Scuola Internazionale Superiore Studi Avanzati (S.I.S.S.A.)
International School for Advanced Studies (I.S.A.S.)

Trieste, Italy

THE POTENTIAL ROLE OF COPPER BINDING SITES IN PRION PROPAGATION

Thesis submitted for the degree of

Doctor of Philosophy

Supervisor

Prof. Giuseppe Legname

Candidate

Thao Phuong Mai

February 20th, 2014

Acknowledgements

I would like to express my deep gratitude to my research supervisor Professor Giuseppe Legname, for giving me the great opportunity to work in his lab and learn more about scientific research, for his useful advice and encouragement in work.

I am also thankful to all my professors, teachers and many other peoples in my University of Medicine in Vietnam, who have taught, supported and given me the best conditions throughout the course of my studies.

I am grateful to Dr. Gabriele Giachin for teaching me from the first PCR to writing a scientific paper. I have learnt a great deal from his experience, not only the prion knowledge but also optimism and sincerity.

I am so thankful to Dr. Tran Hoang Ngoc Ai, Le Tran Thanh Nhat, Dr. Stefano Benvegnù, Dr. Federico Benetti and Dr. Ilaria Poggiolini for their helpful guidance and assistance since my very beginning with experiments. I also want to thank Tran Thanh Hoa for his assistance during this interesting project.

I sincerely thank Erica Sarnataro for the encouragement and patience to read word by word and correct my writings; thanks to all my lab members, Suzana, Lisa, Paola, Diana, Joanna, Andrea ... for your friendship and the time we spent together.

I would also like to extend my thanks for the invaluable support from Tullio, Jessica, Micaela, Massimo, Federica, Andrea, Beatrice, Andrea, Sandra and all SISSA staff, especially the Students' Secretariat, Riccardo and Federica.

Finally, I wish to thank my great parents for their endless love, support and encouragement throughout my life. Mom and Dad are always my great teachers and my closest friends, who make me feel safe and like a little kid. I want to express my deep gratefulness to my husband, who is always by my side sharing my good and bad times, making me more confident in myself and giving me all his sympathy and love. Lastly, I want to thank my little girl - a precious gift coming to

my life, who gives me strength to overcome obstacles; and I wish never to be far away from her since now…

Most of all, thank you for the times here in peaceful Trieste that I will never forget…

Abstract

Transmissible spongiform encephalopathies (TSEs) or prion diseases are caused by a post-translational conversion of the normal cellular form of the prion protein (PrP^{C}) into the pathological and infectious isoform denoted as prion or PrP^{Sc}. PrP^{C} has been shown as a high-affinity copper-binding protein, and to a lesser extent binding to other divalent cations through the octarepeat region (OR) and the non-OR copper binding sites located in the disordered N-terminal domain. Studies on the role of copper in promoting prion conversion and infectivity yielded controversial results. In this work, we explored the role of histidine residues which are crucial for copper coordination in prion conversion using a combination of cell culture and cell-free approaches. The first evidence was derived from chronically prion-infected neuronal murine cells (ScN2a) transiently expressed in murine PrP^{C} carrying artificial mutations at histidines located both at the OR and non-OR regions. We found that the lack of each histidine in the OR has neither effect on prion replication nor protein maturation and trafficking. Intriguingly, mutagenesis of histidine 95 (H95Y) does enhance prion conversion leading to *de novo* infectious material formation and cause aberrant accumulation during protein trafficking. Thus, we hypothesize that H95 could function as molecular switch for prion conversion, and copper bound to this residue may function in protein conformation stabilization. We also propose a cellular model for prion formation in cells expressing the H95Y mutant. Interestingly, our data may establish a platform for rationally designed experiments aimed at elucidating whether the H95Y mutation may cause *de novo* prion diseases in transgenic mice.

TABLE OF CONTENT

LIST OF ABBREVIATIONS

Ab – antibody

ABTS - 2,2'-azino-bis(3-ethylbenzothiazoline-6-sulphonic acid)

Ala (A) – Alanine

ASA - Amyloid seeding assay

Asn – Asparagine

BSE - Bovine Spongiform Encephalopathy

CJD - Creutzfeldt-Jakob disease

CNS – central nervous system

Ctm– C-trans transmembrane

Cy – cytosolic

DAPI – 4',6- diamidinobenzidine

DMSO - dimethyl sulfoxide

EEA1 – Early endosome marker antibody

Endo-H – Endoglycosidase H

EPR – Electron Paramagnetic Resonance

ER – Endoplasmic reticulum

FBS – Fetal Bovine Serum

FFI - Fatal Familial Insomnia

GAG – glycosaminoglycan

GdnHCl - Guanidine hydrochloride

GFP – green fluorescent protein

Gly (G) – Glycine

GSS - Gerstmann-Sträussler-Scheinker Syndrome

H95Y$_{3F4}$ – 3F4-tagged H95Y construct

H95Y$_{3F4}$_PrP^{Sc} seed - PrP^{Sc} from ScN2a cells expressing H95Y$_{3F4}$

His (H) - Histidine

HRP – horseradish peroxidase

Hu – human

kDa – kilo Dalton

KO – knock-out

LAMP2 – Lysosomal associated membrane antibody

M6PR – Mannose 6 phosphate receptor antibody

Mo – Mouse

mRNA – messenger ribonucleic acid

NGS – normal goat serum

Ntm – N-trans transmembrane

O/N – over night

Opti-MEM - Optimal minimum essential medium

OR(s) - octapeptide repeat(s)

PAGE – polyacrylamide gel electrophoresis

PBS – phosphor-buffered saline

PBS-Tween – phosphor-buffered saline with 0.05% Tween

PCR – polymerase chain reaction

Pen/Strep – Penicillin/Streptomycine

PFA – Paraformaldehyde

pH– hydrogen ion concentration

Phe (F) – Phenylalanine

PK - protease K

PK-res – protease-K resistance

PMCA – Protein misfolding cycling amplification

PMSF - phenylmethylsulphonyl fluoride

PNGase-F – Peptide*N*-glycosidase-F

PRNP – prion protein gene (human)

Prnp – prion protein gene (mouse)

Pro (P) – Proline

PrP - Prion protein

PrP^{C} - normal form of prion protein

PrP^{Sc} - disease associated form of prion protein

PTA –phosphotungstic acid

recH95Y – recombinant full-length MoPrP H95Y

recWT – recombinant full-length MoPrP

ROS – reactive oxygen species

rpm– revolutions per minute

RT – Room temperature

SDS – sodium dodexylsulphate

Ser (S) – Serine

SHa – Syrian Hamster

Tfn – Transferrin receptor antibody

ThS or **T** – Thioflavin-S or -T

TSE - Transmissible Spongiform Encephalopathy

Tyr (Y) – Tyrosine

W – Tryptophan

w/w– weight over weight

WT - wild-type

$WT3_{F4}$ – 3F4-tagged WT construct

WT_{3F4}_PrP^{Sc} seed – PrP^{Sc} from ScN2a cells expressing WT_{3F4}

LIST OF FIGURES and TABLES

I. INTRODUCTION

1. Prion diseases

Prion diseases, or transmissible spongiform encephalopathies (TSEs), are a group of rare invariably fatal neurodegenerative diseases affecting human and other mammals (Prusiner, 1984). TSEs etiologically manifest as genetic, sporadic and infectious forms. They include Creutzfeldt-Jakob disease (CJD), inherited Gerstmann-Sträussler-Scheinker syndrome (GSS), Fatal Familial Insomnia (FFI), and kuru in humans; bovine spongiform encephalopathy (BSE) of cattle, scrapie of sheep, chronic wasting disease (CWD) of deer and elk.

Prion disorders are caused by the conformational conversion of the physiological cellular form of the prion protein (PrP^{C}) to the pathological form denoted as scrapie or PrP^{Sc}. The neuropathological hallmarks of prion diseases are astrogliosis, spongiosis and neuronal death, with a generally quite long incubation time and diverse clinical symptoms. Once the symptoms appear, the disease progresses rapidly with motor dysfunction, cognitive impairment, and cerebral ataxia. Neither standard clinical tests for diagnostics nor effective treatments are available so far for prion diseases (**Figure 1**).

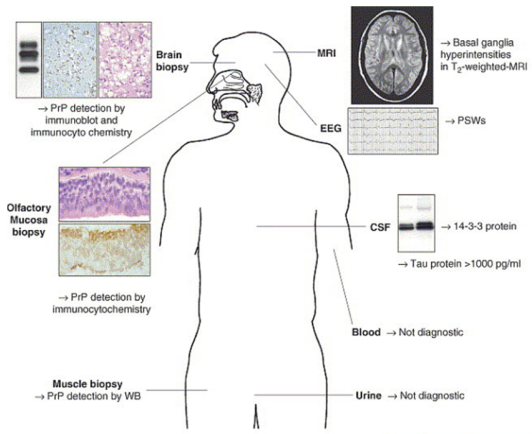

Figure 1. Diagnostic procedures for sporadic Creutzfeldt–Jakob disease. Methods relying on PrP^{Sc} detection include brain and olfactory mucosa biopsies. Currently, examination of blood and urine does not provide diagnostic help. Adapted from (Zanusso and Monaco, 2005).

2. The prion protein

2.1. PrP^C and its biosynthesis

The prion protein (PrP) is conserved among species. It is normally expressed in all tissues and more prominently in the central nervous system. The physiological cellular form PrP^C is largely localized on the outer leaflet of the plasma membrane *via* a GPI anchor, with two short beta-strands (β_1 and β_2) and three alpha-helices (α_1, α_2 and α_3) in structure (Surewicz and Apostol, 2011). This normal form of PrP is α-helical, monomeric, soluble in non-denaturing detergents and protease (PK)-sensitive.

The mammalian *Prnp* gene encodes a protein of approximately 250 amino acids that contains several distinct domains, including an N-terminal signal peptide that directs the protein to the endoplasmic reticulum (ER), a series of five proline- and glycine-rich octapeptide repeat (OR) region, a central hydrophobic segment, and a C-terminal hydrophobic region that is a signal for addition of a glycosylphosphatidylinositol (GPI) anchor (Surewicz and Apostol, 2011) (**Figure 2**). Like other membrane proteins, PrP^C is synthesized in the ER and transits through the Golgi apparatus to the cell surface. After several post-translational modifications, the mature prion protein has 210 amino acids with molecular weight around 26-37 kDa depending on its glycosylation state.

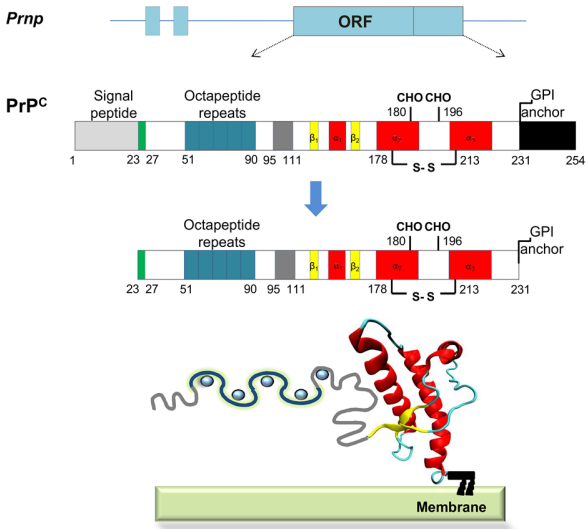

Figure 2. Schematic representation of *Prnp* gene and PrP^C structure. The unstructured N-terminal portion includes a signal peptide (residues 1–22), precedes a **polybasic region**

(residues **23–27**, green) and **five histidine-containing octapeptide repeats** (residues **51–90**, cyan). The central part of the molecule includes **a positively charged region** (residues **95–111**, dark gray) followed by a highly conserved hydrophobic domain (residues 111–130). The C-terminal domain encompasses **two short β-strands** (β_1 and β_2; residues **127–129** and **166–168**, yellow) and **three α-helices** (α_1, α_2 and α_3; residues **143–152**, **171–191** and **199–221**, red). A **C-terminal peptide** (residues 231–254, black) is removed during biosynthesis, followed by attachment of a glycosylphosphatidylinositol (GPI) moiety. PrP^C also contains two N-linked oligosaccharide chains (at Asn180 and Asn196) and a disulfide bond (between residues 178 and 231) (hereafter in mouse numbering).

During its normal biosynthesis, PrP^C undergoes post-translational modifications, including cleavage of the N-terminal signal peptide, addition of N-linked oligosaccharide chains at two sites, formation of a single disulfide bond, and attachment of a GPI anchor (Haraguchi et al., 1989; Stahl et al., 1987; Turk et al., 1988). The GPI anchor, which is added after the cleavage of the C-terminal hydrophobic segment, tethers the mature PrP^C to the cell surface (**Figure 3**). The mature PrP^C is found mostly in the cholesterol- and sphingolipid-rich membrane domains, also known as lipid rafts, which are detergent-resistant membrane domains with many important cellular receptors and other GPI-anchored proteins (Abid et al., 2010).

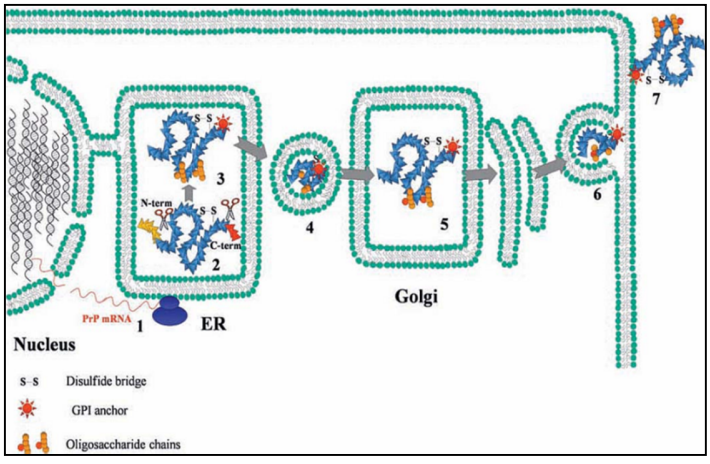

Figure 3. Steps in the biosynthesis of PrP^C. mRNA is translocated from the nucleus and translated by ER-associated ribosomes into the precursor protein (**1**). During its biosynthesis, PrP^C is subject to several post-translational modifications, including the N- and C- terminal signal peptide cleavage, the addition of N-linked oligosaccharide chains, which are high-mannose type (**2**), the formation of disulfide bond and the GPI addition (**3**) in the ER. At the Golgi apparatus, the processes include further modification of oligosaccharide to produce

complex sugar type chains (**4-5**). Mature PrP^C is then trafficked to the cell surface and attached to the outer leaflet *via* a GPI anchor **(6-7)**. Adapted from (Abid et al., 2010).

2.2. PrP^C trafficking and other isoforms of PrP

PrP^C undergoes cyclic rounds of endocytosis (Shyng et al., 1993) with a transit time of around 60 min (Harris, 1999). The process occurs between the surface and the endocytic compartment and it can follow either clathrin-dependent pathways, or be mediated by "caveolae-like" domains (Shyng et al., 1993). From the cell surface, PrP^C can be endocyted to internal endosomal compartments, delivered from early to late endosomes, and routed to lysosomes for degradation or recycled to the cell surface for ensuing cycles (**Figure 4**). Beyond the normal pathway, alternative forms of PrP^C have been found in both cell cultures and *in vivo*. Recent studies suggest that PrP can acquire transmembrane topologies (^{Ctm}PrP and ^{Ntm}PrP) or cytosolic form (cyPrP) (Hegde et al., 1998, 1999). PrP topologies and functions remain nevertheless obscure.

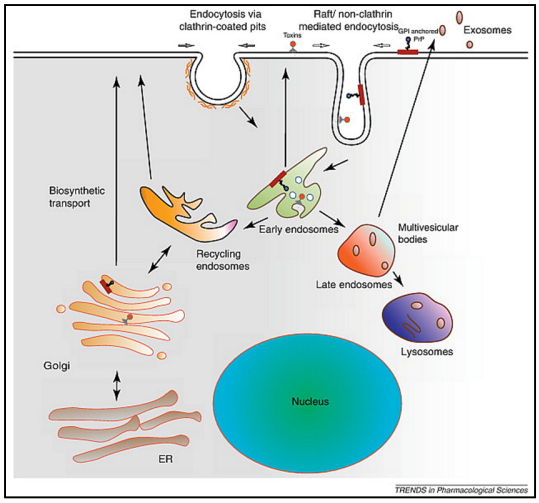

Figure 4. Membrane trafficking in the cell. PrP is internalized via the raft-mediated route. The released clathrin-coated vesicles (CCVs) can undergo fusion with either other CCVs or with existing early endosomes to produce early endosomes. These are sorting endosomes from which proteins could be routed either for degradation *via* late endosomes and lysosomes or for recycling *via* recycling endosomes. PrP travels from the plasma membrane to the Golgi apparatus through early endosomes. Adapted from (Rajendran et al., 2012).

The transmembrane topologies occur when, along the biosynthetic pathway, PrP^{C} is not fully translocated into the ER lumen and its hydrophobic domain (residues 105-140) is inserted within the lipid bilayer of the ER compartments (**Figure 5**). The N-trans transmembrane (^{Ntm}PrP) has the N-terminus of the protein directed toward the ER lumen with the C-terminus accessible to proteases in the cytosol. Alternatively, in the C-trans transmembrane (^{Ctm}PrP) the C-terminus is in the ER lumen with the N-terminus accessible to proteases in the cytosol. These species are generated in small amounts (below 10% of the total) as part of the normal biosynthesis of wild-type (WT) PrP in the ER. Their function still remains unclear, but they may play an important role in disease pathogenesis since the expression of ^{Ctm}PrP in transgenic mice leads to pathological features similar to those of some inherited forms of prion diseases (Hegde et al., 1998). Like many proteins that traffic through the ER, a substantial fraction of PrP normally misfolds, is retrogradely transported to the cytosol, rapidly degraded by proteasomes and undetectable. However, when proteasome activity is compromised, PrP accumulates intracellularly to form cyPrP (Ma and Lindquist, 2001; Taraboulos et al., 1995), but it is not clear whether the cytosolic form is just a WT-PrP occasionally retained in the cytosol, or it serves any physiological function, or it is maybe associated with neuronal pathogenesis. There are multiple potential routes for cyPrP generation. It is conceivable that the access of PrP to the cytoplasm is the neurodegenerative trigger in at least some naturally occurring prion diseases.

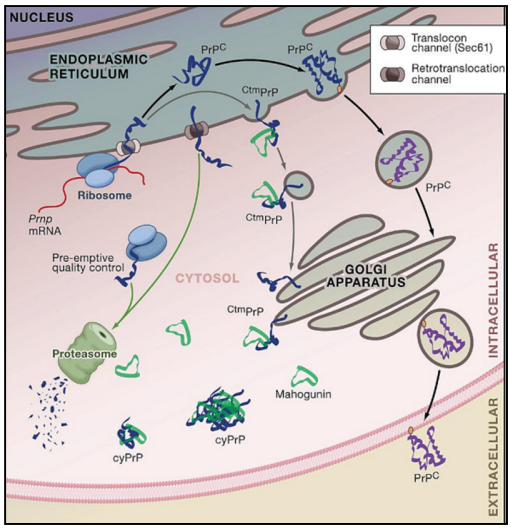

Figure 5. Biosynthesis and localization of other prion protein isoforms. Most PrP^{C} molecules are attached to the outer leaflet of the plasma membrane. However, PrP may acquire transmembrane topologies (^{Ctm}PrP and ^{Ntm}PrP) or cytosolic (cyPrP) form. The N-trans transmembrane (^{Ntm}PrP) has the N-terminus of the protein directed toward the ER lumen with the C-terminus in the cytosol, while the C-trans transmembrane (^{Ctm}PrP) has the C-terminus in the ER lumen with the N-terminus in the cytosol. The cytosolic form of PrP (cyPrP) may arise from proteasome malfunction so the protein cannot reach the cell surface and then accumulate in the cytosol. Adapted from (Hegde et al., 1998; Ma and Lindquist, 2001).

2.3. Putative physiological roles of PrP^{C}

PrP^{C} is most abundantly expressed on neural cells including neurons and glia (Brown et al., 1990; Kretzschmar et al., 1986), as well as in hematopoietic cells (Burthem et al., 2001; Ford et al., 2002). Despite being highly conserved among mammals, the PrP^{C} function has not found a unifying definition yet (Aguzzi et al., 2008). Comparison of WT mice with PrP-knockout (KO) mice or derived cell lines has led to hypothesize PrP^{C} functions in cell adhesion, enzymatic activity, signal transduction, copper metabolism, and programmed cell death. In the nervous system, PrP^{C} is proposed to protect against ischemic trauma, apoptotic agents and reactive oxygen species (Chiarini et al., 2002; McLennan et al., 2004). Moreover, PrP^{C} has been implicated in neuronal transmission (Collinge et al., 1994), neurite outgrowth (Chen et al., 2003), synaptic plasticity (Prestori et al., 2008), circadian rhythm (Tobler et al., 1996), maintenance of peripheral myelin (Bremer et al., 2010) as well as motor

behavior and memory (Nazor et al., 2007; Rial et al., 2009). PrP^C performs important functions also outside the CNS, particularly in the immune system (Isaacs et al., 2006). PrP^C is promptly upregulated in activated T lymphocytes and is redistributed in lipid rafts, together with signaling molecules (Ballerini et al., 2006; Mattei et al., 2004). Not only involved in adaptive immune responses, PrP^C controls hematopoietic cell differentiation including the self-renewal of bone marrow progenitors (Zhang et al., 2006), thymic differentiation (Jouvin-Marche et al., 2006), and the repression of phagocytic activity in macrophages (de Almeida et al., 2005).

Studies on PrP-KO mice showed that they display no major developmental or anatomical abnormalities and have a normal lifespan (Büeler et al., 1994). Nevertheless, some of these animals exhibit subtle phenotypic abnormalities at the behavioral and cellular levels (Steele et al., 2007). A consistent finding in all mice devoid of PrP^C is their resistance to scrapie and their inability to propagate infectivity. The differences in phenotypic abnormalities observed in these KO mice may arise from the way in which disruption of PrP gene was achieved (Moore et al., 1999; Rossi et al., 2001).

2.4. The pathological form of the prion protein (PrP^{Sc})

The pathological isoform of PrP, known as PrP scrapie (denoted as PrP^{Sc}), has distinct characteristics from the physiological form PrP^C. Although sharing the same sequences, the two isoforms of the prion protein bear several biophysical differences. PrP^{Sc} shows a high content of β-sheets, tends to aggregate to form amyloid plaques and cause toxicity, is insoluble in non-denaturing detergents and partially resists to PK digestion. The PK-resistance is often used to distinguish the pathological isoform from the physiological form (**Table 1**). All available evidence indicates that conversion of PrP^C into PrP^{Sc} is conformational rather than covalent, due to their similar primary amino acid sequence and probably the same post-translational additions (Prusiner et al., 1998; Stahl et al., 1993). PrP^{Sc} accumulates in scrapie-infected brains while PrP mRNA levels remain unchanged (Oesch et al., 1985). The conformational change involves a substantial increase in the amount of β-structured motifs of the protein, with possibly a small decrease in the amount of α-helices

(Gasset et al., 1993; Pan et al., 1993; Safar et al., 1993). Although a tertiary structure of PrP^{Sc} has not been well established yet, this isoform is suggested to undergo primarily changes in the unstructured N-terminal half of the protein, including folding of a portion of the N-terminal tail from residues 90 to 121 (and possibly part of the first α-helix) into β-turn (Peretz et al., 1997). Solving the actual structure of PrP^{Sc} is clearly a key challenge in the prion field. It would be very useful to elucidate how this structure is derived from the α-helical PrP^{C} conformation and to explain the existence of several "prion strains" related to different TSEs.

Properties	**PrP^{C}**	**PrP^{Sc}**
Isoform	Monomers	Multimeric aggregates
Protease resistance	No	Stable core (residues 90-231)
Location	Plasma membrane	Intra- or extracellular
Solubility	Soluble	Insoluble
PK-sensitivity	Sensitive	Partially resistant
α-helices	45%	30%
β-sheets	3%	45%
Glycoforms	Mixture of un-, mono-, and diglycosylated forms	Mixture of un-, mono-, and diglycosylated forms
Infectivity	No	Yes
Turnover	Hours	Days

Table 1. Biochemical and biophysical characteristics of PrP^{C} and PrP^{Sc}

The prion neuropathology includes neuronal loss, formation of vacuoles in the gray matter, astrogliosis and amyloid deposits in the brain, leading to neurodegeneration. Although prions are widely thought to exert a destructive effect predominantly within the CNS, the exact cause of their neurotoxicity remains unclear. Yet it is established that PrP^{C} is required for prion replication, as mice devoid of PrP^{C} are resistant to prion infection. Moreover, dimeric PrP^{C} was found to efficiently bind to PrP^{Sc} (Meier et al., 2003), suggesting that prion conversion somehow depends on

PrP^{C}. Although protein misfolding and aggregation are undoubtedly associated with neurodegeneration and diseases, the mechanism by which misfolded aggregates produce neuronal death is unknown. Direct PrP^{Sc} toxicity might be mediated by membrane disturbances, which could have effects on neuronal homeostasis, intercellular contacts, synaptogenesis, synapse functions and axonal transport. Indirect effects may arise from perturbations of glial functions. The accumulation of PrP^{Sc} aggregates may corrupt PrP^{C} functions upon conversion to PrP^{Sc}. In addition, ER stress and oxidative stress are involved in the mechanism for neurodegeneration in prion diseases, or the combination of multiple mechanisms might contribute to the pathology.

3. The "protein-only" hypothesis and the mechanism for prion conversion

The first origin for transmissible spongiform encephalopathies (TSEs) was accidentally discovered in 1937, when a population of Scottish sheep was inoculated against a common virus with a formalin extract of brain tissue derived from an animal with scrapie. In 1966, transmission of kuru in humans was demonstrated among members of the cannibalistic tribes of New Guinea. Initially, the causing agent was thought to be a slow virus, because of the long incubation time from the first exposure to the pathogen to the symptoms onset. However, further studies indicated that this agent was significantly different from viruses or other conventional organisms. In 1967, Alper and his colleagues demonstrated that the causing agent was not destroyed by normal treatments that destroy nucleic acid, such as ionizing radiation or ultraviolet (Alper, 1993; Alper et al., 1967), and the infectious material was too small to be a virus or another type of microorganism (Alper et al., 1966). The "protein-only" hypothesis, first elaborated by Griffith in 1967 to explain Alper's findings, proposed a protein could act as the infectious agent that causes scrapie (Griffith, 1967). But little research was done to test this hypothesis until 1982, when Prusiner and coworkers pioneered an impressive set of discoveries for the prion hypothesis, and coined the term PRION to refer to this proteinaceous infectious agent (Prusiner, 1982) (**Figure 6**).

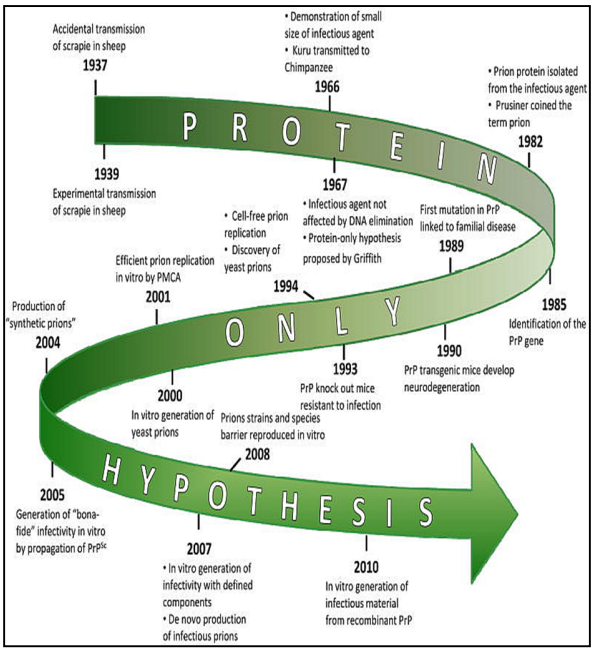

Figure 6. A timeline representation of the milestones in the prion hypothesis. Adapted from (Abid et al., 2010).

3.1. Models for prion replication

Many decades since its first discovery, the mechanism of conversion from physiological PrP^{C} to pathological PrP^{Sc} still remains enigmatic. Although the formation of PrP^{Sc} is accompanied by neurodegeneration in prion disease, PrP^{Sc} is not intrinsically neurotoxic. It needs the presence of PrP^{C} in host cells for the pathology to occur. Two models have been proposed to explain the mechanism by which the pathological isoform PrP^{Sc} could induce the normal cellular form PrP^{C} to acquire a misfolded conformation (**Figure 7**).

The "refolding" or template assistance model proposes the interaction between exogenously introduced PrP^{Sc} and endogenous PrP^{C}, which is induced to transform itself into further PrP^{Sc}. A high energy barrier exists that prevents the spontaneous conversion of PrP^{C} into PrP^{Sc}, thus, the interaction may occur with the presence of "protein X", an unknown chaperone–like protein that facilitates this process (Telling et al., 1995).

The "seeding" or nucleation-polymerization model postulates that PrP^{C} and PrP^{Sc} are in a reversible thermodynamic equilibrium. In physiological state, the

equilibrium could be shifted toward the PrP^{C} conformation, such that only a minute amount of PrP^{Sc} would co-exist with PrP^{C}. The pathological conformation is stabilized only if several monomeric PrP^{Sc} are organized into highly ordered seeds, and PrP^{Sc} could be further recruited and eventually aggregated to form amyloid assemblies. The fragmentation of amyloid aggregates increases the number of replication units, which can recruit further PrP^{Sc} and thus results in an apparent replication agent (Glatzel and Aguzzi, 2001).

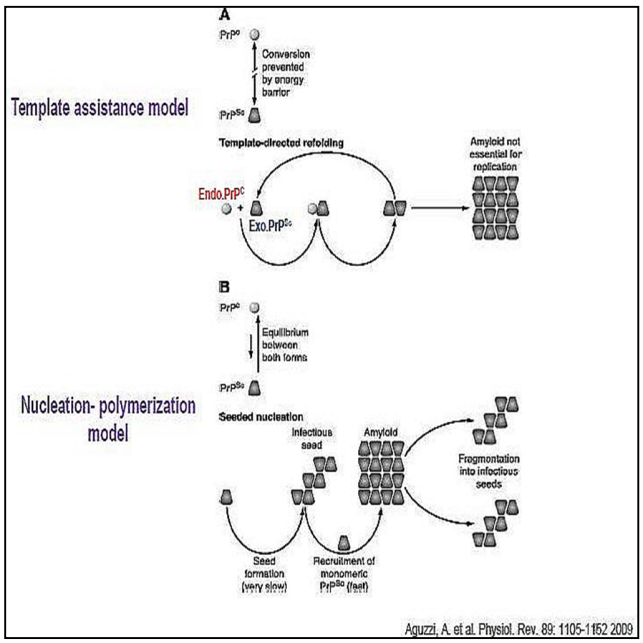

Figure 7. Models for prion replication (A) The "template assistance model" proposes the interaction between exogenous PrP^{Sc} and endogenous PrP^{C} whereas in **(B)** the "nucleation-polymerization model" postulates the imbalance of PrP^{C}–PrP^{Sc} equilibrium that causes the aggregation of PrP^{Sc}. Adapted from (Aguzzi and Calella, 2009).

3.2. Factors involved in prion conversion

Some evidence supports the existence of a conversion factor in the prion replication process (**Figure 8**). This evidence was derived from studies in which transgenic mice expressing both human and mouse PrP^{C} were challenged with human prions. Interestingly, while mice expressing only human PrP^{C} ($HuPrP^{C}$) developed the disease after human PrP^{Sc} inoculation, mice co-expressing both proteins resisted prion replication (Telling et al., 1994). This suggested that mouse PrP^{C} ($MoPrP^{C}$) was able

to inhibit the conversion when co-expressed with $HuPrP^{C}$ by binding to an additional factor. Further studies showed the presence of a factor, termed protein X, able to bind to the C-terminal end of PrP^{C} (Kaneko et al., 1997a). The list of PrP^{C}-binding molecules continues to grow, and it is important to determine whether these molecules also interact with PrP^{Sc}, and characterize the effects of these interactions on PrP^{Sc} formation. As crucial co-factors, the laminin receptor or its precursor have been shown to play an important role in PrP^{Sc} formation in mouse hypothalamic GT1 cells infected with the Chandler scrapie strain. Although it is unclear how glycosaminoglycans (GAGs) affect PrP^{Sc} biogenesis, it is supposed that GAGs might bind to both PrP^{C} and PrP^{Sc} and induce the conversion (Krammer et al., 2009; Lee et al., 2007). Also there is evidence for nucleic acids such as RNA to be involved in prion replication. The first evidence that RNA might play a role in PrP^{res} formation was the finding that pancreatic RNase inhibits PrP^{res} amplification in a dose-dependent manner (Deleault et al., 2003). *In vitro* PrP^{res} amplification was also abolished by purified RNaseA and RNaseT1. PrP molecules are known to traffic to various cell compartments where RNA is normally localized, such as the cytoplasm and nucleus, or even a fraction of PrP molecules exist in a transmembrane form with a cytoplasmic domain (Hegde et al., 1998) that allows the interaction to occur. Moreover, RNA molecules might enter the extracellular space as a result of cell death or active transport. Investigating whether RNA participates in PrP^{Sc} formation in living cells and animals, as it appears to do *in vitro*, will be an important avenue for research in the future (Supattapone, 2004). Metal ions, especially copper ions, have been implicated to have roles in prion replication, but it is unclear whether these ions inhibit or promote the procedures with intriguing results (Bocharova et al., 2005; Lehmann, 2002; Quaglio et al., 2001; Sigurdsson et al., 2003; Thompson et al., 2001).

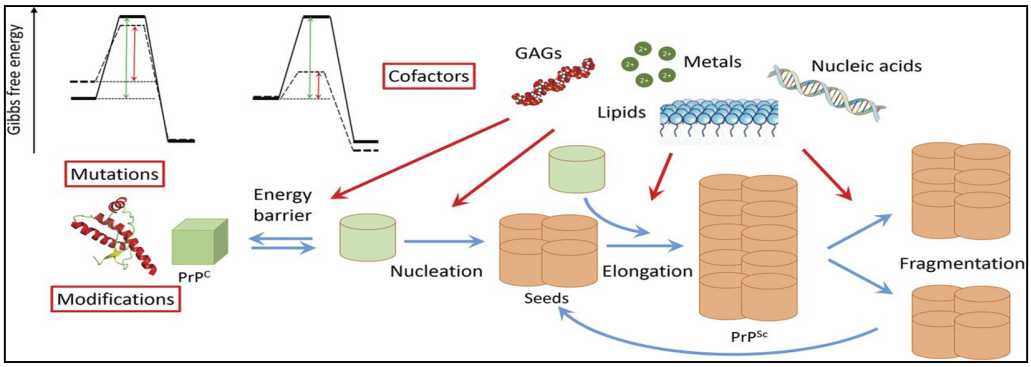

Figure 8. Factors involved in prion conversion. Pathogenic mutations, modifications, co-factors could impact the conformational conversion of PrP^{C} into PrP^{Sc}, which is crucial in prion pathology. Adapted from (Zhou and Xiao, 2013).

3.3. Putative sites for prion conversion

Many putative sites of PrP^{Sc} synthesis have been proposed by analyzing the patterns of distribution for PrP^{C} and PrP^{Sc} in infected cells. The cellular pathways involved in the formation of PrP^{Sc} are summarized in **Figure 9**. PrP^{Sc} is produced from the host PrP^{C} as a result of a conformational change involving increased β-sheet structure in the polypeptide chain. The interaction between exogenous PrP^{Sc} and endogenous PrP^{C} may take place in detergent-resistant rafts on the plasma membrane and/or in endosomal organelles. Once generated, PrP^{Sc} is metabolically stable and becomes localized partly but not exclusively in intracellular organelles, perhaps endosomes and lysosomes, which may be the sites where the N-terminus of the protein is proteolytically cleaved (Caughey et al., 1989, 1991a). Taken together, the results obtained for prion conversion sites greatly vary depending on the cellular models used. Prion conversion possibly occurs via multiple pathways.

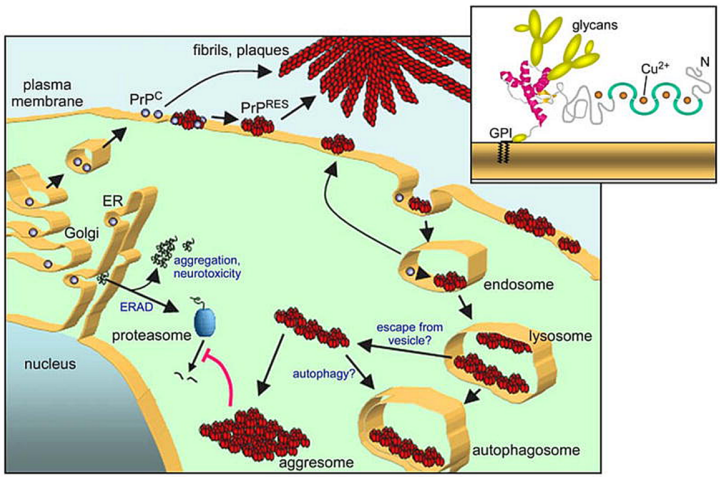

Figure 9. Model of biogenesis and accumulation of PrP^{res} in scrapie-infected cells. In the infectious manifestation of prion diseases, extracellular PrP^{Sc} in the form of a prion particle interacts with PrP^{C} on the cell surface, possibly in detergent-resistant rafts, catalyzing its conversion to PrP^{Sc}. Conversion may also occur after uptake of the proteins into an endosomal compartment. Once PrP^{res} is made, it can accumulate on the cell surface, in intracellular vesicles and aggresomes, or in extracellular deposits. Adapted from (Caughey et al., 2009).

3.4. Transmission of protein misfoding

The prion-like conversion phenomenon could contribute to transmit the pathological misfolded conformation between proteins, within cells and tissues and among individuals. Thus, transmission by infectious proteins can be regarded at different stages (Moreno-Gonzalez and Soto, 2011) (**Figure 10**).

At the molecular level, misfolded proteins can propagate and induce the conformational changes in the native proteins, as the seeding-nucleation model proposes, modifying normal protein functions and inducing cellular stress and damage.

From one cell to another, misfolded aggregates come into contact with the native protein in the neighboring cells *via* several cellular pathways. Misfolded proteins can accumulate intra- or extracellularly. Intracellular aggregates are usually encapsulated in so-called aggresomes that could help in the recruitment of protein aggregates, which are then targeted to elimination by macro-autophagy and degradation into lysosomes. Both autophagosomal and lysosomal vesicles can spread

aggregates within the cell and act as a reservoir for misfolded proteins. Moreover, lysosomal proteolysis could provide more fragmentation of large aggregates leading to the seed amplification. Cell-to-cell transmission of intracellular aggregates requires their release to the extracellular space. Exosomes are assembled in cytoplasmic organelles, known as multivesicular bodies, and secreted *via* exocytosis. Released exosomes can then fuse with other cells and exchange to deliver their content, contributing to spread protein misfolding.

Another potential spreading mechanism of misfolded aggregates is *via* tunneling nanotubes. Tunneling nanotubes are thin membranous bridges between cells for intercellular long distance communication to transfer organelles, vesicles, plasma membrane and cytoplasmic molecules (Rustom, 2009). Tunneling nanotubes have been implicated in propagation of endogenous PrP between dendritic cells and uninfected neurons (Gousset and Zurzolo, 2009; Gousset et al., 2009). Since PrP^{C} is a membrane protein, cell-to-cell spreading may occur by direct contact between the misfolded proteins in one cell with the natively folded protein in the neighboring cells.

Individual-to-individual transmission can occur through vertical or horizontal routes. Horizontal transmission may involve exposure through contaminated surgical tools, organ transplant, human hormone treatment or blood transfusion. All these routes have been demonstrated in the transmission of prion diseases in humans (Brown et al., 2000). It is well established that BSE can be transmitted to humans, inducing the fatal variant CJD (Scott et al., 1999). Prion diseases could be acquired through exposure to or intake of contaminated tissues or fluids and consumption of infected food derived from afflicted animals. Another route for host-to-host transmission is the vertical infection from parents to their offspring.

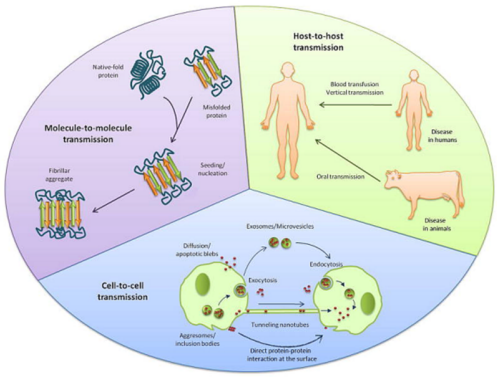

Figure 10. Transmission of protein misfolding between molecules, cells and individuals. Prion-like transmission of protein misfolding may operate at various levels, including molecule-to-molecule, cell-to-cell and host-to-host. Propagation of the pathological conformational changes and downstream effects to cells, tissues and the entire individual appears to be a universal property of misfolded protein aggregates. Adapted from (Moreno-Gonzalez and Soto, 2011).

4. Metal ions and neurodegenerative diseases

Transition metal ions like iron, copper, zinc, manganese etc. are essential for life, but they are also involved in several neurodegenerative mechanisms such as protein aggregation, free radical generation and oxidative stress. Almost all living organisms require transition metals for essential metabolic processes to function properly. In the nervous system, iron is required to support the brain's high respiratory rate as well as for myelination, gene expression and neurotransmitter synthesis; copper is also required for mitochondria respiration, neurotransmitter biosynthesis and as a cofactor for antioxidant enzymes.

Although metal ions are important for life, they can induce free radicals that cause neurotoxicity in several neurodegenerative conditions. Neurodegenerative diseases affect the nervous system and share common features such as selective neuronal death, protein aggregation, oxidative stress, mitochondria dysfunction, transition metal accumulation and inflammation. These elements have been proposed to contribute to neurodegenerative disorders based on the observations that patients with neurodegenerative diseases have alterations of metal levels in their nervous systems. Some studies show that metals such as iron and copper play an important

role in protein aggregation and therefore are likely to link the two pathological processes of protein aggregation and oxidative stress (Gaeta and Hider, 2005).

The prion-metal relation was first reported in the early 1970s when the copper chelator cuprizone was found to induce spongiform changes in the brain of treated mice, which are similar to those induced by scrapie (Pattison and Jebbett, 1973). Later on, several studies on the concentrations of metals in mice affected by prion disease demonstrated the alterations of copper, manganese and iron levels in brain, liver and blood (Brown, 2001; Lehmann, 2002; Thompson et al., 2001). Recent reports suggest that imbalance of brain metal homeostasis is a significant cause of PrP^{Sc}-associated neurotoxicity (Singh et al., 2010). Indeed, oxidative stress events in the brain (lipid peroxidation, decrease in neuronal nitric oxide synthase activity) are detectable in prion disease in both infected animals and cultures (Guentchev et al., 2000; Lehmann, 2002). Proposed hypotheses include a functional role for PrP^{C} in metal metabolism, and loss of this function due to protein misfolding and as the cause of brain metal imbalance. PrP^{C}-metal interaction may induce oxidative damage and also promote the conversion of PrP^{C} to a PrP^{Sc}-like form, but only limited information is available on PrP-metal interaction and its implications on prion disease pathogenesis (Bush, 2000; Davies et al., 2008; Singh et al., 2010). Studies on the interaction of PrP^{C} with metals have been based both on *in vitro* and *in vivo* models. *In vitro* studies have been more revealing due to the simplicity and accuracy of the readout, whereas in animal models, metal metabolism is complex and the interaction of individual proteins with metals is often missed due to low affinity or their transient nature (Singh et al., 2010). *In vitro* studies using refolding full-length recombinant PrP or its fragments, have led to many important findings regarding PrP-metal interaction. PrP can bind to several divalent cations but the protein highly selectively binds to copper at the conserved octapeptide repeat (OR) region with high affinity. It is crucial to study the interaction of PrP^{C} with metals to understand the physiological and pathological implications of this interaction in prion pathogenesis.

4.1. Copper (Cu)

Copper is an essential trace element, which is required as a catalyst for multiple enzymatic reactions. Since it can exist in multiple redox states, an imbalance in copper homeostasis can lead to several detrimental effects. Free Cu rarely exists in organisms; it is always found to be bound to proteins and in highly regulated uptake, sequestration and excretion. When this highly regulated state is disturbed, it can cause CNS disorders, such as Wilson's disease, Menkes disease, Alzheimer's disease and prion diseases (Hung et al., 2010; Scheiber et al.; Zatta et al., 2009). The link between Cu and TSEs arises from studies showing administrations of cuprizone to mice caused a spongiform degeneration of the brain similar to scrapie (Pattison and Jebbett, 1973; Sigurdsson et al., 2003). Indeed, the ORs of PrP^C can bind Cu within the physiological concentration range (Brown et al., 1997a; Kramer et al., 2001), suggesting that PrP^C may play a role in Cu metabolism in the normal brain. Since Cu ions have been proved to stimulate the endocytosis of PrP^C (Pauly and Harris, 1998), it could serve as a recycling receptor for uptake of Cu ions from the extracellular milieu. Recently, the demonstration that there is free Cu in synaptic clefts, also where PrP^C has been found at high concentration, emphasized a further role for PrP^C in Cu homeostasis and redox signaling at synapse (Herms et al., 1999; Hung et al., 2010). Cu binds to PrP at four ORs in the unstructured N-terminal half of the protein and the non-OR or "fifth site" region preceding the highly conserved PrP hydrophobic core has been identified to involve histidine (His) 95 and 110. The affinity of PrP^C for copper is higher compared to zinc, since even a large excess of zinc cannot displace copper from the OR (Jackson and Collinge, 2001; Walter et al., 2007).

4.2 . Zinc (Zn)

Zinc can also bind to the OR region and His 95 of PrP, though with a lower affinity than Cu. The interaction of Zn^{2+} with PrP has an important implication, because about 5-15% of the total Zn^{2+} content of the brain is present at the pre-synaptic vesicles level (Weiss et al., 2000) and the release of Zn^{2+} into the synaptic cleft, together with the localization of PrP near neuronal synapses, proposed the link between PrP-Zn at synapses. PrP can be a candidate in maintaining Zn^{2+} homeostasis by serving as a Zn^{2+} transporter. Indeed, in cell models, at physiological levels, Zn

can alter the distribution of PrP^C-bound Cu and stimulates the protein endocytosis (Watt and Hooper, 2003). These observations indicate that the interaction of PrP^C with Zn may be more significant given the relative abundance of this metal in the brain (Qin et al., 2002; Walter et al., 2007; Watt and Hooper, 2003). Jobling *et al.* showed that both Cu^{2+} and Zn^{2+} can enhance *in vitro* aggregation of PrP derived peptide 106–126 and chelation of the metals prevents the aggregation (Jobling et al., 2001). While studies conducted on peptides showed an enhancing effect of this ion on protein aggregation, experiments on full-length protein demonstrated that Zn^{2+} can prevent conversion to fibril amyloid forms, although this effect was more pronounced in the case of Cu^{2+} (Wadsworth et al., 1999). However, the role of zinc on prion formation remains obscure.

4.3 . Iron (Fe)

Iron is probably one of the most important metals required for survival. The transportation of Fe in and out of the cells must be tightly regulated in physiological systems since Fe exists in two oxidation states (non-toxic ferric Fe^{3+} and highly toxic ferrous Fe^{2+}) and, therefore, its free form can generate oxidative stress (Kaplan, 2002; Thompson et al., 2001). The interaction of PrP^C with Fe indicates a functional role for PrP^C in cellular iron uptake and transport (Basu et al., 2007; Singh et al., 2009). PrP^C influences the cellular Fe pool within a tightly regulated mechanism of Fe uptake, transport, and utilization (Singh et al., 2009). PrP^C has been demonstrated to influence Fe metabolism in cells expressing normal and mutant PrP forms and in PrP-KO mice model (Petersen et al., 1996; Singh et al., 2009). PrP^C does not mediate the efflux of excess Fe from cells, confirming its role as an Fe uptake protein (Singh et al., 2009). But it is unclear whether PrP^C mediates Fe uptake using a novel pathway or by interacting with the conventional pathway of Fe uptake and transport. PrP^C has been hypothesized to influence Fe uptake by interacting with the transferrin or transferrin receptor pathway (Waheed et al., 2002), or function as a ferric reductase to facilitate the transport of ferric iron from endosomes to cytosolic ferritin (Singh et al., 2009). Deletion of PrP^C in PrP-KO mice induces Fe deficiency by decreasing the transport efficiency from the intestinal lumen to the blood stream, and the uptake from the blood by parenchymal cells and cells of the hematopoietic lineage. Re-expression of

PrP^C corrects the Fe deficiency in these mice, confirming the functional role for PrP in Fe uptake (Singh et al., 2009). An important question that remains unanswered is the binding site and the affinity of PrP^C for Fe. *In vitro* experiments using recombinant PrP and its fragments indicate that the OR region of PrP^C is not essential for Fe binding, and the Fe and Cu binding regions of PrP^C do not overlap (Singh et al., 2010).

4.4 . Manganese (Mn)

Manganese is also an essential trace element crucial for survival whose imbalance can cause detrimental disorders of the CNS (Dobson et al., 2004). Mn can bind to PrP^C probably at the C-terminal region between residues 91-230 or overlapping with the copper binding site at His 95 (Brazier et al., 2008; Treiber et al., 2007). Cu and Mn bind to different histidine residues within the fifth site in the full-length protein. When studying the truncated mutant PrP (90-231) this preference is probably lost, as occupancy of the fifth site by one metal excludes binding of the other at this site. This implies a change in coordination of both metals within the fifth site in the truncated protein. The affinity of PrP for Cu is much higher than for Mn (Jackson and Collinge, 2001), but Mn could occupy Cu binding sites and compete equivalently for these sites (Brown et al., 2000). Mn bound to PrP becomes oxidized and is able to displace Cu that already bound to the protein. Studies have shown that mice infected with PrP^{Sc} have increased Mn and decreased Cu content, suggesting that in prion infection, altered metal content could be the initial sign of infection, or it could be due to the infection itself (Thackray et al., 2002). Recombinant PrP, when refolded in the presence of Mn, can transform to a PK-resistant but not pathogenic form (Brown et al., 2000). Protein with Mn bound is able to initiate seeded polymerization of metal-free prion protein (Lekishvili et al., 2004). Initially, Mn binding does not result in an altered conformation, but over time, the protein is more susceptible to oxidative damage that possibly changes the structure of the protein (Tsenkova et al., 2004).

Taken together, the interactions of PrP^C with different divalent metal ions share some of features:

(1) Binding sites in the OR and/or non-OR regions site at His 95/ His110

(2) Linkage between PrP^C expression, function and metal ions

(3) Conformational effects

(4) Related to PrP^{Sc} formation

The effects of metal ions on prion protein are summarized in **Table 2**. The prion protein may serve as a buffer against metal imbalances that neuronal cells encounter during stress conditions. However, since PrP must bind to metal ions within certain physiological concentrations, once metal concentration gets over the threshold level, PrP adopts an altered conformation reminiscent of the protease-resistant PrP^{Sc} form. Limited studies make it difficult to explain the underlying molecular and cellular mechanisms of these abnormalities. Further studies are necessary to fully understand this phenomenon.

Copper	• Superoxide dismutase-like activity • Stimulates endocytosis; increases protein turnover • Converts into PK resistant forms distinct from scrapie • Delays onset of disease • Inhibits conversion into amyloid fibrils • Regulates expression and metabolism
Zinc	• Induces rapid turnover of PrP • Critical for PrP(106–126) aggregation and neurotoxicity
Iron	• Formation of PrP^{res} with PMCA
Manganese	• Amplifies aggregation of PrP; pro-aggregatory effect • Formation of PrP^{res} with PMCA • Increases resistance to proteinase K digestion

Table 2. Summary of metal effects in prion protein. Adapted from (Choi et al., 2006).

5. Copper and prion diseases

A link between copper and prion diseases was first proposed in 1973, when Pattison and Jebbett noticed that cuprizone caused a similarity in the histopathology of scrapie-infected mice.

5.1. Copper binding in PrP^C

It is well established that PrP^C binds to Cu ions both *in vitro* and *in vivo* (Brown et al., 1997b; Hornshaw et al., 1995; Viles et al., 1999; Whittal et al., 2000). Our understanding of the number, location, structure, affinity and cooperativity of the Cu binding sites in PrP continues to expand in the literature. Although the proposed binding affinities differ, most would agree that Cu binds specifically to the OR region in the flexible N-terminus of PrP (Aronoff-Spencer et al., 2000; Hornshaw et al., 1995); however, other sites in the C-terminus of PrP have also been intriguingly identified as potential Cu binding regions.

- **Octapeptide repeat (OR) domain**

Hornshaw *et al*. first suggested that PrP^C binds Cu^{2+} (Hornshaw et al., 1995). The area of the protein first implicated in this activity is the so-called OR region composed of multiple tandem copies of the eight-residue sequence PHGGGWGQ. The OR domain is in the unstructured flexible N-terminal portion of the protein but it can acquire some rigid structures after metal binding. This region spans approximately from residues 60 to 90, with variations arising from different species and the number of ORs. PrP sequences from most species carry four or five copies of this segment. The histidine-glycine-rich sequence is similar to other histidine-rich sequences in other cupro-proteins (Hornshaw et al., 1995). Interestingly, across species, the OR domain is among the most highly conserved regions of the PrP sequence (Wopfner et al., 1999), indicating a correlative role between Cu and PrP (**Figure 11**).

The OR domain takes up approximately six Cu ions, each with a dissociation constant varying from the micromolar to nanomolar range at pH 7.4. Each OR can bind up to one equivalent of Cu^{2+} under saturating conditions, and the complete OR region can bind 3-6 Cu^{2+} with an apparent binding affinity for Cu^{2+} in the micromolar range (Whittal et al., 2000). This domain is highly selective for Cu^2 (Hornshaw et al.,

1995; Stöckel et al., 1998a; Whittal et al., 2000). The binding of metals to the OR region is quite pH-dependent, with only two Cu ions found at pH 6.0 (Miura et al., 2005; Whittal et al., 2000). It has been shown that at pH 5.5, the full-length PrP is capable of binding two Cu^{2+} ions with coordination from multiple histidine imidazole groups. The binding mode at pH 5.5 is similar to that occurring at neutral pH at low Cu^{2+} occupancy, even though at maximum Cu^{2+} coordination is very different (Wells et al., 2006).

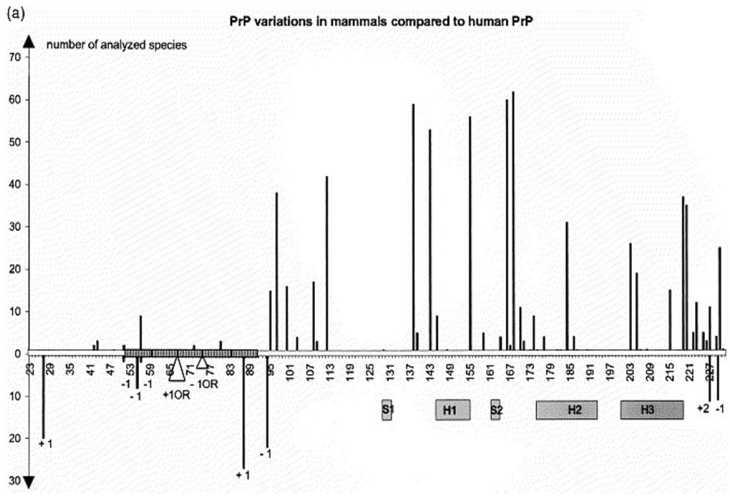

Figure 11. Matrix of the number of variations in mammals as compared to the human PrP for amino acid residues 23-231 (68 mammalian species have been included). Upper columns delineate amino acid substitutions; lower columns represent insertions and deletions; triangles indicate octarepeat insertions (depicted to scale for number of species, but not for the exact localization). Adapted from (Wopfner et al., 1999).

The imidazole ring of histidine residue, present in the PHGGGWGQ repeat, is an avid metal ion binder and is certain to participate in Cu^{2+} coordination. Modeling studies identified a conformation in which the second and third Gly following the His participated in the coordination sphere (**Figure 12**). The minimal sequence HGGGW bound a single Cu^{2+} and captured all the electron paramagnetic resonance (EPR) spectral features of the full four-repeat domain with four bound Cu ions. The number of Cu ions is taken up in a 1:1 fashion. These findings demonstrated that HGGGW constitutes the fundamental copper-binding unit in the OR domain (Aronoff-Spencer et al., 2000).

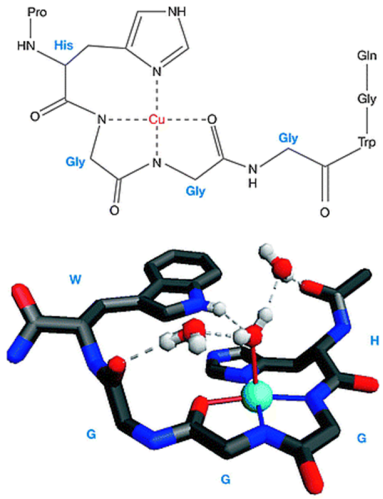

Figure 12. Chemical details of the Cu^{2+}-octarepeat interaction (top panel), determined from **electron paramagnetic resonance (EPR)** constraints, **and the X-ray crystal structure** (bottom panel) of the Cu^{2+}-HGGGW complex. Adapted from (Millhauser, 2004).

Copper binding affinity, as reflected by the dissociation constant K_d, has been demonstrated in the low micromolar to nanomolar range with controversial data (Krammer et al., 2009; Whittal et al., 2000). At low-Cu^{2+} occupancy, which favors multiple His coordination (component 3 spectrum), a single Cu^{2+} coordinates through multiple His side chains with a K_d of 0.12 nM. At high copper occupancy, the component 1 spectrum dominates and reflects the interaction with a single His and de-protonated amide side chains with a K_d in the range 7.0 μM to 12.0 μM. Component 2 is an intermediate state in which each Cu^{2+} is coordinated by two His residues, thus forming large intervening loops. Potentiometric titrations identify distinct de-protonated binding states depending on the ratio of Cu to OR (Valensin et al., 2004). PrP^C binds Cu with several unique coordination modes (**Figure 13**) (Chattopadhyay et al., 2005). It is certainly possible that each mode exhibits distinct characteristics with regard to prion conversion.

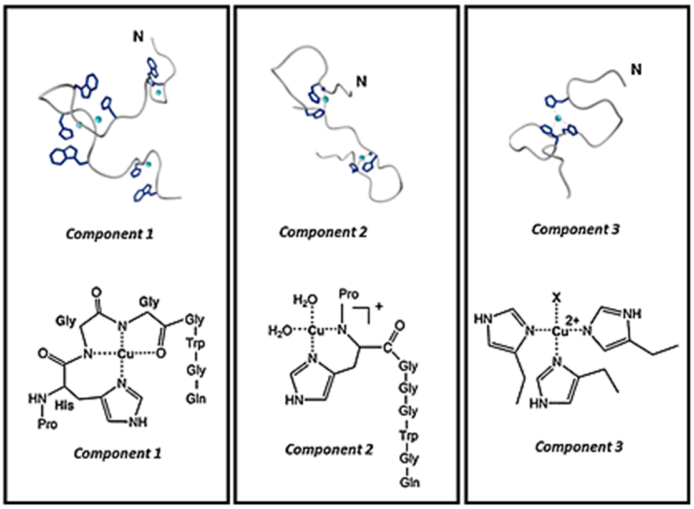

Figure 13. Distinct octarepeat Cu^{2+} binding modes with three, two, or one coordinated His residues, respectively. Low Cu^{2+} occupancy favors component 3; high occupancy favors component 1. Adapted from (Chattopadhyay et al., 2005).

- **The non-OR or fifth copper-binding site**

Treatment of PrP^{Sc} with protease-K (PK) removes approximately from residue 90 but without loss of infectivity, suggesting that the OR domain does not play a role in TSEs. Recent studies show that addition of Cu to PrP^{C} converts the protein to a partially PK-resistant state, and this conversion requires only a single Cu binding site (Quaglio et al., 2001). Studies by Qin (Qin et al., 2002) and Millhauser (Millhauser, 2004) demonstrate that another Cu binding beyond the PK cleavage site takes place at His 95, which is outside the OR region (**Figure 14**).

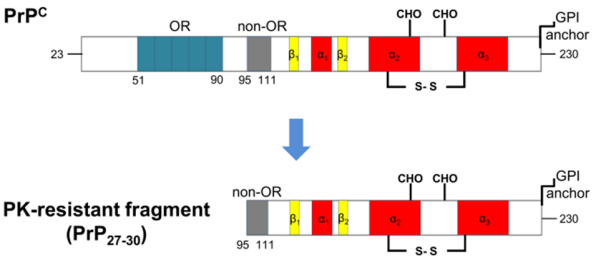

Figure 14. Protease-resistance fragment formation. PK treatment cleaves the protein at residue 90 and the PK-resistant fragment (residues 90-231) remains, including the non-OR copper binding site, proposing a further function of copper in prion propagation.

Using recombinant full-length PrP, a non-OR site has been identified involving H95 and/or H110 (Burns et al., 2003) which precede the hydrophobic segment of the protein and are also in a glycine-rich environment. The fifth site could successfully compete with the OR region for Cu. The location of this particular site has been controversial, with Jones et al. (Jones et al., 2005) arguing that Cu^{2+} coordinates at H110 with higher affinity than at H95, depending on the peptides and methods used for analysis. Several lines of evidence suggest that this site may possess higher affinity for Cu^{2+} than the OR sites within a nanomolar range (Burns et al., 2003) **(Figure 15)**. The location of the non-OR region beyond the PK cleavage site suggests that Cu may be found in the PrP^{Sc} particle, perhaps with a stabilizing role.

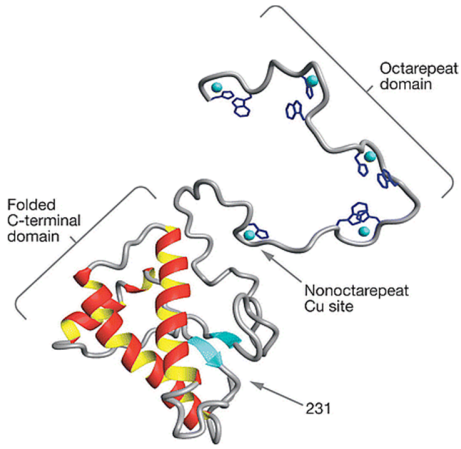

Figure 15. The model of full-length PrP, with all copper sites occupied. Each Cu in the OR domain interacts with the HGGGW residues as shown in **Figure 14**. EPR studies on recombinant full-length protein identified an additional non-OR binding site involving H95. Adapted from (Millhauser, 2004).

- **Copper binding in the C-terminal domain PrP(126-231)**

Several studies suggest other Cu binding sites within the folded C-terminal domain of PrP (**Figure 16**). Experiments using a series of His/Ser mutants of the C-terminal histidines attempted to identify which specific histidine is involved in protein conformational changes. Only the EPR spectrum of the H187S mutant had an altered signal, but this result is not certain yet, since the presence of aggregation in the investigated sample could interfere with accurate analysis (Cereghetti et al., 2003).

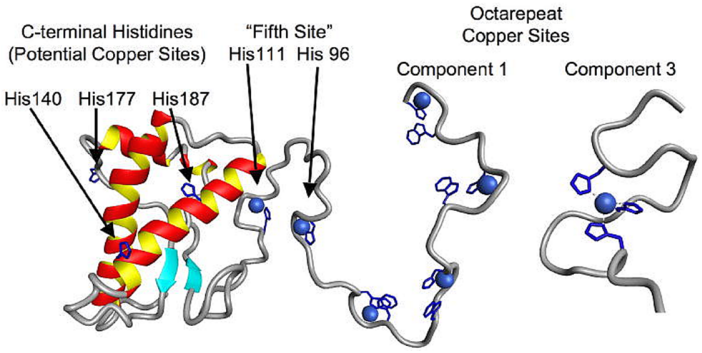

Figure 16. Model representing copper binding sites in the human prion protein. The model on the left shows the N-terminal region at full copper occupancy, as well as the locations of histidines in the globular C-terminal domain. The model on the far right shows the octarepeat region binding in component 3 (low copper occupancy, high affinity, multi-histidine mode). Adapted from (Walter et al., 2009).

5.2. Role of copper in functions and pathogenesis of the prion protein

- **Role of copper in prion protein function**

PrP^C endocytosis transports Cu from the extracellular space to the cell interior (Burns et al., 2002; Pauly and Harris, 1998; Rachidi et al., 2003; Waggoner et al., 2000; Whittal et al., 2000). PrP^C may act as a Cu transporter (Urso et al., 2010, 2012) or perhaps as a Cu chelator, preventing Cu from participating in redox reactions that generate reactive oxygen species (ROS) which are toxic to cells, especially neuronal cells (Miura et al., 2005). PrP^C is also implicated in Cu buffering (Millhauser, 2004), sensing (Vassallo and Herms, 2003), signal transduction (Mouillet-Richard et al., 2000), anti-apoptosis (Roucou et al., 2004) and neuron development (Kanaani et al., 2005). Furthermore, Hornshaw *et al.* (Hornshaw et al., 1995) noted that the Cu binding to PrP^C leads to a conformational change of the protein structure, whose functions are still argued.

(a) Endocytosis

Cu can stimulate the endocytosis of PrP^C into the endosome and portions of the Golgi (Brown and Harris, 2003). Elimination of the OR results in less efficient rates of PrP endocytosis (Pauly and Harris, 1998). Recombinant PrP, in which the histidine residues in the repeat segments are removed, is poorly endocytosed when exposed to Cu. This suggests that it is the binding of metal that induces the

endocytosis rather than another protein that indirectly controls endocytosis (Brown et al., 1999; Jackson et al., 2001). Insertions of extra OR from four to nine more ORs, such as those found in familial CJD (Goldfarb et al., 1991), abolished the endocytosis activity of the protein. The authors concluded that the ORs, not any other Cu-binding site, are critical for Cu-induced endocytosis of PrP^C. The ORs do not bind Cu ions independently but rather cooperatively; additional copies of the repeat region inhibit the Cu-binding endocytosis of PrP^C and may inhibit its other functions or interactions (Perera and Hooper, 2001a). PrP endocytosis transports Cu from the extracellular space to the cell interior (Burns et al., 2002; Pauly and Harris, 1998; Whittal et al., 2000). There may be a pH-dependent process for PrP^C to detect Cu in the extracellular matrix or to release Cu in the endosome (Burns et al., 2002; Miura et al., 1999). Such a mechanism would explain the results of studies demonstrating that PrP^C protects cells from copper toxicity. In addition, the capability of Cu^{2+} to bind at pH 5.5 indicates that Cu^{2+} binding could be maintained during the cycling of PrP through acidic endosomal compartments (Shyng et al., 1993), which have been postulated to be the site of PrP^{Sc} formation (Mayer et al., 1992). It was noted that the increased PrP expression in the presence of Cu seems to be involved in the capability of Cu to induce the endocytosis of the prion protein or delay its degradation.

(b) Antioxidant activity

Several studies suggest that PrP^C can protect cells from deleterious redox activity of free Cu (Brown and Besinger, 1998; Rachidi et al., 2003). The level of Cu/Zn dismutase activity is thought to reflect Cu status in different tissues. PrP-KO mice exhibit significant increases in lipid and protein oxidation, as well as reduction of superoxide dismutase and catalase function when compared to WT-mice (Klamt et al., 2001). Restriction of Cu in the diet of animals leads to a decrease of Cu/Zn SOD activity, but addition of $CuCl_2$ restores enzyme reactivity (Harris, 1992). These findings raise the possibility that PrP^C is involved in the supply or regulation of Cu^{2+} in the brain. Moreover, PrP^C might also act as a “sink” for free Cu to reduce the generation of lethal ROS catalyzed by Cu ions. So far, the attempts at identifying SOD activity have been inconsistent. Studies with PrP-KO mice show decreased SOD activity, but do not mention increased susceptibility to oxidative stress (Brown and

Besinger, 1998; Brown et al., 1997b). Several lines of investigation have firmly established that PrP^C helps maintain the integrity of neurons. Transgenic mice lacking PrP, as they age, present widespread tissue damage, mainly through protein and lipid oxidation (Klamt et al., 2001). This suggests that PrP^C functions as a Cu buffer that helps maintain neuron integrity in the Cu-rich environment of the CNS, and somehow indicate that PrP^C increases antioxidant levels directly or indirectly. In contrast, other groups have shown that PrP does not exhibit SOD-like activity *in vivo* or *in vitro* (Hutter et al., 2003; Jones et al., 2005). However, with chemical and structural considerations, PrP localization at synapses may be part of a protective mechanism in which Cu sequestration induces deleterious redox activity during synaptic depolarization.

(c) Copper uptake

Brains from PrP-KO mice show significantly low levels of Cu as compared to those from WT mice (Brown et al., 1997b, 1998). Likewise, PrP^{Sc}-infected mice also have significantly lower levels of Cu compared to brains of WT mice (Thackray et al., 2002; Wong et al., 2001). This evidence suggests a role of the prion protein as a possible Cu transporter in the CNS. PrP^C is concentrated at presynaptic membranes (Herms et al., 1999), where neurotransmitter release drives communication between neurons. Interestingly, the presynaptic membrane is also a region of high Cu localization and flux (Hartter and Barnea, 1988; Hopt et al., 2003; Kardos et al., 1989). Cu moves from the cell interior to the synaptic space through both exocytosis and neuronal depolarization, thus, its efflux may be an obligatory event associated with vesicle fusion, leading to neurotransmitter release (Vassallo and Herms, 2003).

As mentioned above, PrP-Cu coordination, depending on different Cu concentrations, exhibits a distinct binding mode. The transition among binding modes may serve as a switch that facilitates specific cellular processes. For example, Cu concentrations in excess of 100 μM stimulate PrP endocytosis (Pauly and Harris, 1998); the transition from component 3 to component 1 coordination may be the trigger for this process. Takeuchi and colleagues (Miura et al., 2005) suggested that, once in the endosome, component 3 coordination facilitates reduction to Cu^+ as part of Cu transport to the intracellular space.

(d) Anti-apoptosis

Programmed cell death, termed apoptosis, is an essential process for regulating the number of cells in a living system. Several studies show that PrP^C has an anti-apoptotic property (Drisaldi et al., 2004; Kim et al., 2004; Roucou et al., 2004; Solforosi et al., 2004). For example, PrP^C protects against the cellular death brought on by the expression of the Doppel protein (a homolog of C-terminal PrP) (Drisaldi et al., 2004) or by serum deprivation (Kim et al., 2004). Mutagenesis experiments show that the OR domain is a required element for protection against Doppel-protein toxicity (Drisaldi et al., 2004). Thus, Cu toxicity may occur through two mechanisms, including its inherent redox activity and a lowering of the apoptosis threshold. In turn, PrP's anti-apoptotic function may arise from its ability to sense Cu at the extracellular membrane surface or to regulate the transmembrane movement of Cu.

- **Role of copper in the pathogenesis of prion diseases**

Cu has been shown to convert PrP into PK-resistant and detergent-insoluble forms under certain *in vitro* conditions (Quaglio et al., 2001). Although some of these biochemical changes are commonly associated with initial stages of PrP^{Sc} formation, additional studies have shown that Cu-induced biochemical changes were distinct and reversible. Interestingly, Cu can also modulate the PK-res of PrP^{Sc} molecules (Nishina et al., 2004). A study showed that PrP^{Sc} formed in the absence of Cu was 20 times more susceptible to PK digestion, whereas addition of Cu reinstated the normal PK-resistance. Furthermore, protein misfolding cyclic amplification (PMCA) experiments showed that PrP^{res} with Cu could propagate and form more PrP^{res} from PrP^C (Kim et al., 2005). Additional support for the role of Cu in the pathogenesis of prion diseases is that chelating Cu delays the onset of the disease (Sigurdsson et al., 2003). Constrastly, Cu was reported to inhibit formation of fibrils from recombinant PrP (Bocharova et al., 2005). In addition, previous studies have shown that copper chelation (using cuprizone) resulted in spongiform-like degeneration in mouse brains (Blakemore, 1972; Kimberlin and Millson, 1976). Of note, homeostatic balance of Cu in the CNS is crucial for its functioning, and the pathogenesis of prion disease. However, it is not well establsihed how PrP- Cu interplays in PrP^C functions and in the conversion of PrP^C to PrP^{Sc}.

The OR segment is unstructured without Cu (Viles et al., 1999), but PrP^{C} can adopt a new conformation when bound to Cu, which is restricted to the N-terminal region (Wong et al., 2000). This shows that Cu-binding to PrP^{C} causes a physical change in the protein that is related to its functionality (Brown and Harris, 2003). There are several differing views about conformational changes in PrP^{C} when it binds to Cu. One study found that the binding of Cu^{2+} to the OR propagates an α-helical structure (Miura et al., 1996) based on the fact that correct incorporation of Cu into recombinant PrP^{C} stabilizes the protein and makes it more soluble (Daniels and Brown, 2002). Another study showed that PrP^{C} bound with Cu tends to shift from an α-helical secondary structure to a β-sheet aggregate (Stöckel et al., 1998b). This shift arises from the fact that each Cu^{2+}-HGGGW segment on the OR is separated by a Gly-Gln-Pro link, in which the Gly and Pro molecules are associated with β-turns (Aronoff-Spencer et al., 2000), and the conformational change that occurs when Cu^{2+} binds to the repeat segment is expected to be a β-turn (Bonomo et al., 2000). It is evident that Cu contributes to the conformation of PrP^{C}, but Viles *et al.* (Viles et al., 1999) found it was only in turns and structured loops, as opposed to α-helices or β-sheets, as other studies mentioned. These authors supposed that the competitive results arose from different buffer and OR segments used for Cu binding.

In addition to proposed conformational changes and stabilization in the protein secondary and tertiary structures (Gustiananda et al., 2002), Cu-binding can also cause the protein to acquire other PrP^{Sc}-like properties. Incubation of recombinant PrP with Cu^{2+} generated a PK-resistant PrP that formed aggregates. This transformation to the recombinant PrP fragment needed no acidic pH, denaturants or reduction agents (Qin et al., 2000). Other studies show that in the presence of Cu, PrP^{Sc} brain denatured abnormally and regained PK-resistance (McKenzie et al., 1998). PrP106-126 aggregation and fibril formation was restored in the presence of Cu^{2+}, indicating that Cu binding to PrP106-126 may cause the peptide to interact with PrP^{C} (Jobling et al., 2001). Notably, studies using PrP^{C} extracted from transgenic mice and recombinant PrP show that Cu causes these proteins to adopt a PK-resistant and detergent-insoluble form, similar to, but structurally different from PrP^{Sc}.

Human prion diseases may arise not only as a consequence of transmission, but also of mutations in the *Prnp* gene. In addition to about 20 different point mutations, there are also deletions or insertions of a stretch of octarepeats in the amino-proximal region of PrP, suggesting that this region might be important for the spontaneous conversion of the prion protein. A question is raised whether the OR region of PrP is essential for sustaining prion replication and scrapie.

(a) Octapeptide repeat deletion

PrP-KO mice develop and behave normally (Büeler et al., 1992) but are resistant to prion disease. Introduction of the *Prnp* gene into such mice restores susceptibility to scrapie (Fischer et al., 1996), thus demonstrating the essential role of PrP^{C} in developing prion diseasesb. Studies on cell models showed that mutant PrP lacking all five ORs or with only one OR was still efficiently converted into PrP^{Sc} in scrapie-infected neuroblastoma cells despite the lack of the copper binding motif (Hiraga et al., 2009; Rogers et al., 1993). Indeed, Fischer *et al.* (Fischer et al., 1996) showed that in PrP-KO mice overexpression of truncated PrP with a deletion of codons 32–80, which retains only one of the five ORs, still sustained replication of the infectious agent and development of disease. They also showed that PrP with a deletion of codons 32–93 and thus devoid of all five ORs, also efficiently restores susceptibility to scrapie in PrP-KO mice. All animals succumbed to scrapie-like disease, showing that the truncated PrP was competent in this regard. However, incubation times to first symptoms and to terminal stage of disease were longer than for WT controls (Flechsig et al., 2000). While in WT mice accumulation of prions and PrP^{Sc} is followed within weeks by clinical symptoms and death (Büeler et al., 1994), the prion titers in the brains and spleens of mice expressing PrP devoid of all five ORs (PrPΔ32–93) were lower at all stages of the disease. Interestingly, while PrP devoid of the ORs sustains scrapie-like disease in response to scrapie, no typical histo-pathological changes were detected in the brain but neuronal loss and astrogliosis were noticed in the cervical spinal cord (Flechsig et al., 2000). In 2008, Sakudo *et al.* (Sakudo et al., 2008) evaluated the PrP^{Sc} level in HpL3-4, a *Prnp* gene-deficient cell line expressing various deletion mutants of PrP^{C} after prion infection, to identify whether specific regions of PrP^{C} for the production of PrP^{Sc} exist. They

suggested that removal of the OR abolished the ability to produce PrP^{Sc}, while the full-length PrP^{C} leads to the production of PrP^{Sc} at an early stage (Sakudo et al., 2008).

(b) Octapeptide repeat insertion

Insertions of one to nine extra ORs, resulting in the expansion of the N-terminal domain, cause CJD and GSS in human. Interestingly, there is a correlation between the number of inserted ORs and progression and onset age of the disease (Campbell et al., 1996). With one to four extra ORs, the average onset age is 64 years, whereas five to nine extra ORs result in an average onset age of 38 years. OR expansions alter the properties of PrP and its interactions with cellular components. When expressed in various cell lines, PrP with additional repeats displays detergent-insolubility, resistance to PK digestion similar to PrP^{Sc} (Lehmann and Harris, 1996), altered cell surface expression (Priola and Chesebro, 1998), and hindered export to the cell surface (Ivanova et al., 2001). Similar effects can be observed in transgenic mice with OR expansion (Chiesa et al., 1998, 2000). Moreover, recombinant protein containing insert mutations forms amyloid fibrils faster than WT (Moore et al., 1999).

The WT-PrP with four repeats responds to increasing copper concentrations by transitioning from component 3 to component 1 coordination. However, for eight repeat segments (four inserts beyond WT) and beyond, this transition is significantly inhibited (**Figure 17**). Eight total repeats allow for two equivalents of component 3 coordination and exhibit an approximate 10-fold increase in Cu^{2+} binding affinity. This affinity shift contributes to the decrease in component 1 coordination for OR domains with four or more inserts beyond WT (Stevens et al., 2009).

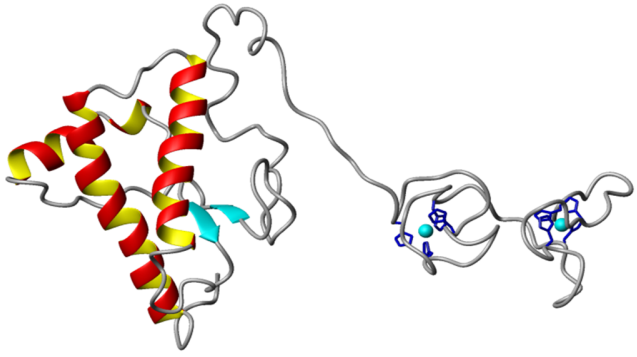

Figure 17. Three-dimensional model of the prion protein with eight total repeats (four inserts) coordinated to two equivalents of Cu^{2+} in the component 3 mode. (N-terminal

residues 23–59 are not shown.) Results presented here demonstrate that this structure is persistent and, in contrast to wild-type PrP, resists transitioning to component 1 coordination. Adapted from (Stevens et al., 2009).

Taken together, these findings demonstrate a very strong relationship between changes in copper binding properties and early-onset prion disease. Although the OR domain is not part of the protease resistant scrapie particles, it nevertheless modulates disease progression. The role of the OR in prion disease is enigmatic. It is postulated that the OR, which binds Cu through histidine residues, is not essential for sustaining prion replication and disease but does affect the level of prion accumulation and pathogenesis in the brain and regulate the ability to produce PrP^{Sc} at an early stage. However, it remains unclear whether these activities of PrP^{C} are the result of Cu-binding, and which residues of the OR are relevant to PrP^{Sc} production. Several aspects of Cu binding likely help explain these divergent results. The non-OR involving His95 is in the region of PrP that typically remains after proteolytic cleavage, liberating amyloidogenic, C-terminal PrP^{Sc}. Thus, Cu may modulate PrP^{Sc} formation even in the absence of the ORs, as shown by Cox *et al*. (Cox et al., 2006). Despite the contradictory arguments regarding the actual role of Cu in prion diseases, there is evidently strong agreement that Cu has a crucial function in prion protein aggregation, and the PrP-Cu relationship is still the focus of ongoing research.

II. AIM OF THE STUDY

My study aims to elucidate the potential role of copper binding sites in prion replication and propagation through the following steps:

- Generate a library of histidine/tyrosine substitutions in murine PrP coding sequence in eukaryotic expressing vector
- Analyze the biochemical properties and the distribution of murine PrP mutants in cell model
- Investigate the kinetics of mutant protein (His95Tyr) by using fibrillization assay

III. MATERIALS AND METHODS

3.1. Plasmid constructions

The open reading frame (ORF) encoding for the pre-pro MoPrP from residue 1 to 254 was amplified by PCR from genomic murine DNA and cloned by restriction free methods (van den Ent and Löwe, 2006) in pcDNA3.1(-) (Invitrogen). The 3F4-epitope tag (residues 108-111, LKHV) as well as the single point mutations (H60Y, H68Y, H76Y, H84Y and H95Y) were inserted into the pcDNA3.1::MoPrP(1-254) using the Quick Change site-directed mutagenesis kit (Stratagene). Histidine residues in the OR and non-OR regions were also named H1 to H5. The introduction of 3F4-epitope tag into MoPrP constructs made it possible to distinguish mutant PrP and endogenous PrP using the monoclonal antibody 3F4 (Kaneko et al., 1997b; Kascsak et al., 1987).

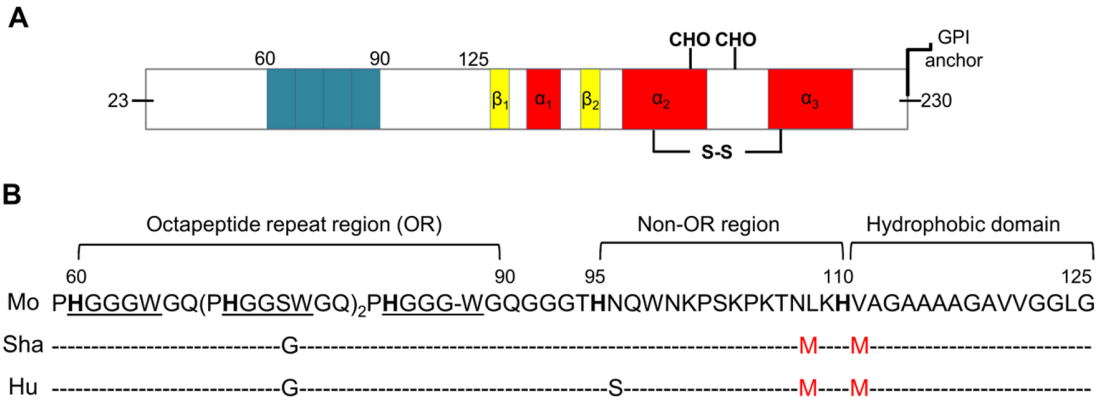

Figure 18. Schematic secondary structure representation of mature full-length MoPrP. **(A)** The unstructured N-terminal portion includes the octapeptide repeat domain (OR, highlighted in blue, residues 59-90) and the non-OR copper binding sites. The C-terminal domain (residues 128-230) encompasses two short β-strands and three α-helices with a disulfide bond (S-S), two N-linked glycosylation sites, and a GPI moiety anchor. **(B)** Comparison of amino acid sequence (residues 59 to 125) including the OR and non-OR regions of mouse (Mo), Syrian hamster (SHa) and human (Hu) PrPs. The 3F4-epitope specific for SHa and Hu PrPs is highlighted in red.

Primer	FORWARD PRIMER	REVERSE PRIMER
H60Y	CAGCCCTACGGTGGTGGCTGGGGACAA	TTGTCCCCAGCCACCACCGTAGGGCTG
H68Y	GGGGACAACCCTATGGGGGCAGCTGG	CCAGCTGCCCCCATAGGGTTGTCCCC
H76Y	AGCTGGGGACAACCTTATGGTGGTAGTTGGG	CCCAACTACCACCATAAGGTTGTCCCCAGCT
H84Y	TGGGGTCAGCCCTATGGCGGTGGATGG	CCATCCACCGCCATAGGGCTGACCCCA
H95Y	CAAGGAGGGGGTACCTATAATCAGTGGAACAAGC	GCTTGTTCCACTGATTATAGGTACCCCCTCCTTG

Table 3. Pairs of primers used for His/Tyr mutations.

3.2. Cell culture and transfection

Mouse neuroblastoma (N2a) cells, and scrpaie neuroblastoma (ScN2a) cells chronically infected with RML prion were cultivated in Opti-MEM medium (Gibco) supplemented with 10% FBS and penicillin-streptomycin (100 IU/mL penicillin and 100 mg/mL streptomycin). All cell lines were grown in a humidified incubator at 37°C with 5% CO_2.

Cells were transfected with X-treme gene DNA transfection reagent (Roche Biochemicals) according to the manufacturer directions. The amounts of cells, DNA and transfection reagents were chosen by preliminary experiments to ensure a modest level of transfection in most experiments, and analyzed 72 h later.

3.3. Protein extraction

Cells were washed once with cold phosphate-buffered saline (PBS), harvested in cold cell lysis buffer (10 mM TrisHCl pH 8.0, 150 mM NaCl, 0.5% Nonidet P-40 substitute, 0.5% sodium deoxycholate), centrifuged at 2,000 rpm at RT for 5 min, quantified by BCA protein assay kit (Pierce) and stored at -20^{o}C until use.

pcDNA 3.1 MoPrP (1-254), L108M,V111M	
1.	H60Y
2.	H68Y
3.	H76Y
4.	H84Y
5.	H95Y
6.	H12/ Y12
7.	H13/ Y13
8.	H14/ Y14
9.	H15/ Y15
10.	H23/ Y23
11.	H24/ Y24
12.	H25/ Y25
13.	H34/ Y34
14.	H35/ Y35
15.	H45/ Y45
16.	H123/ Y123
17.	H124/ Y124
18.	H125/ Y125
19.	H134/ Y134
20.	H135/ Y135
21.	H145/ Y 145
22.	H234/ Y234
23.	H235/ Y235
24.	H345/ Y345
25.	H1234/ Y1234
26.	H1235/ Y1235
27.	H1245/ Y1245
28.	H1345/ Y1345
29.	H2345/ Y2345
30.	H12345/ Y12345
31.	Wild-type

Table 4. Histidine/tyrosine MoPrP with 3F4-tag constructs in *pcDNA 3.1(-)*

3.4. PrP^{Sc} detection by immunoblot

For protease-K (PK) digestion assay, 500 µg of protein was treated with 20 µg/mL PK (Roche, ratio protein: PK = 50:1, w/w) for 1 h at 37°C. Digestion was stopped by adding phenylmethyl-sulphonyl fluoride (PMSF) to a final concentration of 2 mM. Then, samples were ultracentrifuged at 55,000 rpm (Optima TL, Beckman) for 1 h at 4°C and resuspended in loading buffer. Samples were loaded onto a 10% SDS-PAGE and transferred on nitrocellulose membranes. Membranes were blocked with 5% (w/v) non-fat milk protein in TBS-T (0.05% Tween) for 2 h at RT, incubated with anti-PrP antibodies D18 mAb (1:1,000, InPro Biotechnology) or 3F4 (1:10,000, Covance) in blocking buffer for 2 h at RT or O/N at 4°C, prior to 1-hour incubation in the secondary HRP-conjugated antibodies (1:5,000, Pierce). The signals were

visualized using enhanced chemiluminescence (GE Healthcare) and acquired on the UVI software (UVITEC, Cambridge).

3.5. Endo-H and PNGase-F digestion

Fifty μg of total protein was denatured in 1× glycoprotein denaturing buffer (0.5% SDS, 1% β-mercaptoethanol; New England Biolabs) at 100°C for 10 min prior to incubation with Endo-H and PNGase-F (250,000 units/ml; New England Biolabs) in 1% Nonidet 40 and 1× G5 or G7 reaction buffer (New England Biolabs) at 37°C for 16 h. The reaction was terminated by adding an equal amount of 2×loading buffer and boiling to 100 °C for 2 min.

3.6. Stability to protease treatment

N2a cells were transiently transfected with the constructs and harvested as previously described. In order to evaluate the stability of the H95Y mutant to PK treatment according to concentration and incubation time, 250 μg of protein was treated with different concentrations of PK (from 1 to 15 μg/mL of PK) for 30 min at 25°C, or incubated with 2 μg/mL PK for different times (10-20-30-60 min) at 25°C. The reaction was stopped and precipitated as previously described.

3.7. Immunofluorescence imaging

Common protocol for the detection of PrP and organelles

Cells were grown on poly-L-lysine coated coverslips for 24 h before fixation with 4% paraformaldehyde (PFA) in phosphate-buffered saline (PBS) for 20 min at RT. Subsequently, cells were washed with PBS prior blocking in 10% FBS, 0.3% Triton X-100 diluted in PBS for 1 h at RT. After blocking, cells were incubated at 4°C O/N with primary antibody in dilution buffer (1% FBS in PBS with 0.3% Triton X-100). The next day, coverslips were washed 2 times in PBS and given an additional washing in high-salt PBS for 2 min to decrease the unspecific binding of the antibody. After one more washing with PBS, cells were incubated for 1 h at RT in the dark with secondary antibody conjugated with AlexaFluor (1:500; Invitrogen) in dilution buffer. Cells were further washed before mounting on Vectashield with DAPI (VECTOR Laboratories). Images were acquired with a DMIR2 confocal microscope equipped with Leica Confocal Software (Leica). Primary antibodies used to detect PrP are D18 mAb for endogenous MoPrPs, and 3F4 mAb for transfected MoPrPs. All

organelle markers were purchased from Abcam, as were the ER marker (anti-Calnexin), the early endosome marker (anti-EEA1), the recycling endosome (anti-Transferrin receptor Tfn), the late endosome marker (anti-Mannose-6 phosphate receptor M6PR) and the lysosome marker (anti-LAMP2). Secondary antibodies were goat anti-human, goat anti-mouse, goat anti-rabbit, donkey anti-rat conjugated with AlexaFluor-488 or -594, in accordance with manufacturer's guidelines.

Surface staining

Cells were placed on ice for 15 min then stained with Opti-MEM containing anti-PrP 3F4 mAb (1:1000) for 20 min. After the fixation, cells were washed with PBS for 3 times to remove residual fixative. Finally, cells were incubated with fluorescence-conjugated secondary antibody without permeabilization.

Endocytosis imaging

Cells were surface-labeled on ice with anti-PrP 3F4 mAb in Opti-MEM, and returned to 37°C for 1 h to induce PrP internalization. Later, cells were washed twice with PBS, treated with 0.5% trypsin on ice for 90 sec to remove surface proteins, and fixed for 20 min at RT in 4% PFA. Cells were permeabilized with 0.2% Triton X-100 for 5 min at RT, blocked for 1 h in 2% FBS in PBS, and stained with AlexaFluor-488 anti-mouse antibody for 1 h. Finally, coverslips were washed with PBS for 3-4 times and mounted on glass (Westergard et al., 2011).

Thioflavin-S (ThS) staining

For ThS staining to detect aggregates, transfected cells were fixed with 4% PFA/4% sucrose/1% Triton X-100 in PBS. Subsequently, fixed cells were incubated with 0.025% ThS (Sigma) for 8 min and washed three times with 80% ethanol, once with double-distilled water and once with PBS, 5 min for each wash, before the antibody incubations (Ostrerova-Golts et al., 2000; Volpicelli-Daley et al., 2011).

Assay for the detection of PrP^{Sc}

Fixed transfected cells were incubated with PK (20µg/ml) for 15 min at 37ºC. Digestion was stopped with 2 mM PMSF for 15 min at RT. The cells were then denatured with 6 M GdnHCl for 10 min (Veith et al., 2009a). After some washes, cells were blocked in 10% FBS, 0.1% Triton X-100 diluted in PBS for 2 h at RT, incubated with antibodies as previously described.

3.8. Protein expression and purification

The plasmid pET-11d (Novagen) encoding for the full-length MoPrP (residues 23-230) was kindly provided by Dr. J.R. Requena (University of Santiago de Compostela, Santiago de Compostela, Spain). The H95Y mutation was inserted into the pET-11a::MoPrP using the Quick Change site-directed mutagenesis kit (Stratagene). An overnight culture of *E. coli* BL21 (DE3) (Novagen) freshly transformed with the plasmid was added at 37°C to 2 L of LB. Cells were grown in a 2 L fermenter system (Sartorius), harvested after 24 h and lysed by homogenizer (Panda plus, GEA Niro Soavi). Inclusion bodies were washed and solubilized according to (Ilc et al., 2010). MoPrP was purified using its octapeptide repeat sequence as natural affinity tag for nickel or copper. MoPrP was loaded onto a 5-mL HisTrap column (GE Healthcare) equilibrated in binding buffer (2 M GdnHCl, 500 mM NaCl, 20 mM Tris, pH 8) and eluted with 500 mM imidazole. Subsequently, the protein was purified by size exclusion chromatography (HiLoad 26/600 SUPERDEX 200 PG column, GE) and eluted in buffer 25 mM Tris, 6 M GdnHCl, 5 mM EDTA, pH 8. The purified protein was buffer exchanged against acetate buffer (25 mM NaOAc, 6 M GdnHCl, pH 5) or Tris buffer (25 mM Tris-HCl, 6 M GdnHCl, pH 7).

3.9. Preparation of scrapie cell lysate seed by sodium phosphotungstic acid

One mg of ScN2a cell lysate in 500 µl was used to precipitate prions (Ai Tran et al., 2010). Samples were incubated with 500 µl of PBS/4% sarkosyl/protease inhibitor and sodium phosphotungstic acid **(**PTA, Sigma) at final concentration of 0.5%, with constant shaking (350 rpm) for 1 h at 37°C. After the incubation, samples were centrifuged at 13,200 rpm for 30 min at RT. Then, we washed the pellet with 500 µl of PBS/2% Sarkosyl/protease inhibitor and centrifuged it again at 13,200 rpm for 30 min at RT. The pellet was resuspended in 150 µl of water and stored at −80°C until use. The PTA pellet was denatured in 2 M GdnHCl for 2 h at RT. Ten µl of denatured PTA pellet and 90 µl of PBS/BSA were added to each well of a 96-well ELISA plate coated with anti-PrP 3F4 antibody. The plate was incubated O/N at 4°C, washed three times with TBS-T, and 100 µl of the antibody-enzyme conjugate HRP was added per well. After 1 h incubation at RT, the plate was washed seven times

with TBS-T and developed with 100 µl of ABTS (KPLM). Absorbance was measured at 405 nm to determine soluble PrP in each well relative to the recombinant PrP ladder. Each assay was performed in duplication of 4 wells.

3.10. Monitoring the kinetics of *in vitro* amyloid formation

Lyophilized recMoPrP WT and recMoPrP H95Y were dissolved in 6 M GdnHCl with a protein concentration of 5mg/ml and stored at −80°C until use. A final protein concentration of 100 µg/ml was incubated in PBS buffer (pH 7) or in acetate buffer (pH 5), GdnHCl, and 10 µM ThT in a reaction volume of 200 µl per well in 96-well plates (BD Falcon 353945; BD Biosciences). One 3-mm glass bead (Fisher Scientific) was added to each well to increase agitation.

For amyloid seeding experiments, resuspended PTA pellets were quantified by Western blot, diluted in water and re-confirm by Westeren blot and ELISA to ensure the same amount of PrP^{Sc} seeds in all reactions. PrP^{Sc} seed was added to each well for a final volume of 200 µl. Samples were normally run with four replicates. The 96-well plates were covered with sealing tape (235307; Fisher Scientific) and incubated at 37°C with continuous shaking on a plate reader (SpectraMax M5 fluorescence plate readers; Molecular Devices). The kinetics of fibril formation was monitored by bottom reading of ThT fluorescence intensity every 5 min by using 444-nm excitation and 485-nm emission filters.

3.11. *De novo* prion formation in N2a cells

N2a cells were transiently transfected with either 3F4-tagged WT or H95Y MoPrP and regularly passaged every 7 days up to passage (P) 8. Subsequently, the protein extracts were analyzed by PK digestion to monitor the presence of PK-resistant PrP^{Sc} levels through passages. Additionally, the *de novo* prion formation was assessed by cells seeding experiments. PTA-extracted PrP^{Sc} from transfected N2a cells were inoculated into N2a cells and regularly passaged every 7 days up to P8. The PrP^{Sc} detection was assessed by PK digestion as previously described.

3.12. Cell viability

Cells were seeded in a 96-well tissue culture plate one day before transfection and then transiently transfected with MoPrP constructs. Seventy-two hours after the transfection, the medium was removed and the cells were incubated with 200 µL of

MTT (Sigma) working solution (5 mg/mL of MTT in sterile PBS) for 4 h at 37°C. Cell viability was assessed by the conversion of MTT (yellow) to a formazan product (purple). The solution was removed and formazan products were dissolved by adding 200 μL of DMSO to each well. The optical density was read at 570 nm and the background subtracted at 690 nm using a VersaMax plate reader (Molecular Device). Each assay was performed in duplication of 4 wells.

Statistical analysis

Two-sample *t* tests were used for statistical analysis of the data. Differences were considered significant when $p<0.05$. Data were analyzed using Origin 8.6 software.

IV. RESULTS

4.1. The non-OR H95Y mutant promotes prion conversion

To investigate the effect of His residues on prion replication, ScN2a cells were transiently transfected with 3F4-tagged wild-type (WT_{3F4}) and $MoPrP^{C}$ constructs where the His located inside the OR and non-OR were substituted by Tyr (hereafter designated as H60Y, H68Y, H76Y, H84Y and H95Y mutations). The introduction of the 3F4-epitope tag into these constructs does not affect cell viability **(Figure S1)** but allows the discrimination between transfected MoPrPs and endogenous $MoPrP^{C}$ (Kaneko et al., 1997b; Kascsak et al., 1987; Taraboulos et al., 1990) **(Figure S2 A and S2 B)**. The effect of the H110Y mutant was not considered in this study as it is located inside the 3F4-epitope, thus precluding the detection by the anti-PrP 3F4 mAb. His to Tyr substitutions in $MoPrP^{C}$ constructs did not affect the total PrP expression levels **(Figure 19 A)**. Conversely, the PK-digestion profiles showed remarkably different PrP^{Sc} levels among the mutants. While WT_{3F4} and H60Y, H68Y, H76Y, H84Y displayed similar PK-resistant PrP^{Sc} levels, the non-OR $H95Y_{3F4}$ mutant yielded in a significantly higher PrP^{Sc} signal, providing the first evidence of this mutation role in affecting prion replication (**Figure 19 B and 19 C,** $**p=0.003$). The higher PrP^{Sc} level of H95Y-expressing ScN2a cells was re-confirmed by ELISA analysis (**Figure 19 D**, $***p = 5*10^{-5}$).

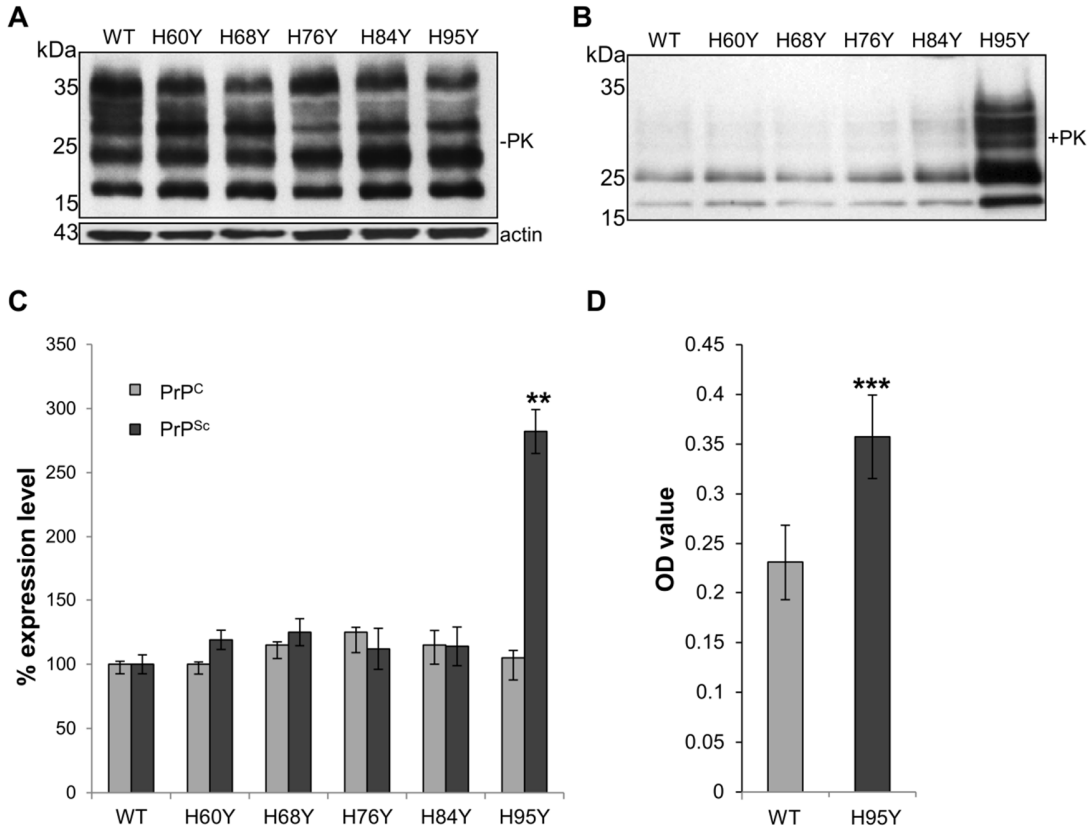

Figure 19. The non-OR H95Y mutation promotes prion conversion. (A) Fifty µg of undigested lysates from ScN2a cells expressing 3F4-tagged WT and mutated PrPs was applied to each lane. β-actin was used as internal control. **(B)** Five hundred µg of cell lysates was digested with PK (20 µg/mL) at 37°C for 1 h. PrPs were detected by anti-PrP 3F4 mAb. **(C)** Quantitative analysis of PrP expression (PrP^{C}) and PrP^{Sc} PK-resistance levels (PrP^{Sc}) in transfected constructs. **(D)** ELISA signal densities analysis of PrP^{Sc} levels (n = 4, $^{**}p < 0.005$, $^{***}p < 0.0005$).

4.2. H95Y-derived PrP^{Sc} accelerates prion polymerization in the amyloid seeding assay (ASA)

Prion diseases are caused by misfolded proteins. Alternatively folded proteins can adopt a β-sheet rich conformation that facilitates polymerization into amyloid fibers. After observing that the $H95Y_{3F4}$ mutant significantly affects PrP^{Sc} level in transiently expressing ScN2a cells, we reasoned whether chemically purified PrP^{Sc} from these cells may promote the amyloid formation of WT recombinant full-length MoPrP without 3F4-tag (WT_recMoPrP). In these experiments, we compared the kinetics of WT_recMoPrP fibrillizations seeded by either PrP^{Sc} extracted from ScN2a cells expressing 3F4-tagged WT MoPrP (WT_{3F4}_PrP^{Sc} seed) or PrP^{Sc} purified from ScN2a cells expressing the 3F4-tagged H95Y mutant ($H95Y_{3F4}$_PrP^{Sc} seed). PrP^{Sc} seeds purified using phosphotungstate (PTA) precipitation (Colby et al., 2007) were added into the reactions containing WT_recMoPrP as substrate, 2M GdnHCl, at two different pH values (neutral and acidic pH) under continuous shaking for 72 h. Using chaotropic agent Gdn at this concentration has been demonstrated to facilitate aggregation efficiency (Polano et al., 2009). *In vitro*, the kinetics of amyloid formation usually exhibits an initial lag phase, in which no detectable amyloid forms, whereas monomers nucleate to form fibrils. Monomeric molecules adopt partially denatured conformations which assemble into multimeric species. The kinetic profiles of amyloid fibril formation was obtained by measuring changes in Thioflavin-T (ThT) fluorescence intensity. This dye is a highly sensitive indicator and is used as a marker for newly generated amyloid structural motives (Rogers, 1965). Sigmoidal kinetic profiles typical for amyloid formation were obtained for both WT and H95Y_PrP^{Sc} seeds at two pH values (**Figure 20**). Differently from the WT_{3F4}_PrP^{Sc} seed, we found that adding the $H95Y_{3F4}$_PrP^{Sc} seed significantly accelerated the fibrillization reactions. At pH 7, the lag phase of the reaction seeded by $H95Y_{3F4}$_PrP^{Sc} was shorter (25.8 ± 4.7 hrs) than that seeded by WT_{3F4}_PrP^{Sc} (37.5 ± 5 hrs) (**Figure 20 A and 20 B**). The same effect was obtained at pH 5: $H95Y_{3F4}$_PrP^{Sc} reduced the lag phase to 20.4 ± 3.8 hrs, whereas in the presence of WT_{3F4}_PrP^{Sc} the fibrillization reaction started later (29 ± 2.5 hrs) (**Figure 20 C and 20 D**). Interestingly, at acidic pH the lag phase was shortened by 20% compared to neutral pH for both

fibrillization reactions seeded by H95Y$_{3F4}$_PrP^{Sc} and WT$_{3F4}$_PrP^{Sc}. This observation is in agreement with previous cell biological studies indicating that acidic condition as likely environment facilitating conformational conversion (Borchelt et al., 1992; Cruite et al., 2011; Taraboulos et al., 1990). We also noted that reactions performed with H95Y$_{3F4}$_PrP^{Sc} seed always exhibited higher ThT signals (**Figure 20 A and 20 C**).

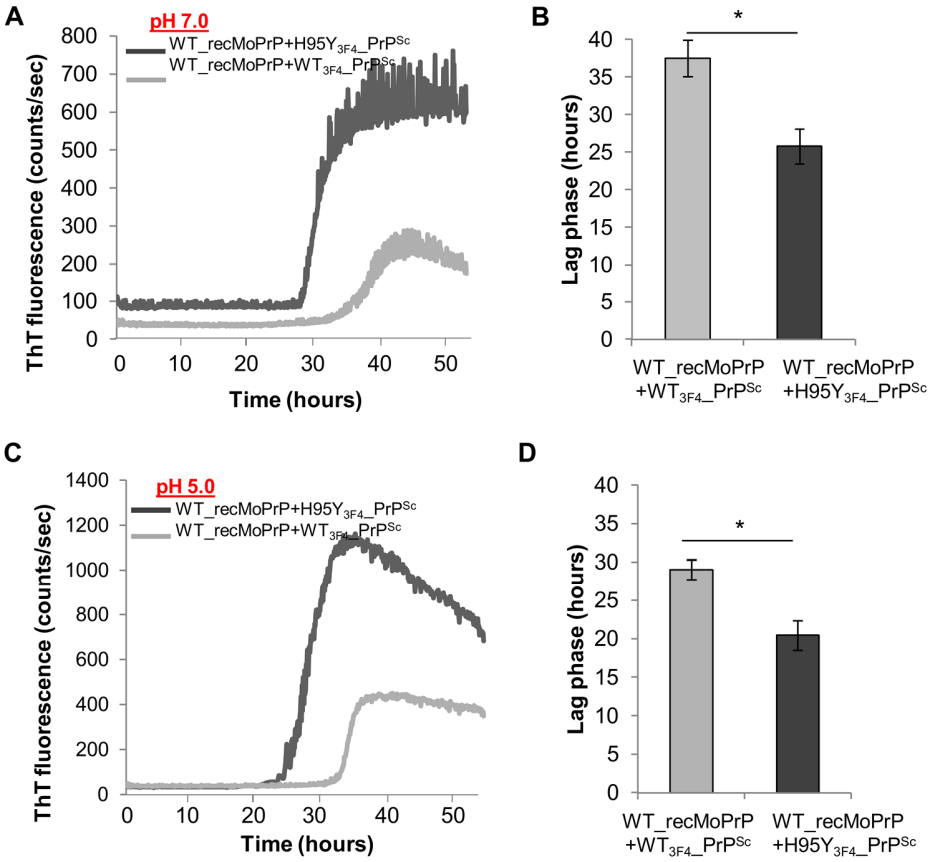

Figure 20. **H95Y-derived PrP^{Sc} accelerates prion polymerization in the amyloid seeding assay (ASA).** H95Y$_{3F4}$_PrP^{Sc} significantly reduced the lag phases at both pH conditions and exhibited higher ThT signals, as compared to WT$_{3F4}$_PrP^{Sc} (Student's *t* test, *$p \leq 0.05$, n=4)). ASA of WT_recMoPrP seeded by 3F4-tagged WT PrP^{Sc} (WT$_{3F4}$_PrP^{Sc}) and H95Y PrP^{Sc} (H95Y$_{3F4}$_PrP^{Sc}) at pH 7 **(A)** and at pH 5 **(C)**. Mean values of the lag phases (in hours) for ASA are shown at the two pH values **(B and D)** (*p<0.05, n=4)

4.3. The H95Y mutant displayed PK-resistance when expressed in N2a cells

The enhanced resistance to protease digestion is a primary feature to discriminate between PrP^{C} and PrP^{Sc} (Caughey et al., 1990; McKinley et al., 1983). Since the transient expression of the $H95Y_{3F4}$ mutant in ScN2a resulted in higher PK-resistant PrP^{Sc} signal, we reasoned whether the same result would be observed also in non-infected N2a cells expressing the same mutant construct. N2a cells were transiently transfected with WT_{3F4} or the $H95Y_{3F4}$ mutant, and treated under different PK conditions. Interestingly, at low PK concentration (2 μg/mL) an immunoreactive PrP signal was visible in the cell lysate of N2a expressing $H95Y_{3F4}$ mutant, whereas in the cell expressing WT_{3F4} PrP^{C}, no signals were detectable at either 2 or 5 μg/mL of PK treatments (**Figure 21 A**).

To gain detailed insights into the PK-resistant profile of the $H95Y_{3F4}$ mutant, we further assessed its stability according to a wide range of PK concentrations and time-dependent PK reactions. The digestion was performed at 25°C instead of 37°C in order to better monitor PK-resistance levels. Cell lysates of N2a transient expressing WT_{3F4} and the $H95Y_{3F4}$ mutant were treated with increasing concentrations of PK for 30 min (**Figure 21 B**); or incubated with the same concentration of PK (protein:PK 250:1, w/w) for different time periods (**Figure 21 C**). According to PK concentration, at the concentration of 2 and 15 of PK, there was no difference between WT_{3F4} and $H95Y_{3F4}$ ($p.> 0.05$). However, we found that $H95Y_{3F4}$ is significantly resistant to PK digestion than WT_{3F4} at PK concentration of 3 and 10 μg/mL ($p < 0.05$) (**Figure 21 B**). We next analyzed the stability of $H95Y_{3F4}$ compared to WT_{3F4} over time. Interestingly, PK-resistance of $H95Y_{3F4}$ were significantly higher than WT_{3F4} at all time points (**Figure 21 C**). When compared the mean PK-resistance values over PK concentration and over time, these experiments consistently confirmed the higher PK-resistant $H95Y_{3F4}$ mutant under investigated conditions.

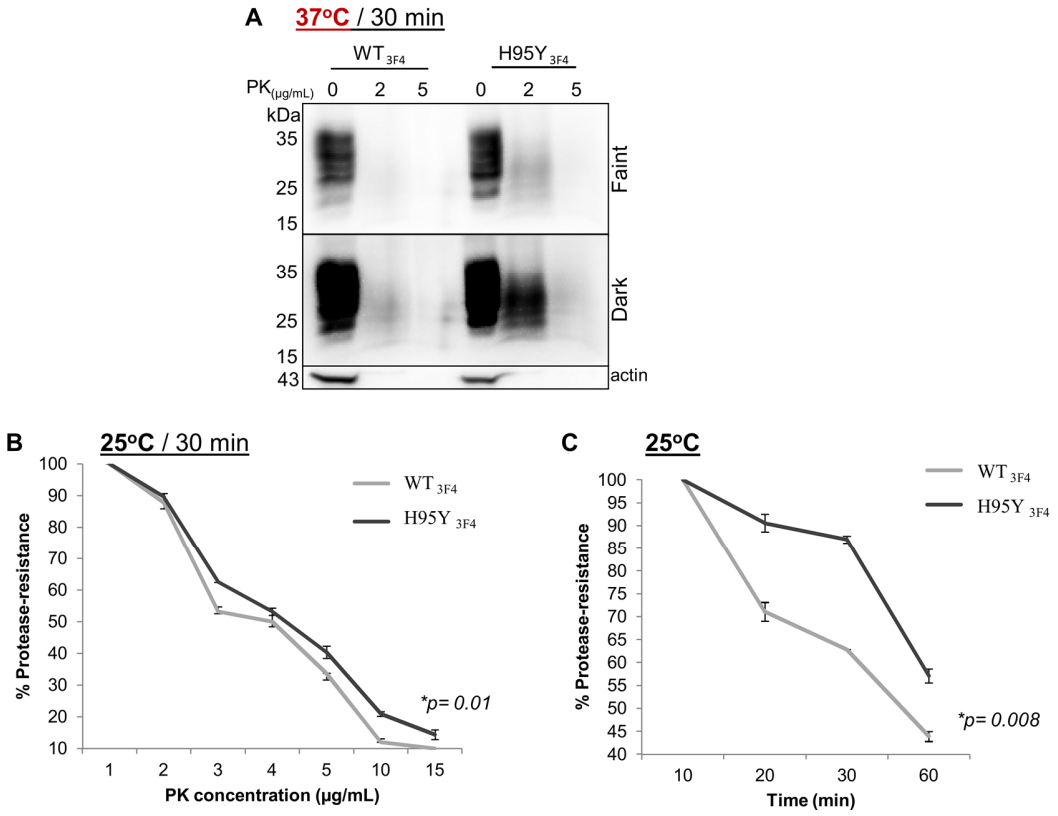

Figure 21. The H95Y mutant displayed PK-resistance when expressed in N2a cells. N2a cells were transiently expressed WT_{3F4} and $H95Y_{3F4}$ mutant. **(A)** Cell lysates were treated with 2 or 5 µg/mL of PK at 37°C for 30 min. Two exposures of the same blot are shown (Faint: 30 sec exposure; dark: 6 min exposure). PrPs were detected by anti-PrP 3F4 mAb. β-actin was used as internal control. **(B)** Lysates were digested with different concentrations of PK at 25°C for 30 min; or **(C)** treated with 2 µg/mL of PK at 25°C for different time periods. Percentages of protease-resistance levels were quantified by calculating the ratio of PK-resistance signal densities at each condition. Comparison of the mean PK-resistance values over PK concentration and over time was performed (n = 3, *p< 0.05).

4.4. The OR and non-OR mutations share similar glycosylation patterns and proteolytic features as wild-type PrP^C

To further elucidate whether the PK-resistance of the $H95Y_{3F4}$ mutant may be due to altered cellular maturation processes, we analyzed the glycosylation patterns of all 3F4-tagged $MoPrP^C$ constructs employed in our study. Western blot analysis showed that all mutation MoPrPs display the same glycosylation patterns as the WT PrP^C, migrating with three bands corresponding to the diglycosylated, monoglycosylated and unglycosylated PrP^C forms (**Figure 22 A**).

PrP^C is synthesized in the endoplasmic reticulum (ER). During its post-translational modifications, the protein undergoes the cleavage of N- and C-terminal signal peptides, the addition of *N*-linked oligosaccharide chains, disulfide bond formation and the attachment of a GPI moiety. All the processes occur through ER and Golgi apparatus, and result in the mature PrP^C embedded at the outer leaflet of the membrane *via* a GPI anchor. To better biochemically characterize mutant PrPs, we performed the deglycosylation assays using Endo-H and PNGase-F enzymes. Endo-H can only remove high-mannose oligosaccharides, whereas PNGase-F removes all types of asparagine-linked oligosaccharides. Endo-H enzyme is used for evaluating the correct protein glycosylation pattern occurring in the Golgi compartments (Maley et al., 1989). Thus, Endo-H sensitivity is considered a sign of protein immaturity, as proteins acquire Endo-H resistance upon transport to the Golgi apparatus. Immunoblotting of 3F4-tagged WT and mutant MoPrP constructs treated with Endo-H showed no difference between the WT and mutated PrP glycoforms (**Figure 22 B**). Also the treatments with the PNGase-F displayed clear unglycosylated PrP bands having the same molecular weight of WT_{3F4} full-length $MoPrP^C$, and an additional faint band of about 20 kDa —corresponding to the major C-terminal fragment of PrP^C— denoted as C2 (Liang and Kong, 2012) was also visible (**Figure 22 C**). Taken together, these data suggest that these mutant proteins were successfully processed through ER and Golgi compartments during their maturation.

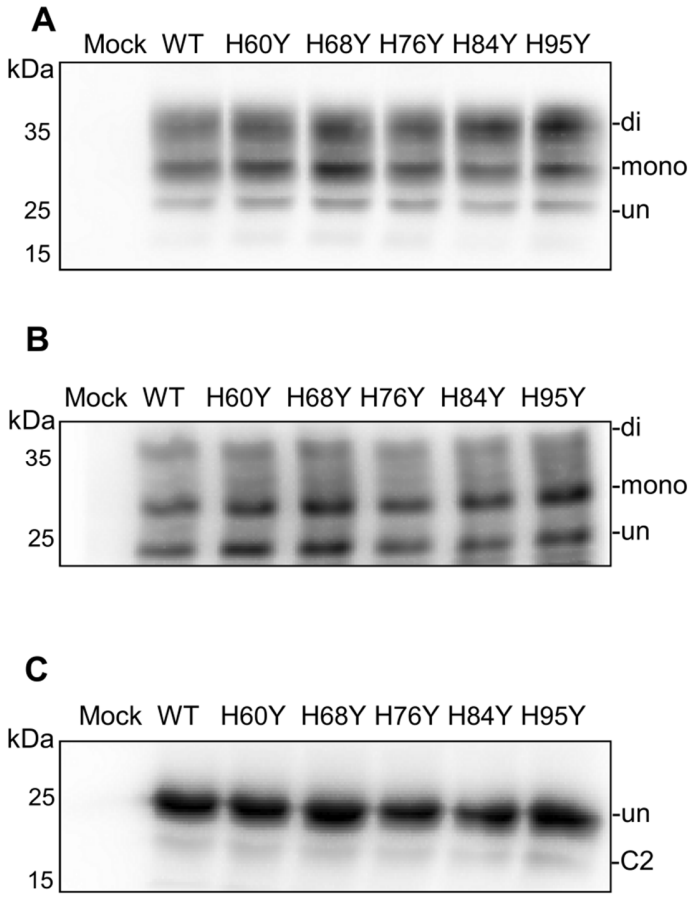

Figure 22. The OR and non-OR mutations share the same glycosylation patterns and proteolytic features as the WT MoPrP^{C}. N2a cells were transiently transfected with 3F4-tagged WT and mutant MoPrP constructs. **(A)** Fifty µg of cell lysates was applied to each lane. **(B)** Lysates were either digested with Endo-H or **(C)** PNGase-F. Mutant proteins were detected with anti-PrP 3F4 mAb. The positions of diglycosylated, monoglycosylated and unglycosylated forms (denoted as di, mono and un) of PrP^{C} and the C-terminal fragment (C2) are on the right of each blot.

4.5. Intracellular accumulation of the H95Y mutant

The OR and non-OR His mutants were expressed in N2a cells and selectively visualized by immunofluoresence with the 3F4 mAb. The 3F4-tagged WT and mutated PrPs were found predominantly on the cell surface, with some intracellular punctated deposits. The distribution of WT and mutant PrPs found in this study is similar to previous reports (McKinley et al., 1991; Negro et al., 2001) **(Figure 23 and 24)**. However, a closer analysis on N2a cells expressing the H95Y$_{3F4}$ mutant

displayed robustly punctated immunoreactive signals consistent with intracellular PrP accumulation (**Figure 23, H95Y panels**).

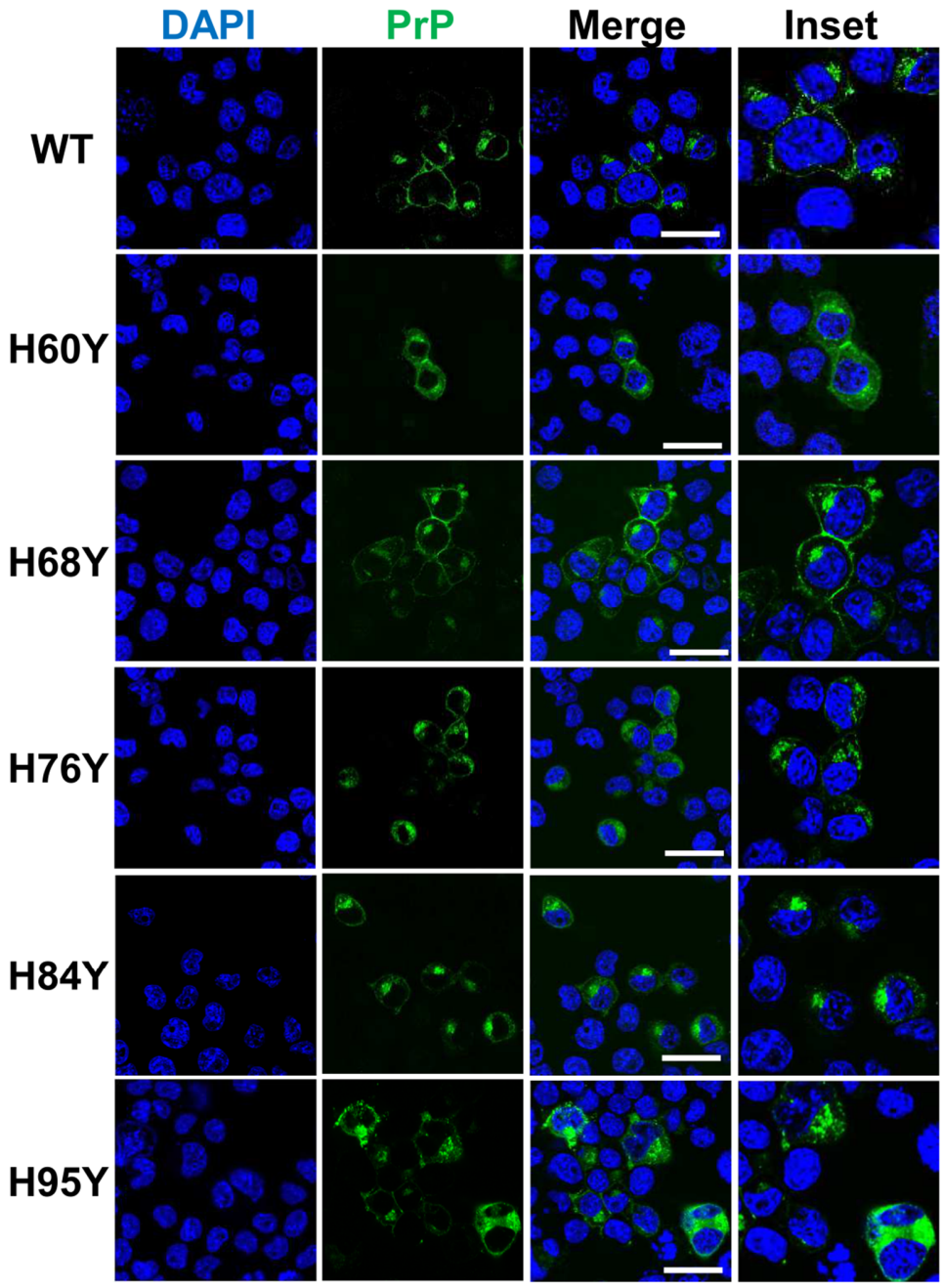

Figure 23. H95Y PrP is accumulated in the perinuclear region of N2a cells. PrPs in N2a cells expressing 3F4-tagged MoPrP constructs were detected by anti-PrP 3F4 mAb. Insets show magnifications of some cells in the merge images. Blue fluorescence for nucleus; green fluorescence for PrP. Scale bars: 24 μm.

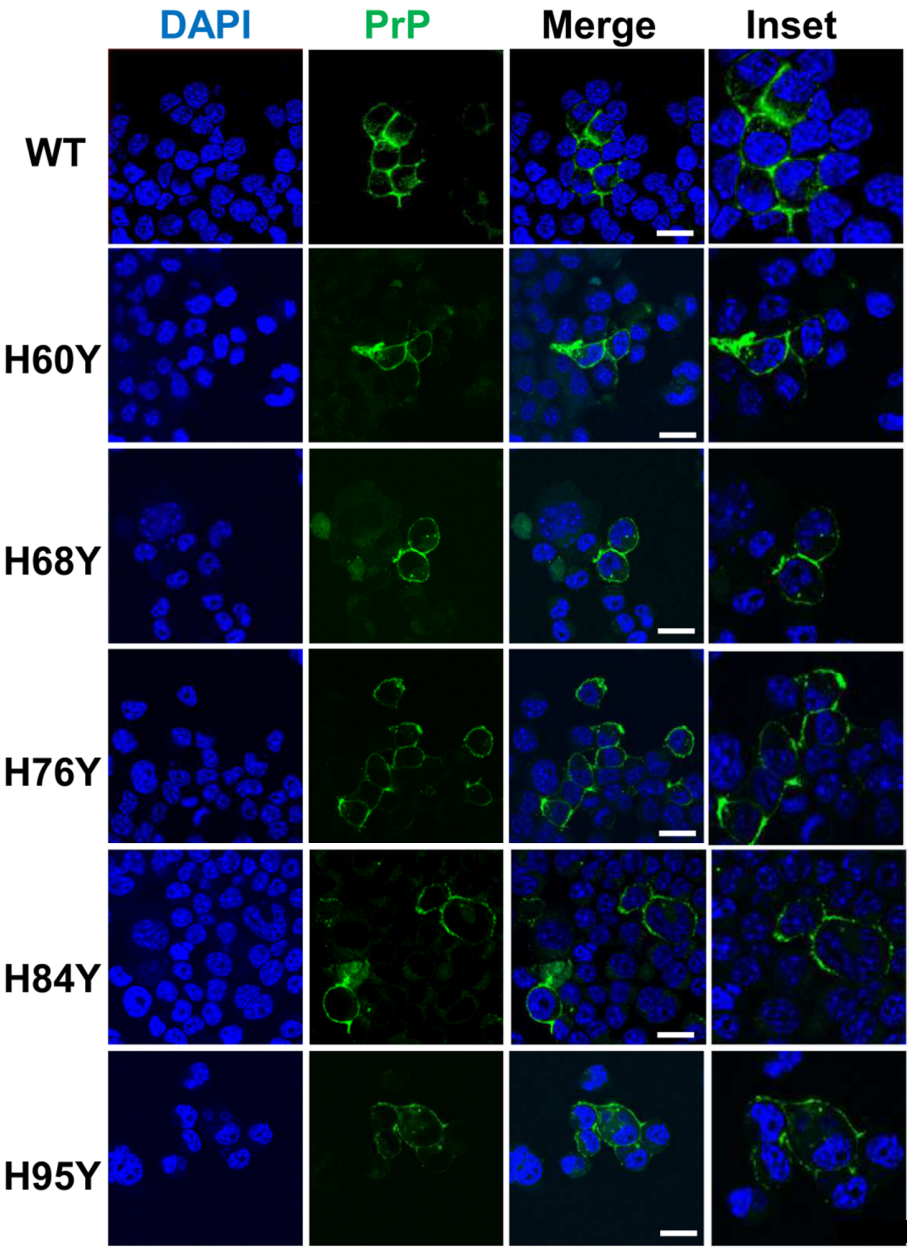

Figure 24. Mutant PrPs are predominantly expressed on cell surface as wild-type PrP^{C}. PrPs on cell surface were detected by anti-PrP 3F4 mAb without permeabilization. Insets represent magnifications of some cells in the merge images. Blue fluorescence for nucleus; green fluorescence for PrP. Scale bars: 24 μm.

One of the numerous characteristics of PrP^{Sc} is its accumulation inside the cells (Harris, 1999; Taraboulos *et al.*, 1990). Here, we reasoned whether the intracellular $H95Y_{3F4}$ accumulation is a sign of prions or not. Prion diseases are caused by misfolding proteins that can accumulate to form amyloids characterized by β-sheet structure. This structure can be recognized by some specific dyes, such as Congo Red and thiazole dyes (Thioflavin-S and Thioflavin-T). We double-stained cells with Thioflavin-S (ThS) and anti-PrP antibodies to obtain more information about the $H95Y_{3F4}$ conformation. N2a and ScN2a cells were used as negative and positive controls, respectively, to ascertain that ThS signals were due to aggregates, not artifacts. Data demonstrated that only scrapie cells with PrP^{Sc} existence showed ThS-positive signals. In $H95Y_{3F4}$ transfected N2a cells, only few of the perinuclear inclusions were strongly stained with ThS, while other regions of $H95Y_{3F4}$ expressing cells were ThS-negative **(Figure 25)**. This finding supports the idea that $H95Y_{3F4}$ aggregates may possess prion-like features. In order to confirm this hypothesis, we performed PrP^{Sc} detection assay by immunofluorescence imaging (Veith et al., 2009). As shown in **Figure 26**, the PrP^{C} signal of N2a cells disappeared while abundant PrP^{Sc} signal could be found mostly intracellularly and less at the plasma membrane after PK treatment. The same phenomenon can be seen in N2a cells expressing the $H95Y_{3F4}$ mutant, but not as frequently as in scrapie cells. These results are consistent with those of our Western blot analysis **(Figure 19 and 21)**. It could be hypothesized that a subpopulation of $H95Y_{3F4}$ mutant can acquire a β-sheet enriched conformation.

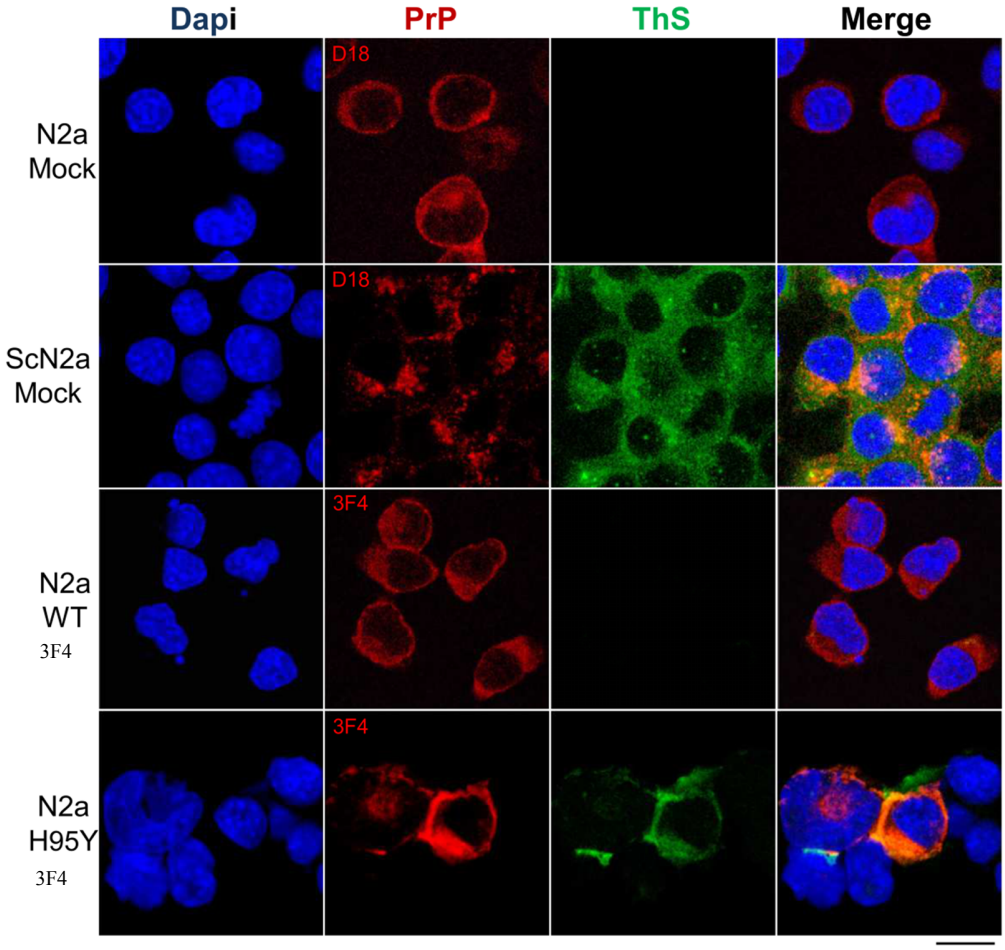

Figure 25. ThS-positive H95Y MoPrP aggregates detected in N2a cells. N2a cells were transiently transfected with WT_{3F4} or with the $H95Y_{3F4}$ mutant and stained with anti-PrP antibody and thioflavin-S (ThS) for β-structured aggregates detection. Untransfected N2a and ScN2a (N2a-mock and ScN2a-mock) were used as controls. Blue fluorescence for nucleus; red fluorescence for PrP; green fluorescence for aggregate. Scale bar: 12 µm.

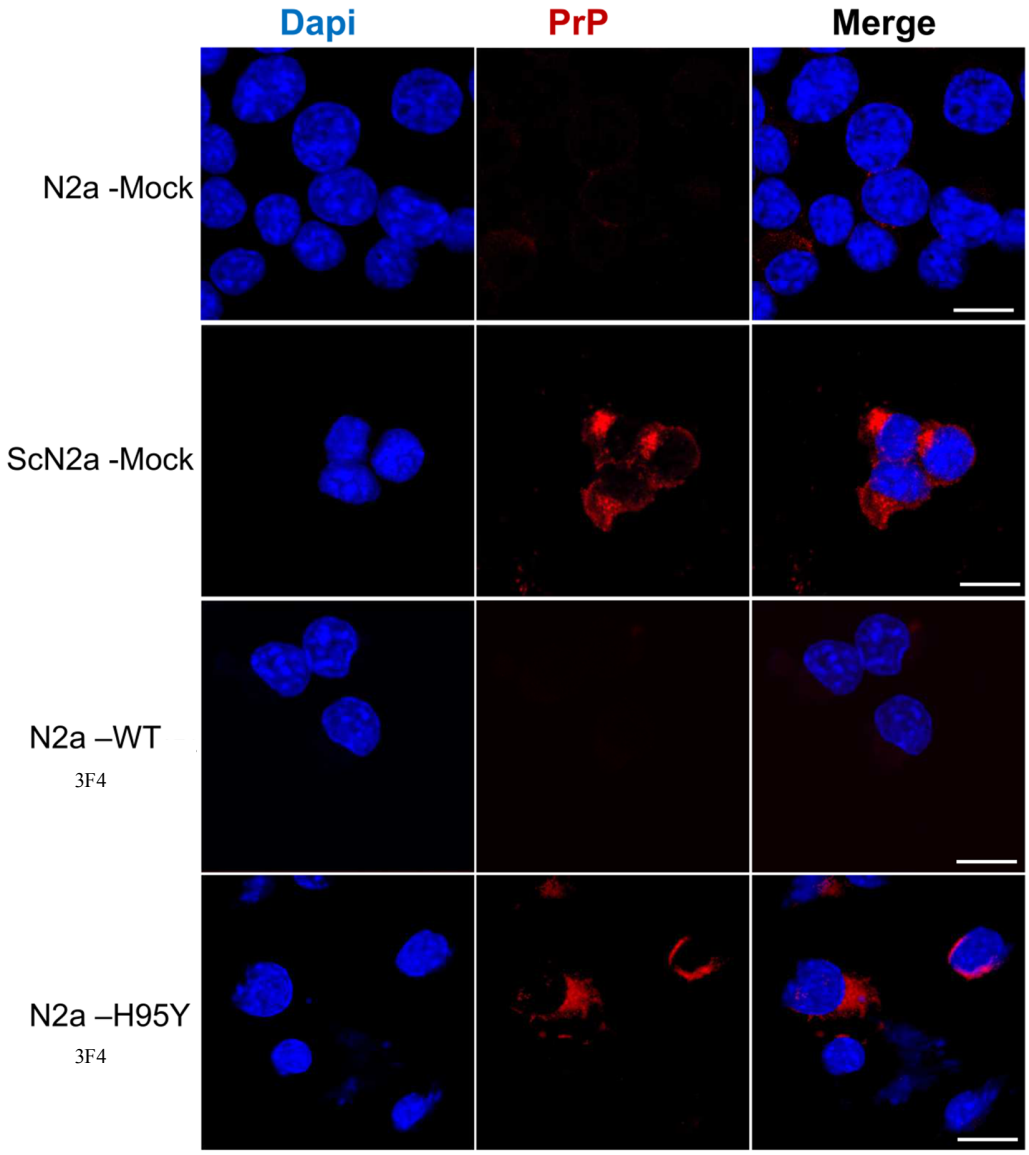

Figure 26. PrP^{Sc} detection in N2a cells expressing the H95Y mutant by immunofluorescence imaging. N2a transiently expressed WT_{3F4} and $H95Y_{3F4}$ mutant were treated with PK to remove PrP^{C} signals and guanidine to expose the PrP^{Sc} epitope. Blue fluorescence indicates nucleus; red fluorescence indicates PrP. Untransfected N2a and ScN2a (N2a-mock and ScN2a-mock) were used as controls. Scale bars: 12 µm.

4.6. Protein trafficking is not impaired in N2a cells expressing mutants

PrP^C is trafficked through the secretory pathway to the cell surface, and sequentially recycled through the endosomal system. More than 90% of surface PrP^C is internalized within 2 min and returned to the plasma membrane within 6 min (Sunyach et al., 2003). The copper binding depending on the histidine residues, particularly in the OR, has been previously implicated in several properties of PrP^C, one of which is the endocytic trafficking (Lee et al., 2001; Pauly and Harris, 1998; Perera and Hooper, 2001a). This endocytic recycling pathway has been involved in certain steps of PrP^C-PrP^{Sc} conversion. Moreover, the existence of this pathway also suggests that PrP^C might serve as a receptor to uptake extracellular ligands, and copper ion is an attractive partner. Here we investigated whether lacking of copper binding *via* His in the OR or non-OR may have an effect on the endocytosis, and whether the accumulation of the $H95Y_{3F4}$ mutant is correlated with this pathway or not. For this purpose, we specifically immunolabelled the transfected proteins that were localized only intracellulary, after removing the extracellular PrP^C by trypsin treatment (Westergard et al., 2011). We observed that all mutant PrPs exhibited punctated intracellular fluorescence signals corresponding to endosomal compartments to which antibody-labeled PrP had been delivered, and as shown, $H95Y_{3F4}$ was efficiently endocyted as WT_{3F4} **(Figure 27)**. We concluded that His mutations do not impair PrP^C internalization from cell surface, and the accumulation of $H95Y_{3F4}$ could not be attributable to endocytosis. It is needed to be more evidently confirmed by other experiments. However, it could be in agreement with a previous study showing that cells expressing the OR region ablation in the PrP construct failed to result in endocytosis (Perera and Hooper, 2001b) despite the copper binding to other sites out of ORs (Whittal et al., 2000). Nevertheless, the number of OR efficient for copper-mediated internalization is intriguing. It was reported that even if one OR unit is lacking, the protein is still sufficient for the endocytosis (Pauly and Harris, 1998). Conversely, Perera and Hooper, based on the investigation of the construct containing two mutated histidines (H68 and H76), have concluded that disruption of one or more ORs drastically compromises the endocytosis of PrP (Perera and Hooper, 2001b). Our data add evidence that one histidine substitution could not impair the

endocytosis, since identical effects were obtained for all four H60/68/76/84 mutations.

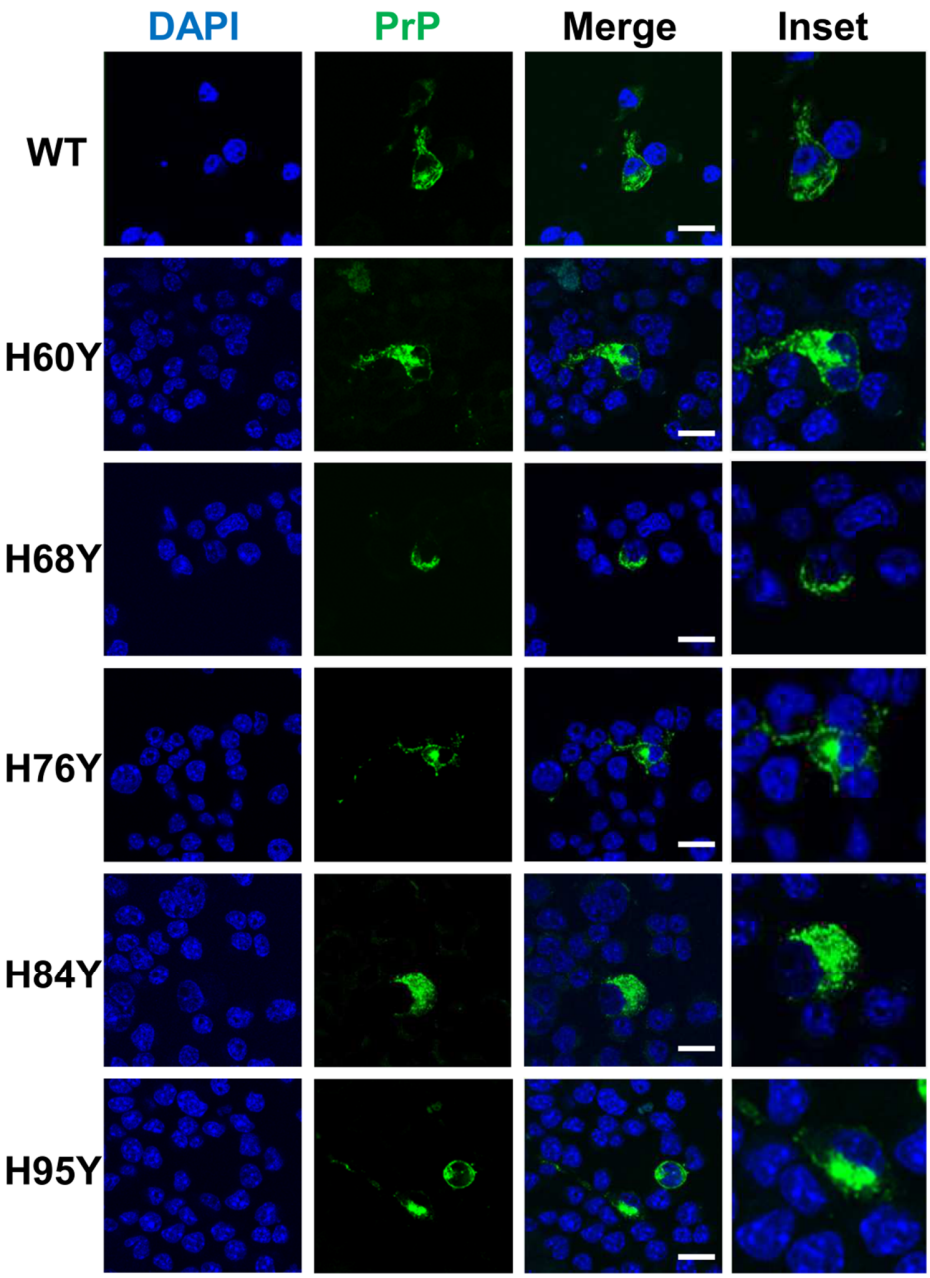

Figure 27. Substitution of a single histidine residue in the OR and non-OR regions does not impair PrP endocytosis. N2a cells were transiently transfected with 3F4-tagged MoPrP constructs. Only intracellular transfected PrPs were immunolabeled after removing extracellular PrP^{C} by trypsin. PrPs were detected by the 3F4 mAb. Insets show magnifications of cells in the merge images. Scale bars: 24 µm.

4.7. The H95Y mutant accumulates in early and recycling endosomes

Conversion of PrP^{C} to PrP^{Sc} is the key event in prion pathogenesis. To date there is no direct evidence for the involvement of any specific intracellular compartments in this event, as several compartments have been proposed as possible location depending on different systems (Arnold et al., 1995; Barmada and Harris, 2005; Caughey et al., 1991b; Godsave et al., 2008; McKinley et al., 1991; Pimpinelli et al., 2005). It is important to characterize the putative intracellular localization where PrP^{C} to PrP^{Sc} conversion occurs. On the basis of our results, we further identified the primary intracellular compartments where H95Y accumulation may occur. For this purpose, we selectively analyzed the localization patterns of 3F4-tagged WT and the H95Y mutant with some organelle markers.

We demonstrated here that most WT_{3F4} PrP^{C} is found on cell surface, while there is a small portion in the endosomes and lysosomes. These results are consistent with those obtained from previous works analyzing the distribution of WT PrP^{C} in different cell lines (Lainé et al., 2001; Mironov et al., 2003). Some punctated deposits found in WT expressing cells were colocalized with lysosome marker LAMP2 while the majority of 3F4-positive signals were on plasma membrane **(Figure 28 A)**. The same general patterns of intracellular labeling were seen in cells expressing the $H95Y_{3F4}$ mutant. Double labeling analysis using Calnexin (an ER marker) indicates a correct trafficking through the ER; and taken together with biochemical analysis **(Figure 22 B and 22 C),** the H95Y mutant is not blocked in this compartment. A significant population of intracellular $H95Y_{3F4}$ mutant showed co-localization with EEA1 (an early endosome marker) and Tfn (a recycling endosome marker) suggesting a $H95Y_{3F4}$ MoPrP accumulation in early and recycling endosomes. Additionally, a smaller fraction of $H95Y_{3F4}$ mutant was found in the late endosomes and lysosomes **(Figure 28 B)**. $H95Y_{3F4}$-PrP distribution in early and recycling endosomes is somehow identical to PrP^{Sc} in scrapie-infected cells **(Figure S7)**. Similar findings were observed in previous reports (Marijanovic et al., 2009; Uchiyama et al., 2013).

Acidic pH has been suggested as a critical condition for changes in PrP conformation (Hornemann and Glockshuber, 1998) and a change in the balance of

distinct mechanisms of internalization may facilitate conversion of PrP^{C} to PrP^{Sc}, by diverting the protein to distinct intracellular compartments. Furthermore, mutations in PrP^{C} related to prion diseases have been demonstrated to alter protein subcellular trafficking (Ivanova et al., 2001; Negro et al., 2001). Our data support the idea that early and recycling endosomes could be the principal intracellular sites where $PrP^{C} \rightarrow PrP^{Sc}$ conversion may occur. Previous studies have shown that the transition of PrP from its native state to soluble oligomers is a pH-dependent process (Gerber et al., 2008). Acidic conditions appear to favor the existence of soluble PrP oligomers (Baskakov et al., 2002). Potentially, the mutation might provoke alterations in the cell sorting and protein processing, inducing a suitable surrounding environment for PrP^{Sc} formation.

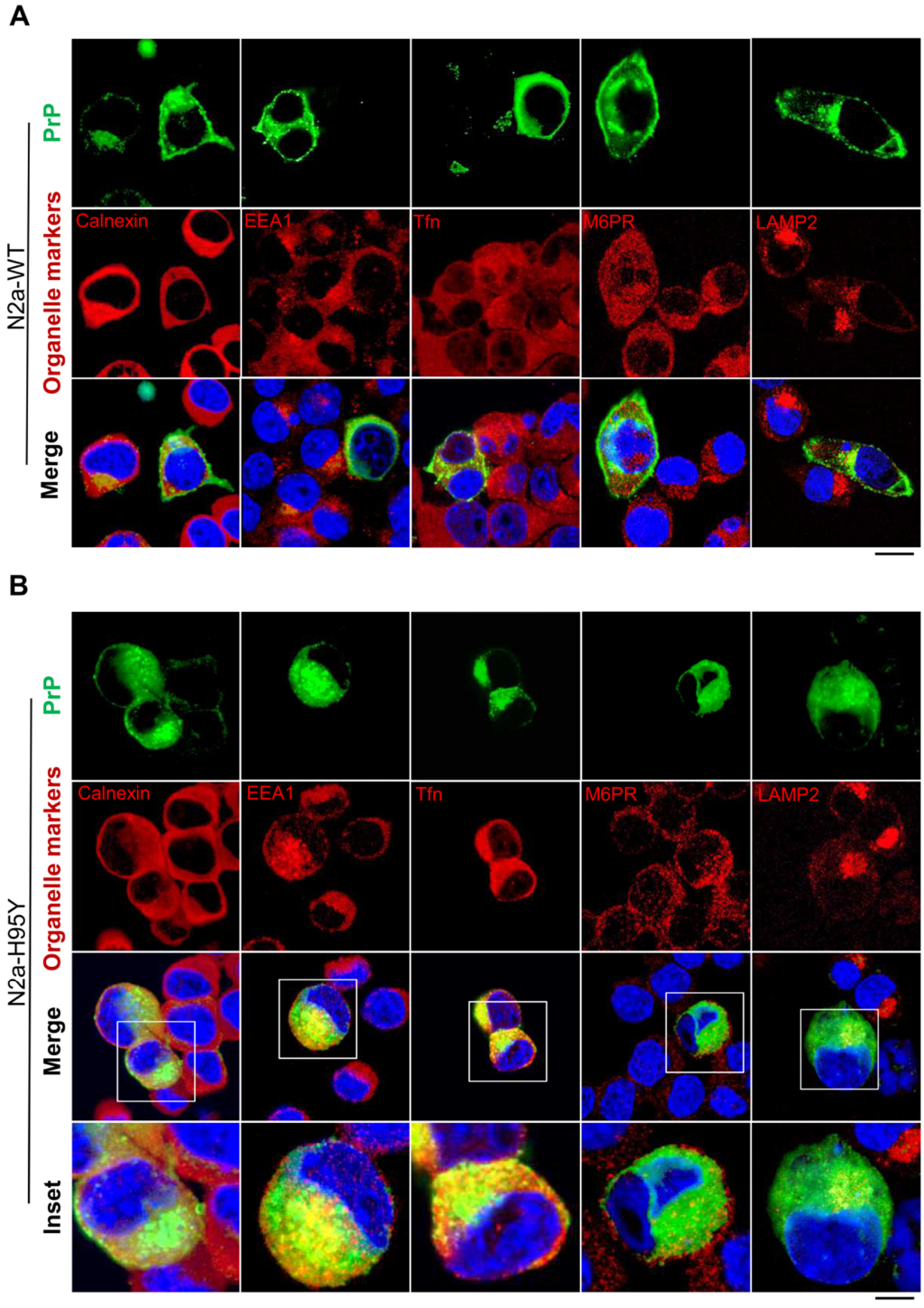

Figure 28. The H95Y$_{3F4}$ MoPrP mutant displays intracellular accumulation in early and recycling endosomes. PrP localization in N2a cells expressing the WT$_{3F4}$ MoPrP **(A)** or the H95Y$_{3F4}$ MoPrP **(B)**. Nuclei are labeled with DAPI (blue), PrPs are detected by 3F4

antibody (green), while organelle markers, as Calnexin (ER marker), EEA1 (early endosomes marker), Tfn (recycling endosomes marker), M6PR (late endosomes marker) and LAMP2 (lysosomes marker), are labeled in red. Insets in (B) show a magnification of the merged panels (white boxed areas). Scale bars: 12 μm.

4.8. The H95Y mutant can induce *de novo* prion formation in N2a cells

Often referred to as the prion agent (Prusiner et al., 1998), PrP^{Sc} derives its infectious nature from its unique ability to induce additional PrP^{C} molecules to acquire its own β-sheet rich PrP^{Sc} conformation. However, the mechanistic details of the conversion process are not completely clear. In sporadic prion disorders, the conversion of PrP^{C} to PrP^{Sc} is believed to occur as a spontaneous event. The newly formed PrP^{Sc} can favor the conversion of PrP^{C} into additional PrP^{Sc} and cause the accumulation of pathological isoforms, as prions. On the basis of these results, we reasoned whether the $H95Y_{3F4}$ mutant expressed in N2a cells may behave as an infectious prion. To test this hypothesis, N2a cells were transiently transfected with WT_{3F4} or $H95Y_{3F4}$ mutant and regularly passaged, up to passage (P) 8 (**Figure 29 A**). Using D18 mAb, which allows for the detection of both transfected and endogenous MoPrPs, we found the immunoreactive PK-resistant PrP bands starting at P4, remaining unchanged till P7, and slightly increasing at P8.

Alternatively, we isolated the $H95Y_{3F4}$ "seed" from transiently transfected N2a cells by PTA precipitation, subjected this seed to uninfected N2a and sequentially passaged up to P8 (**Figure 29 B**). Interestingly, we observed an increment in PrP^{Sc} PK-resistance levels through passages when compared to WT expressing cells at P8, thus indicating that the H95Y seed acted as a real infectious agent inducing *de novo* conformational conversion of PrP^{C} to PrP^{Sc} and propagating itself over passages. To explain these observations, we proposed that isolated H95Y seeds were more than sufficient to induce endogenous PrP^{C} to change its native structure to misfolded PrPs. These misfolded PrPs could continue the process and amplify PrP^{Sc} population. Conversely, in N2a cells transiently expressed H95Y and sequentially passaged, the existing misfolded H95Y was possibly trapped inside the cells and thus less efficient in exhibiting its infectivity; this resulted in unchanged PrP^{Sc} PK-resistance levels over passages.

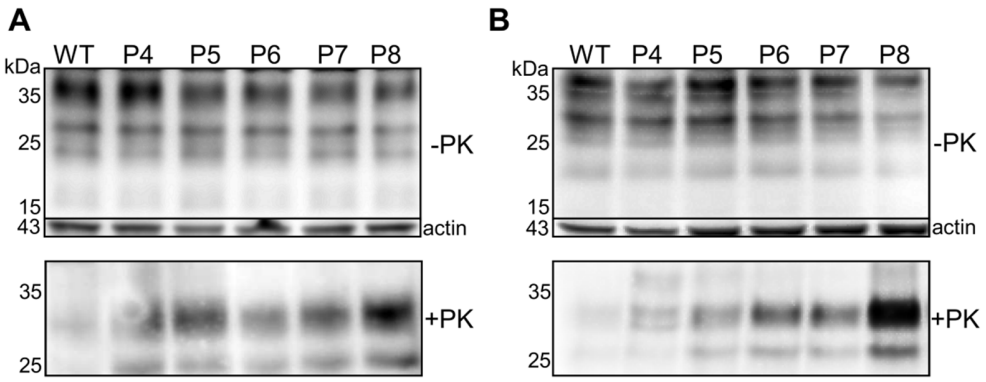

Figure 29. The H95Y mutant induces *de novo* prion formation. (A) N2a cells were transiently transfected with WT_{3F4} and $H95Y_{3F4}$ MoPrP and regularly passaged every 7 days up to passage (P) 8. **(B)** PTA-extracted PrP^{Sc} from N2a cells transfected with either WT_{3F4} MoPrP or $H95Y_{3F4}$ MoPrP were subjected to N2a cells and regularly passaged every 7 days up to P8. The PrP^{Sc} detection was assessed by PK digestion over subsequent passages. PrP^{C} and PrP^{Sc} expressions were detected by D18 antibody. β-actin was used as internal loading control.

We further analyzed the kinetics of recMoPrP H95Y compared to recMoPrP WT in fibrillization reaction. In this assay, we used the recombinant proteins without 3F4-tag. Moreover, in order to directly evaluate the effect of H95Y mutation in the spontaneous conversion process, we initiated the reaction without preformed PrP^{Sc}. We obtained typical sigmoidal kinetics for amyloid formation for both recMoPrP_WT and recMoPrP_H95Y. At neutral condition and low concentration of 1 M Gdn denaturant, we could not detect any clear difference in lag phase (**Figure 30 A**). However, recMoPrP_H95Y showed considerably reduced lag phases as compared to recMoPrP_WT at higher concentrations of Gdn. In this experimental setup, we observed the same effect as amyloid seeding assay in the presence of preformed $H95Y_{3F4}$_PrP^{Sc} seed. The fibrillization of recMoPrP_H95Y started more quickly at both pH 5 and 7, indicating that this mutation significantly promotes the β-structured formation (**Figure 30 B)**. We also noticed that the variability between replicates in the reaction of recMoPrP H95Y was always lower than that of recMoPrP_ WT.

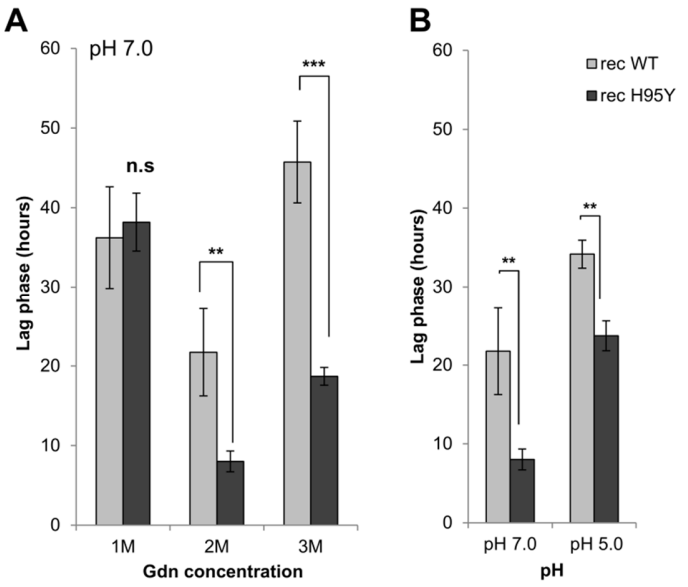

Figure 30. recMoPrP H95Y mutant dramatically promotes polymerization processes. recMoPrP_WT (recWT) and recMoPrP_H95Y (recH95Y) were adding into fibrillization reactions at different concentrations of Gdn **(A)** or at two pH conditions in 2 M Gdn **(B)**. Comparison of mean lag phase values was performed. (n = 4, n.s: non-significant, ** $p< 0.005$, ***$p<0.001$).

V. DISCUSSION

The central molecular event in prion diseases is the conversion of the normal cellular form, PrP^{C}, into the disease-specific isoform, PrP^{Sc}. Despite numerous investigations on PrP, the physiological functions of PrP^{C} as well as its conversion mechanism leading to the conformational change remain elusive. Several lines of evidence have suggested that PrP^{C} specifically binds to copper, an essential trace metal. Regardless of contradictory results on the actual role of copper in prion diseases, there is evidently strong agreement that copper binding has a pivotal impact on protein aggregation. Previous studies have been based mostly on spectroscopic analysis of protein native structure and copper binding mode. Although these methods are powerful approaches to study PrP conformation and binding affinities, they still fail to completely investigate the protein in its physiological environment. By combining cell culture and cell-free approaches, we first explore that the lack of each histidine in the OR has neither effect on prion replication nor protein maturation and trafficking. Conversely, we found a critical implication of histidine 95 in prion conversion. To explain these results, we hypothesize a compensatory effect between the four identical OR units. A single OR is a sufficient primary unit for copper binding and to sustain the replication (Cruite et al., 2011; Flechsig et al., 2000). Thus, ablation of one OR unit or substitution of the histidine residue in each unit may not significantly alter protein conformation and copper coordination. Another possibility is that the non-OR copper-binding site at H95, not the OR region, is much more crucial for prion propagation and infectivity. This finding supports previous studies on a higher affinity for copper coordination at the non-OR region, particularly the H95 (Jones et al., 2004; Millhauser, 2007; Qin et al., 2000; Quaglio et al., 2001). Moreover, H95 is in the region of PrP that typically remains after proteolytic cleavage, thus, copper may modulate PrP^{Sc} formation even in the absence of the ORs, as shown by Cox *et al*. (Cox et al., 2006). We showed that the $H95Y_{3F4}$ MoPrP follows normal maturation and internalization processes. The mutant can transit to the ER, successfully exit the Golgi apparatus and finally attach to the outer leaflet of the plasma membrane. From the cell surface, the mutant can be endocyted to internal endosomal compartments and routed to lysosomes and proteasomes for degradation.

Along its trafficking, a substantial fraction of $H95Y_{3F4}$ may misfold and acquire PrP^{Sc}-like characteristics. This subpopulation can act as a template to recruit and convert normal PrP^{C} into PrP^{Sc} **(Figure 31)**.

On the basis of our findings, we propose that the H95Y mutant acts as a pathogenic mutation located in the N-terminal domain causing spontaneous conversion to prion. This is in line with structural data on full-length and truncated recombinant PrP, which define the N-terminal half of the protein as flexibly disordered or random coil (Viles et al., 1999); the region containing H95 does not adopt a regular secondary structure (Berti et al., 2007; Emwas et al., 2013). Indeed, this unstructured portion of PrP undergoes rearrangements in PrP^{Sc} (Peretz et al., 1997). Instead of causing a significant change in folded structure like other pathogenic mutations in the globular domain, H95Y may alter the interaction between distinct portions in protein structure, whose changes are required for oligomerization into fibrillar species. The importance of residue 95 has not been thoroughly studied yet. We propose that copper binding at this site may impact the interaction between different regions of the protein, possibly to accelerate the copper-binding to the octapeptide domain with the hydrophobic domain or the C-terminal globular domain. This finding supports a previous study showing that the interaction of copper to a peptide including the non-OR and the hydrophobic regions (residues 91-115) induces aggregation of β-sheet enriched structures (Jobling et al., 2001). A recently published study proposes that N-terminal mutations may alter backbone flexibility and intra-molecular contacts in the OR and non-OR regions, thus affecting copper coordination as well as the binding with other physiological interacting partners (Cong et al., 2013).

Copper seems to play an important role for PrP^{C} stability and conversion to prion (Bocharova et al., 2005; Bonomo et al., 2000; Brown, 2001; Brown and Harris, 2003; Brown and Sassoon, 2002; Brown et al., 1998; Chattopadhyay et al., 2005; Cox et al., 2006; Cui et al., 2003; Garnett and Viles, 2003). Experiments on the connection between copper and PrP^{Sc} formation have yielded contradictory results. Since PrP^{C} binds Cu with several unique coordination modes (Chattopadhyay et al., 2005; Millhauser, 2004), it is certainly possible that each mode exhibits distinct

characteristics with regard to prion conversion. The interaction with Cu ions could stabilize PrP conformation but it remains to be seen in what way the binding of Cu to the N-terminal repeats and the concomitant adoption of structure influences the structural transitions that potentially take place in H95 and/or H110.

Recent studies have shown that the copper binding site has the same structure for both Cu (II) and Cu (I) in the WT HuPrP, whereas the coordination site changes drastically from the oxidized to the reduced form of the copper ion in the Q212P mutant, which is related to human GSS (Ilc et al., 2010). Mutation at H95 may change the copper coordination between the OR-H95 and/ or H110, therefore facilitate prion conversion. How Cu^{2+} and other metal ions influence the flexibility of the N-terminal part and, subsequently, the interaction between PrP^{Sc} and PrP^{C} *in vivo* and *in vitro* have not yet been well understood. Whether the N-terminal region of PrP stabilizes the C-terminal domain of the molecule or modulates the binding of PrP^{C} to an auxiliary molecule that participates in PrP^{Sc} formation remains to be established (Wadsworth et al., 1999).

From our cell analysis, we found that mutation at H95 induces alterations in PrP biochemical features and trafficking. These findings raise the question whether the changes in copper binding may influence on the protein distribution in compartments that facilitate protein misfolding to form some intermediate states of structural organization before finally ending up as aggregates. Acidic pH has been suggested to be ideal for conformational changes (Hornemann and Glockshuber, 1998). Thus, a change in the balance of distinct mechanisms of internalization may facilitate conversion of PrP^{C} to PrP^{Sc}, by diverting the protein to distinct intracellular compartments. Identifying the organelles involved in PrP^{C} trafficking is of clear interest, as pH and other factors that may facilitate conversion can change in the endocytic pathway. Recent studies have shown the participation of early endosomes and retrograde trafficking to the Golgi and ER in PrP^{res} conversion (Béranger et al., 2002; Yamasaki et al., 2012).

In some cell models, a small percentage of PrP^{C} normally misfolds, is retrogradely transported to the cytosol, also rapidly degraded by the lysosomal/proteasomal system and becomes undetectable (Ma and Lindquist, 2001;

Yedidia et al., 2001). However, when proteasome activity is compromised, PrP accumulates intracellularly to form cytosolic PrP (Ma and Lindquist, 2001; Taraboulos et al., 1995). It is not well established whether the accumulation of protein in the disease is the cause or the consequence of cellular protective system dysfunction. We observed a population of H95Y acquiring high PK-resistance and accumulating in acidic endosomal compartments, whose environments evolved to promote protein unfolding at low pH prior to degradation by acid-activated proteases. Consequently, this population could escape from or even inhibit the cellular quality control mechanisms (Ashok and Hegde, 2009; Zanusso et al., 1999). Or, the increment of misfolded species may lead to saturation of the trafficking pathway to lysosomes and compromise the proper function of this compartment. Several different pathogenic mutations impair PrP trafficking and cause a portion to accumulate in intracellular compartments (Drisaldi et al., 2003; Ivanova et al., 2001; Massignan et al., 2010; Negro et al., 2001; Petersen et al., 1996). Our data proposed that the effects of H95Y on PrP structure and cellular distribution are related, and endosomal accumulation may be a consequence of PrP misfolding and aggregation. Although a small number of prions could be cleared by multiple different protein degradation pathways, accumulation above a certain threshold would inhibit the self-defense mechanism. Pathogenic mutants do not exert a uniform effect on the stability of PrP. Thus, it was not possible to apply a common mechanism based solely on the alteration of protein intrinsic structure or the impairment of cellular quality control system.

Studying the artificial mutant H95Y provides an invaluable model not only for investigating molecular mechanisms, but also the structural events of $PrP^{C} \rightarrow PrP^{Sc}$ conversion *in vitro* of pathogenic mutations in the N-terminal of PrP. Our results add evidence to explain the existence of this highly evolutionary conserved region in the *Prnp* gene. The substitution of H95 with tyrosine has a dramatic effect in promoting the generation of novel cell-to-cell infectious prion particles. Thus, H95 in the non-OR region may act as molecular switch for prion conversion. We therefore argue that copper, or other metal ions, bound to H95 may stabilize this segment preventing possible misfolding events that occur in the region from residue 95 to 125.

The data presented in this work may also provide a platform for rationally designed experiments aimed at elucidating whether the H95Y mutation may cause *de novo* prion diseases when expressed in Tg mice. Interestingly, the non-OR region has recently been found as the principal site for amyloid-β peptide (Aβ) oligomers binding and modulating Aβ neurotoxicity (Lauren et al., 2009). Aβ is a pathological hallmark of Alzheimer's disease (AD), the prevalent form of dementia in aging population (Hardy and Selkoe, 2002). It has been found that oligomeric Aβ does bind specifically to PrP, not to the PrP paralogs Doppel or Shadoo. Although PrP^C is supposed to mediate the impairment of synapticity induced by Aβ oligomers, it is interesting to elucidate how this binding contributes to AD and prion pathogenesis. It is possible that through PrP-Aβ interaction coupled with the mediation of copperhomeostasis, these molecules effect protein conformational changes and accumulation in the CNS, leading to neurological disorders. It would be interesting to investigate the interaction between the H95Y mutant and Aβ oligomers in Tg mice model to possibly define a relation among copper, PrP^C function and oligomeric Aβ in neurodegenerative disorders.

In addition, building a library of histidine substitutions in MoPrP constructs allowed us to investigate the role of copper coordination at each OR unit as well as the non-OR site, and provided useful information about their role in prion replication. Understanding the molecular mechanism of PrP conformational conversion and misfolding is essential for the biomedical research and treatment of prion diseases.

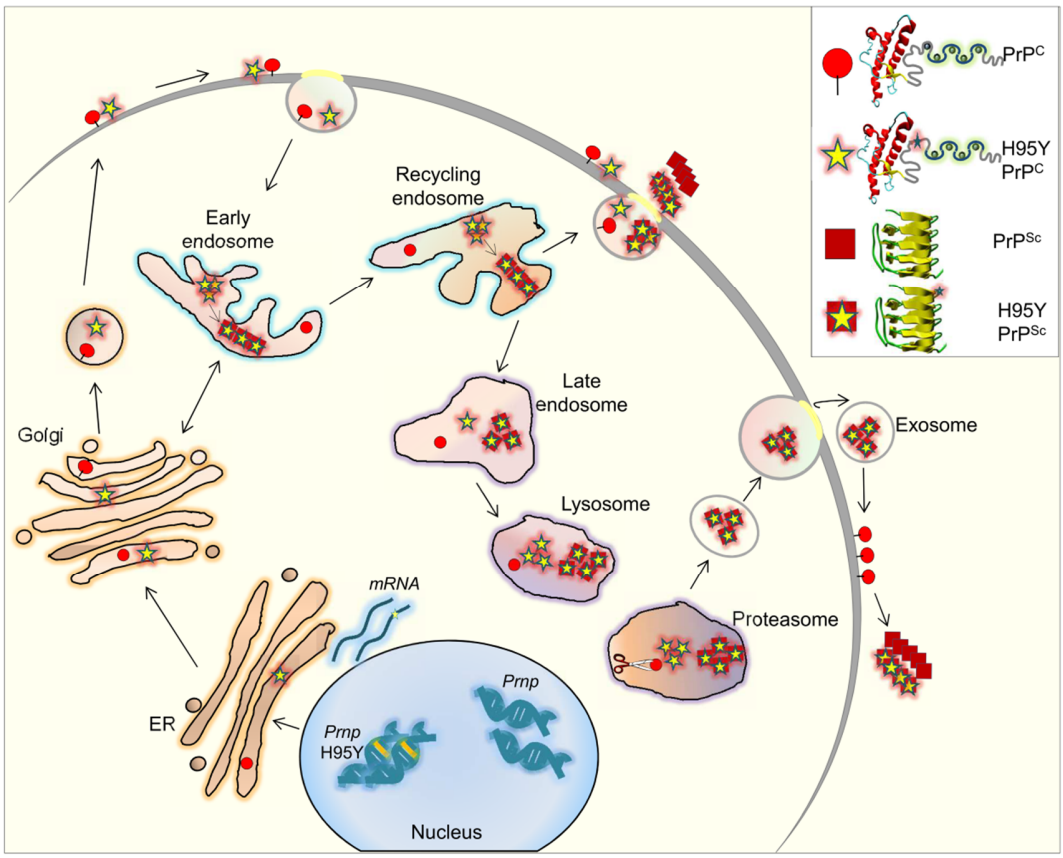

Figure 31. Proposed model for prion conversion in cells expressing H95Y MoPrP. The WT and H95Y MoPrP are synthesized in the ER, undergo post-translational modifications in Golgi apparatus, and result in the mature PrP^{C} embedded in the plasma membrane *via* a GPI anchor. From the cell surface, the proteins can be internalized to early and recycling endosomes. In these compartments, the H95Y MoPrP accumulates and may undergo conformational conversion into prion. Aberrant H95Y mutant aggregates could be delivered and accumulated into late endosomes, lysosomes and proteasomes. The presence of protease-resistant H95Y mutant aggregates may impair the cellular quality control mechanisms leading to the secretion of H95Y PrP^{Sc} via exosomes. H95Y PrP^{Sc} may template the prion conversion of both endogenous WT and mutant MoPrP on the cell surface.

Supplementary information

A. Mutant proteins are not toxic to cell cultures

To evaluate the toxicity of the inserted mutants, ScN2a and N2a cells were incubated in a 96-well tissue culture plate and transfected with 3F4-tagged MoPrP constructs as per manufacturer's instructions. Seventy-two hours after the transfection, the medium was removed and the MTT assay performed as described.

The growth rate was calculated by dividing the absorbance value of the last day with the value measured on the transfection day and compared to the untransfected (Mock) sample. Each assay was performed in duplication of 4 wells and analyzed from at least three separate experiments. Expressions of 3F4-tagged WT and mutant MoPrP constructs and the cell transfection procedures had no detectable effect on the N2a and ScN2a cell viability (**Figure S1 and S2**), indicating that expression of mutant PrP per se was not cytotoxic.

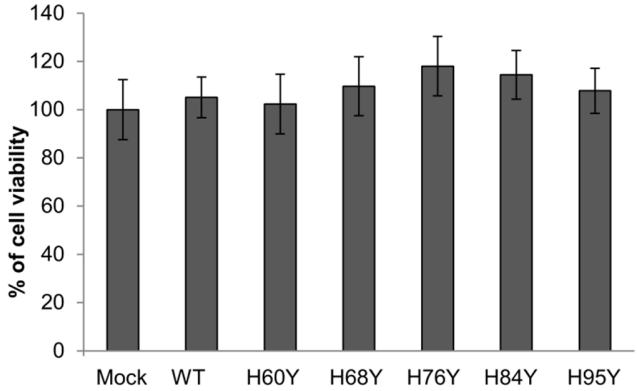

Figure S1. The histidine substitutions in the OR and non-OR regions are not toxic for cell culture. Quantitative analysis of the cell viability percentage in transfected constructs (n = 4, p>0.05).

To ascertain that the protein expression levels were comparable in all experiments, we quantified the signal densities by both Western blotting and immunofluorescence analysis. It was shown that either the protein expression levels of all MoPrP constructs employed in our study or the transfection efficiency were relevant to those for WT-PrP **(Figure S2 and S3**).

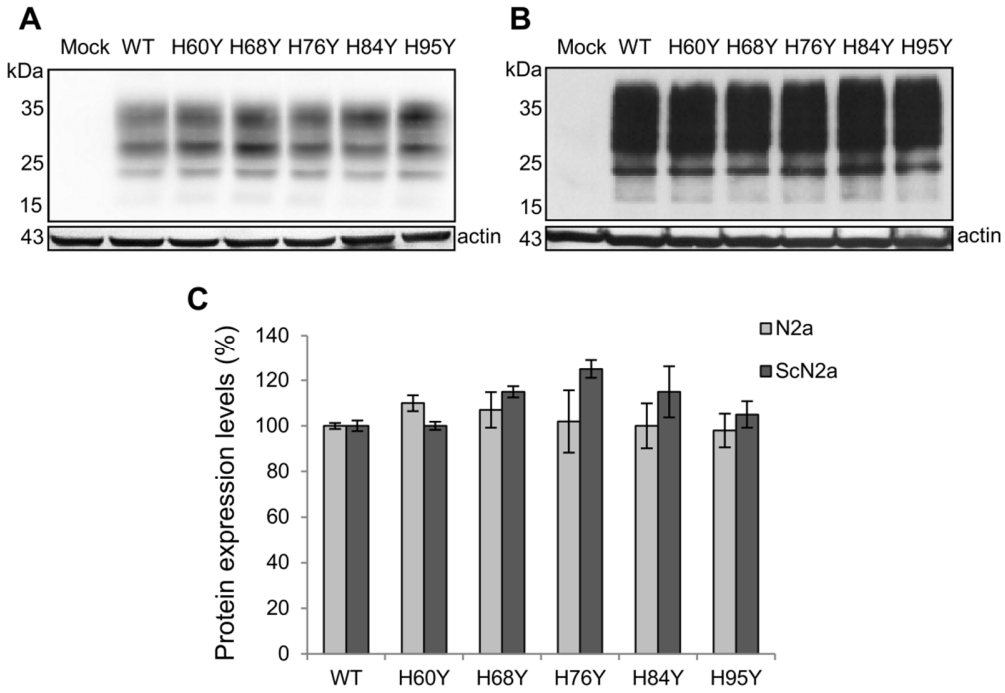

Figure S2. Protein expression levels of 3F4-tagged MoPrPs were equivalent in all experiments. Western blot of MoPrP glycosylation pattern was detected by 3F4 antibody in N2a **(A)** and ScN2a **(B)** cells transfected with the 3F4-tagged constructs. β-actin was used as internal control. Quantitative analysis of actin-normalized PrP expression levels in both N2a and ScN2a cells (n = 4, p>0.05) **(C)**.

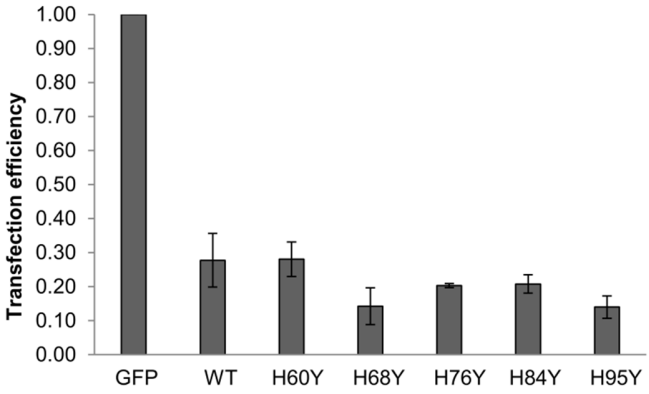

Figure S3. Relevant transfection efficiency between mutated MoPrP constructs. Quantitative analysis of GFP-normalized PrP expression levels in N2a cells (n = 4, p>0.05).

B. The 3F4–epitope tag has no influence on prion replication

As mentioned, the 3F4-epitope tag is a powerful tool to distinguish between introduced and endogenous MoPrPs. To confirm that this tag has no effect on protein expression, and especially on prion replication, we transiently transfected ScN2a cells with a blank vector, or with a vector containing *Prnp* with and without 3F4-tag encoding gene, and treated with PK to evaluate PrP^{Sc} PK-resistance levels. Western blotting with anti-PrP D18 antibody showed relevant PK-resistance among cells expressing WT with and without 3F4-tag (**Figure S4**).

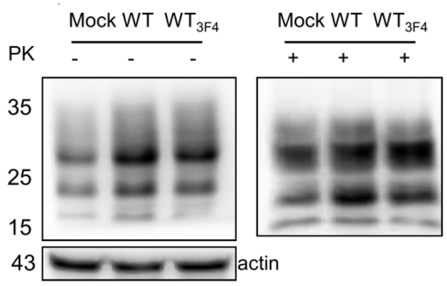

Figure S4. Characterization of 3F4-epitope tag on PK-resistance. Western blot of ScN2a cells transiently expressing MoPrP constructs with or without 3F4-tag compared to untransfected cells (mock). PrP^{C} and PrP^{Sc} were detected by anti-PrP D18 antibody. β-actin was used as internal control.

C. The presence of Histidine-95 is critical for prion replication

To understand whether the high protease-resistance of H95Y was due exclusively to the absence of the fifth histidine residue, and not to the introduction of any specific amino acid, we generated series of PrP molecules containing different amino acid substitutions at residue 95, two molecules from the group of small molecules (alanine and glycine), two of the aromatic molecule group (phenylalanine and tyrosine), and one negatively-charged molecule.

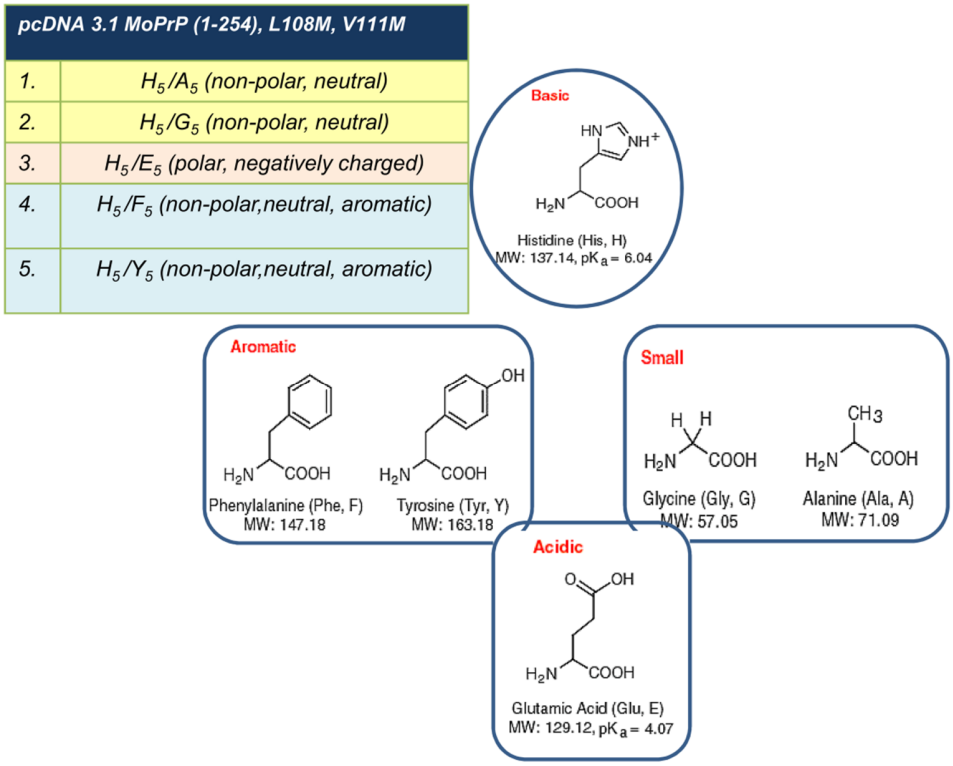

Figure S5. Histidne-95/amino acid substitutions MoPrP mutants in *pcDNA3.1(-)* and general physicochemical properties of these amino acids. Alanine (Ala, A), Glycine (Gly, G), Glutamic acid (Glu, E), Phenylalanine (Phe, F), Tyrosine (Tyr, Y).

We confirmed that the lack of the histidine at residue 95, not the substitution of tyrosine, makes the protein prone to prion propagation. Interestingly, cells expressing Ala and Gly substitutions, which belong to the group of small and neutral molecules, showed less resistance than H95Y, whereas Tyr and Phe that share similar aromatic structure and relevant molecular mass as His, clearly showed PK-resistance. Interestingly, we found that the introduction of a negatively charged molecule at residue 95 significantly reduced PrP^{Sc} level. We proposed that H95E may interact with Cu^{2+} in some different manner from H95, and exhibit a dominant negative effect on prion conversion. It would be interesting to analyze H95E in detail to understand the underlying mechanism. From these data, it is clear that histidine at position 95 plays a critical role in prion conversion and replication. Depending on the characteristics of the introduced molecule, in particular the polarity, it may enhance

or inhibit the conversion process, possibly *via* copper coordination mode. However, H95Y-expressing cells yielded the best protein expression level among amino acid substitutions, so H95Y proved to be the best candidate for our studies **(Figure S6)**.

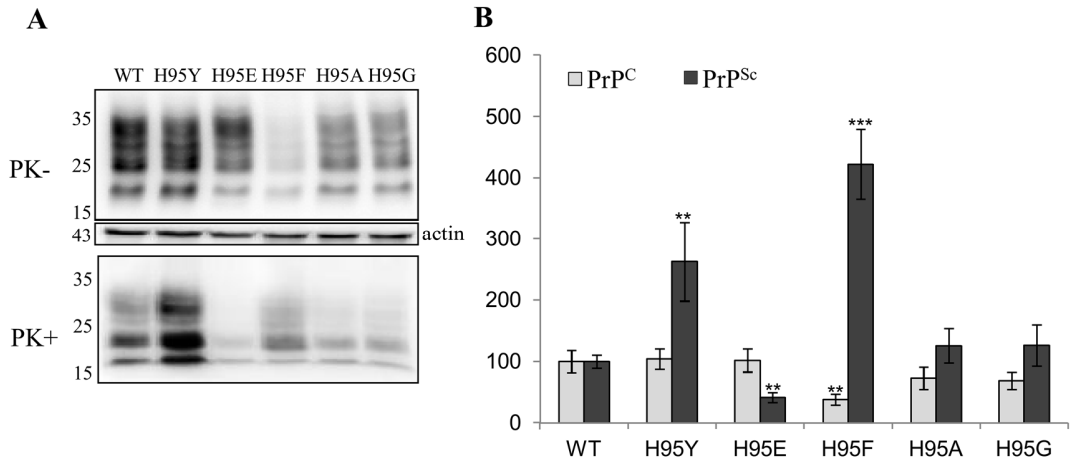

Figure S6. Evaluation of other amino acid substitutions at Histidine 95. (A) Western blot of ScN2a cells transiently expressing MoPrP constructs in which H95 was substituted by different amino acids. PrP^{C} and PrP^{Sc} were detected by anti-PrP 3F4. **(B)** Quantitative analysis of PrP expression (PrP^{C}) and PrP^{Sc} PK-resistance levels (PrP^{Sc}) in transfected cells, calculated from (A) (n = 3, *$p<0.05$, **$p<0.05$, ***$p<0.005$).

D. The localization of PrP^{Sc} in ScN2a cells

The localization of PrP^{Sc} is not well established because of the lack of specific antibodies and the need for protein denaturation by guanidine-hydrochloride (GdnHCl) to expose PrP^{Sc} epitopes (Taraboulos et al., 1990; Veith et al., 2009). Moreover, depending on the cell lines used for investigation, the distribution of the proteins may vary. But it is certain that the majority of PrP^{Sc} molecules is intracellular, and seems to be accumulated in endosomal compartments (Godsave et al., 2008; Marijanovic et al., 2009; McKinley et al., 1991; Taraboulos et al., 1990; Veith et al., 2009). To confirm PrP^{Sc} distribution in ScN2a cells, we briefly analyzed the localization patterns of PrP^{Sc} in some organelle markers **(Figure S7)**. In order to visualize PrP^{Sc}, ScN2a cells were treated with GdnHCl and PK before incubation with the anti-PrP antibody. We found that PrP^{Sc} was predominantly intracellular. Most intracellular proteins are localized throughout the endocytic compartments, particularly in the early endosome, recycling endosome and lysosome. These data agree with previous studies (Marijanovic et al., 2009; McKinley et al., 1991; Uchiyama et al., 2013).

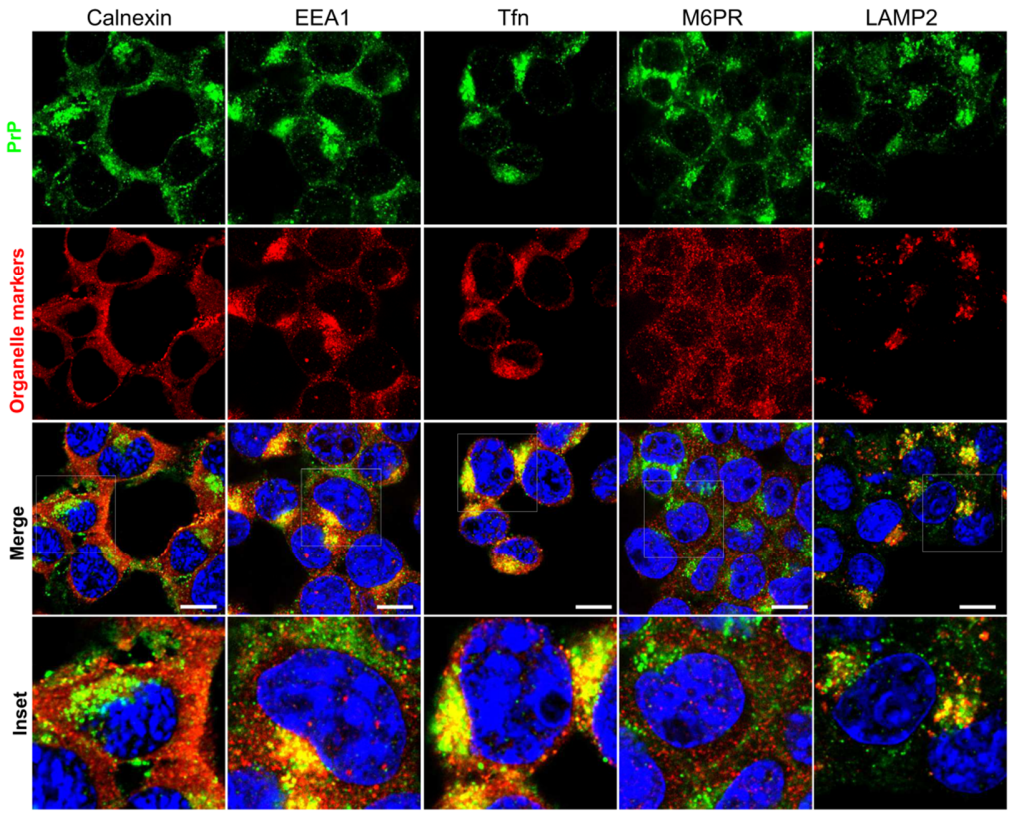

Figure S7. Subcellular localization PrP^{Sc} in ScN2a cells. Nuclei are labeled with DAPI (blue), PrPs are detected by D18 antibody (green), whereas organelle markers, as Calnexin (ER marker), EEA1 (early endosomes marker), Tfn (recycling endosomes marker), M6PR (late endosomes marker) and LAMP2 (lysosomes marker) are labeled in red. Insets show a magnification of the merged panels (white boxed areas). Scale bars: 12 µm.

References

1. Abid, K., Morales, R., and Soto, C. (2010). Cellular factors implicated in prion replication. FEBS Lett. *584*, 2409–2414.

2. Aguzzi, A., and Calella, A.M. (2009). Prions: Protein Aggregation and Infectious Diseases. Physiol. Rev. *89*, 1105–1152.

3. Aguzzi, A., Sigurdson, C., and Heikenwaelder, M. (2008). Molecular mechanisms of prion pathogenesis. Annu. Rev. Pathol. *3*, 11–40.

4. De Almeida, C.J.G., Chiarini, L.B., da Silva, J.P., E Silva, P.M.R., Martins, M.A., and Linden, R. (2005). The cellular prion protein modulates phagocytosis and inflammatory response. J. Leukoc. Biol. *77*, 238–246.

5. Alper, T. (1993). The scrapie enigma: insights from radiation experiments. Radiat. Res. *135*, 283–292.

6. Alper, T., Haig, D.A., and Clarke, M.C. (1966). The exceptionally small size of the scrapie agent. Biochem. Biophys. Res. Commun. *22*, 278–284.

7. Alper, T., Cramp, W.A., Haig, D.A., and Clarke, M.C. (1967). Does the agent of scrapie replicate without nucleic acid? Nature *214*, 764–766.

8. Arnold, J.E., Tipler, C., Laszlo, L., Hope, J., Landon, M., and Mayer, R.J. (1995). The abnormal isoform of the prion protein accumulates in late-endosome-like organelles in scrapie-infected mouse brain. J. Pathol. *176*, 403–411.

9. Aronoff-Spencer, E., Burns, C.S., Avdievich, N.I., Gerfen, G.J., Peisach, J., Antholine, W.E., Ball, H.L., Cohen, F.E., Prusiner, S.B., and Millhauser, G.L. (2000). Identification of the Cu2+ binding sites in the N-terminal domain of the prion protein by EPR and CD spectroscopy. Biochemistry (Mosc.) *39*, 13760–13771.

10. Ashok, A., and Hegde, R.S. (2009). Selective processing and metabolism of disease-causing mutant prion proteins. PLoS Pathog. *5*, e1000479.

11. Ballerini, C., Gourdain, P., Bachy, V., Blanchard, N., Levavasseur, E., Grégoire, S., Fontes, P., Aucouturier, P., Hivroz, C., and Carnaud, C. (2006). Functional implication of cellular prion protein in antigen-driven interactions between T cells and dendritic cells. J. Immunol. Baltim. Md 1950 *176*, 7254–7262.

12. Barmada, S.J., and Harris, D.A. (2005). Visualization of prion infection in transgenic mice expressing green fluorescent protein-tagged prion protein. J. Neurosci. Off. J. Soc. Neurosci. *25*, 5824–5832.

13. Baskakov, I.V., Legname, G., Baldwin, M.A., Prusiner, S.B., and Cohen, F.E. (2002). Pathway complexity of prion protein assembly into amyloid. J. Biol. Chem. *277*, 21140–21148.

14. Basu, S., Mohan, M.L., Luo, X., Kundu, B., Kong, Q., and Singh, N. (2007). Modulation of proteinase K-resistant prion protein in cells and infectious brain

homogenate by redox iron: implications for prion replication and disease pathogenesis. Mol. Biol. Cell *18*, 3302–3312.

15. Béranger, F., Mangé, A., Goud, B., and Lehmann, S. (2002). Stimulation of PrP(C) retrograde transport toward the endoplasmic reticulum increases accumulation of PrP(Sc) in prion-infected cells. J. Biol. Chem. *277*, 38972–38977.

16. Berti, F., Gaggelli, E., Guerrini, R., Janicka, A., Kozlowski, H., Legowska, A., Miecznikowska, H., Migliorini, C., Pogni, R., Remelli, M., et al. (2007). Structural and dynamic characterization of copper(II) binding of the human prion protein outside the octarepeat region. Chem. Weinh. Bergstr. Ger. *13*, 1991–2001.

17. Blakemore, W.F. (1972). Observations on oligodendrocyte degeneration, the resolution of status spongiosus and remyelination in cuprizone intoxication in mice. J. Neurocytol. *1*, 413–426.

18. Bocharova, O.V., Breydo, L., Salnikov, V.V., and Baskakov, I.V. (2005). Copper(II) inhibits in vitro conversion of prion protein into amyloid fibrils. Biochemistry (Mosc.) *44*, 6776–6787.

19. Bonomo, R.P., Imperllizzeri, G., Pappalardo, G., Rizzarelli, E., and Tabbì, G. (2000). Copper(II) binding modes in the prion octapeptide PHGGGWGQ: a spectroscopic and voltammetric study. Chem. Weinh. Bergstr. Ger. *6*, 4195–4202.

20. Borchelt, D.R., Taraboulos, A., and Prusiner, S.B. (1992). Evidence for synthesis of scrapie prion proteins in the endocytic pathway. J. Biol. Chem. *267*, 16188–16199.

21. Brazier, M.W., Davies, P., Player, E., Marken, F., Viles, J.H., and Brown, D.R. (2008). Manganese binding to the prion protein. J. Biol. Chem. *283*, 12831–12839.

22. Bremer, J., Baumann, F., Tiberi, C., Wessig, C., Fischer, H., Schwarz, P., Steele, A.D., Toyka, K.V., Nave, K.-A., Weis, J., et al. (2010). Axonal prion protein is required for peripheral myelin maintenance. Nat. Neurosci. *13*, 310–318.

23. Brown, D.R. (2001). Copper and prion disease. Brain Res. Bull. *55*, 165–173.

24. Brown, D.R., and Besinger, A. (1998). Prion protein expression and superoxide dismutase activity. Biochem. J. *334 (Pt 2)*, 423–429.

25. Brown, D.R., and Sassoon, J. (2002). Copper-dependent functions for the prion protein. Mol. Biotechnol. *22*, 165–178.

26. Brown, L.R., and Harris, D.A. (2003). Copper and zinc cause delivery of the prion protein from the plasma membrane to a subset of early endosomes and the Golgi. J. Neurochem. *87*, 353–363.

27. Brown, D.R., Qin, K., Herms, J.W., Madlung, A., Manson, J., Strome, R., Fraser, P.E., Kruck, T., von Bohlen, A., Schulz-Schaeffer, W., et al. (1997a). The cellular prion protein binds copper in vivo. Nature *390*, 684–687.

28. Brown, D.R., Schulz-Schaeffer, W.J., Schmidt, B., and Kretzschmar, H.A. (1997b). Prion protein-deficient cells show altered response to oxidative stress due to decreased SOD-1 activity. Exp. Neurol. *146*, 104–112.

29. Brown, D.R., Schmidt, B., and Kretzschmar, H.A. (1998). Effects of copper on survival of prion protein knockout neurons and glia. J. Neurochem. *70*, 1686–1693.

30. Brown, D.R., Wong, B.S., Hafiz, F., Clive, C., Haswell, S.J., and Jones, I.M. (1999). Normal prion protein has an activity like that of superoxide dismutase. Biochem. J. *344 Pt 1*, 1–5.

31. Brown, H.R., Goller, N.L., Rudelli, R.D., Merz, G.S., Wolfe, G.C., Wisniewski, H.M., and Robakis, N.K. (1990). The mRNA encoding the scrapie agent protein is present in a variety of non-neuronal cells. Acta Neuropathol. (Berl.) *80*, 1–6.

32. Brown, P., Rau, E.H., Johnson, B.K., Bacote, A.E., Gibbs, C.J., Jr, and Gajdusek, D.C. (2000). New studies on the heat resistance of hamster-adapted scrapie agent: threshold survival after ashing at 600 degrees C suggests an inorganic template of replication. Proc. Natl. Acad. Sci. U. S. A. *97*, 3418–3421.

33. Büeler, H., Fischer, M., Lang, Y., Bluethmann, H., Lipp, H.P., DeArmond, S.J., Prusiner, S.B., Aguet, M., and Weissmann, C. (1992). Normal development and behaviour of mice lacking the neuronal cell-surface PrP protein. Nature *356*, 577–582.

34. Büeler, H., Raeber, A., Sailer, A., Fischer, M., Aguzzi, A., and Weissmann, C. (1994). High prion and PrPSc levels but delayed onset of disease in scrapie-inoculated mice heterozygous for a disrupted PrP gene. Mol. Med. Camb. Mass *1*, 19–30.

35. Burns, C.S., Aronoff-Spencer, E., Dunham, C.M., Lario, P., Avdievich, N.I., Antholine, W.E., Olmstead, M.M., Vrielink, A., Gerfen, G.J., Peisach, J., et al. (2002). Molecular features of the copper binding sites in the octarepeat domain of the prion protein. Biochemistry (Mosc.) *41*, 3991–4001.

36. Burns, C.S., Aronoff-Spencer, E., Legname, G., Prusiner, S.B., Antholine, W.E., Gerfen, G.J., Peisach, J., and Millhauser, G.L. (2003). Copper coordination in the full-length, recombinant prion protein. Biochemistry (Mosc.) *42*, 6794–6803.

37. Burthem, J., Urban, B., Pain, A., and Roberts, D.J. (2001). The normal cellular prion protein is strongly expressed by myeloid dendritic cells. Blood *98*, 3733–3738.

38. Bush, A.I. (2000). Metals and neuroscience. Curr. Opin. Chem. Biol. *4*, 184–191.

39. Campbell, T.A., Palmer, M.S., Will, R.G., Gibb, W.R., Luthert, P.J., and Collinge, J. (1996). A prion disease with a novel 96-base pair insertional mutation in the prion protein gene. Neurology *46*, 761–766.

40. Caughey, B., Race, R.E., Ernst, D., Buchmeier, M.J., and Chesebro, B. (1989). Prion protein biosynthesis in scrapie-infected and uninfected neuroblastoma cells. J. Virol. *63*, 175–181.

41. Caughey, B., Neary, K., Buller, R., Ernst, D., Perry, L.L., Chesebro, B., and Race, R.E. (1990). Normal and scrapie-associated forms of prion protein differ in their sensitivities to phospholipase and proteases in intact neuroblastoma cells. J. Virol. *64*, 1093–1101.

42. Caughey, B., Raymond, G.J., Ernst, D., and Race, R.E. (1991a). N-terminal truncation of the scrapie-associated form of PrP by lysosomal protease(s): implications regarding the site of conversion of PrP to the protease-resistant state. J. Virol. *65*, 6597–6603.

43. Caughey, B., Baron, G.S., Chesebro, B., and Jeffrey, M. (2009). Getting a grip on prions: oligomers, amyloids, and pathological membrane interactions. Annu. Rev. Biochem. *78*, 177–204.

44. Caughey, B.W., Dong, A., Bhat, K.S., Ernst, D., Hayes, S.F., and Caughey, W.S. (1991b). Secondary structure analysis of the scrapie-associated protein PrP 27-30 in water by infrared spectroscopy. Biochemistry (Mosc.) *30*, 7672–7680.

45. Cereghetti, G.M., Schweiger, A., Glockshuber, R., and Van Doorslaer, S. (2003). Stability and Cu(II) binding of prion protein variants related to inherited human prion diseases. Biophys. J. *84*, 1985–1997.

46. Chattopadhyay, M., Walter, E.D., Newell, D.J., Jackson, P.J., Aronoff-Spencer, E., Peisach, J., Gerfen, G.J., Bennett, B., Antholine, W.E., and Millhauser, G.L. (2005). The octarepeat domain of the prion protein binds Cu(II) with three distinct coordination modes at pH 7.4. J. Am. Chem. Soc. *127*, 12647–12656.

47. Chen, S., Mangé, A., Dong, L., Lehmann, S., and Schachner, M. (2003). Prion protein as trans-interacting partner for neurons is involved in neurite outgrowth and neuronal survival. Mol. Cell. Neurosci. *22*, 227–233.

48. Chiarini, L.B., Freitas, A.R.O., Zanata, S.M., Brentani, R.R., Martins, V.R., and Linden, R. (2002). Cellular prion protein transduces neuroprotective signals. EMBO J. *21*, 3317–3326.

49. Chiesa, R., Piccardo, P., Ghetti, B., and Harris, D.A. (1998). Neurological illness in transgenic mice expressing a prion protein with an insertional mutation. Neuron *21*, 1339–1351.

50. Chiesa, R., Drisaldi, B., Quaglio, E., Migheli, A., Piccardo, P., Ghetti, B., and Harris, D.A. (2000). Accumulation of protease-resistant prion protein (PrP) and apoptosis of cerebellar granule cells in transgenic mice expressing a PrP insertional mutation. Proc. Natl. Acad. Sci. U. S. A. *97*, 5574–5579.

51. Choi, C.J., Kanthasamy, A., Anantharam, V., and Kanthasamy, A.G. (2006). Interaction of metals with prion protein: possible role of divalent cations in the pathogenesis of prion diseases. Neurotoxicology *27*, 777–787.

52. Colby, D.W., Zhang, Q., Wang, S., Groth, D., Legname, G., Riesner, D., and Prusiner, S.B. (2007). Prion detection by an amyloid seeding assay. Proc. Natl. Acad. Sci. U. S. A. *104*, 20914–20919.

53. Collinge, J., Whittington, M.A., Sidle, K.C., Smith, C.J., Palmer, M.S., Clarke, A.R., and Jefferys, J.G. (1994). Prion protein is necessary for normal synaptic function. Nature *370*, 295–297.

54. Cong, X., Casiraghi, N., Rossetti, G., Mohanty, S., Giachin, G., Legname, G., and Carloni, P. (2013). Role of prion disease-linked mutations in the intrinsically disordered N-terminal domain of the prion protein. J. Chem. Theory Comput.

55. Cox, D.L., Pan, J., and Singh, R.R.P. (2006). A mechanism for copper inhibition of infectious prion conversion. Biophys. J. *91*, L11–13.

56. Cruite, J.T., Abalos, G.C., Bellon, A., and Solforosi, L. (2011). Histidines in the octapeptide repeat of PrPC react with PrPSc at an acidic pH. Biochemistry (Mosc.) *50*, 1618–1623.

57. Cui, T., Daniels, M., Wong, B.S., Li, R., Sy, M.-S., Sassoon, J., and Brown, D.R. (2003). Mapping the functional domain of the prion protein. Eur. J. Biochem. FEBS *270*, 3368–3376.

58. Daniels, M., and Brown, D.R. (2002). Purification and preparation of prion protein: synaptic superoxide dismutase. Methods Enzymol. *349*, 258–267.

59. Davies, P., Fontaine, S.N., Moualla, D., Wang, X., Wright, J.A., and Brown, D.R. (2008). Amyloidogenic metal-binding proteins: new investigative pathways. Biochem. Soc. Trans. *36*, 1299–1303.

60. Deleault, N.R., Lucassen, R.W., and Supattapone, S. (2003). RNA molecules stimulate prion protein conversion. Nature *425*, 717–720.

61. Dobson, A.W., Erikson, K.M., and Aschner, M. (2004). Manganese neurotoxicity. Ann. N. Y. Acad. Sci. *1012*, 115–128.

62. Drisaldi, B., Stewart, R.S., Adles, C., Stewart, L.R., Quaglio, E., Biasini, E., Fioriti, L., Chiesa, R., and Harris, D.A. (2003). Mutant PrP is delayed in its exit from the endoplasmic reticulum, but neither wild-type nor mutant PrP undergoes retrotranslocation prior to proteasomal degradation. J. Biol. Chem. *278*, 21732–21743.

63. Drisaldi, B., Coomaraswamy, J., Mastrangelo, P., Strome, B., Yang, J., Watts, J.C., Chishti, M.A., Marvi, M., Windl, O., Ahrens, R., et al. (2004). Genetic mapping of activity determinants within cellular prion proteins: N-terminal modules in PrPC offset pro-apoptotic activity of the Doppel helix B/B' region. J. Biol. Chem. *279*, 55443–55454.

64. Emwas, A.-H.M., Al-Talla, Z.A., Guo, X., Al-Ghamdi, S., and Al-Masri, H.T. (2013). Utilizing NMR and EPR spectroscopy to probe the role of copper in prion diseases. Magn. Reson. Chem. MRC *51*, 255–268.

65. Van den Ent, F., and Löwe, J. (2006). RF cloning: a restriction-free method for inserting target genes into plasmids. J. Biochem. Biophys. Methods *67*, 67–74.

66. Fischer, M., Rülicke, T., Raeber, A., Sailer, A., Moser, M., Oesch, B., Brandner, S., Aguzzi, A., and Weissmann, C. (1996). Prion protein (PrP) with amino-proximal deletions restoring susceptibility of PrP knockout mice to scrapie. EMBO J. *15*, 1255–1264.

67. Flechsig, E., Shmerling, D., Hegyi, I., Raeber, A.J., Fischer, M., Cozzio, A., von Mering, C., Aguzzi, A., and Weissmann, C. (2000). Prion protein devoid of the octapeptide repeat region restores susceptibility to scrapie in PrP knockout mice. Neuron *27*, 399–408.

68. Ford, M.J., Burton, L.J., Morris, R.J., and Hall, S.M. (2002). Selective expression of prion protein in peripheral tissues of the adult mouse. Neuroscience *113*, 177–192.

69. Gaeta, A., and Hider, R.C. (2005). The crucial role of metal ions in neurodegeneration: the basis for a promising therapeutic strategy. Br. J. Pharmacol. *146*, 1041–1059.

70. Garnett, A.P., and Viles, J.H. (2003). Copper binding to the octarepeats of the prion protein. Affinity, specificity, folding, and cooperativity: insights from circular dichroism. J. Biol. Chem. *278*, 6795–6802.

71. Gasset, M., Baldwin, M.A., Fletterick, R.J., and Prusiner, S.B. (1993). Perturbation of the secondary structure of the scrapie prion protein under conditions that alter infectivity. Proc. Natl. Acad. Sci. U. S. A. *90*, 1–5.

72. Gerber, R., Tahiri-Alaoui, A., Hore, P.J., and James, W. (2008). Conformational pH dependence of intermediate states during oligomerization of the human prion protein. Protein Sci. Publ. Protein Soc. *17*, 537–544.

73. Glatzel, M., and Aguzzi, A. (2001). The shifting biology of prions. Brain Res. Brain Res. Rev. *36*, 241–248.

74. Godsave, S.F., Wille, H., Kujala, P., Latawiec, D., DeArmond, S.J., Serban, A., Prusiner, S.B., and Peters, P.J. (2008). Cryo-immunogold electron microscopy for prions: toward identification of a conversion site. J. Neurosci. Off. J. Soc. Neurosci. *28*, 12489–12499.

75. Goldfarb, L.G., Brown, P., McCombie, W.R., Goldgaber, D., Swergold, G.D., Wills, P.R., Cervenakova, L., Baron, H., Gibbs, C.J., Jr, and Gajdusek, D.C. (1991). Transmissible familial Creutzfeldt-Jakob disease associated with five, seven, and eight extra octapeptide coding repeats in the PRNP gene. Proc. Natl. Acad. Sci. U. S. A. *88*, 10926–10930.

76. Gousset, K., and Zurzolo, C. (2009). Tunnelling nanotubes: a highway for prion spreading? Prion *3*, 94–98.

77. Gousset, K., Schiff, E., Langevin, C., Marijanovic, Z., Caputo, A., Browman, D.T., Chenouard, N., de Chaumont, F., Martino, A., Enninga, J., et al. (2009). Prions hijack tunnelling nanotubes for intercellular spread. Nat. Cell Biol. *11*, 328–336.

78. Griffith, J.S. (1967). Self-replication and scrapie. Nature *215*, 1043–1044.

79. Guentchev, M., Voigtländer, T., Haberler, C., Groschup, M.H., and Budka, H. (2000). Evidence for oxidative stress in experimental prion disease. Neurobiol. Dis. *7*, 270–273.

80. Gustiananda, M., Haris, P.I., Milburn, P.J., and Gready, J.E. (2002). Copper-induced conformational change in a marsupial prion protein repeat peptide probed using FTIR spectroscopy. FEBS Lett. *512*, 38–42.

81. Haraguchi, T., Fisher, S., Olofsson, S., Endo, T., Groth, D., Tarentino, A., Borchelt, D.R., Teplow, D., Hood, L., and Burlingame, A. (1989). Asparagine-linked glycosylation of the scrapie and cellular prion proteins. Arch. Biochem. Biophys. *274*, 1–13.

82. Hardy, J., and Selkoe, D.J. (2002). The amyloid hypothesis of Alzheimer's disease: progress and problems on the road to therapeutics. Science *297*, 353–356.

83. Harris, D.A. (1999). Cellular biology of prion diseases. Clin. Microbiol. Rev. *12*, 429–444.

84. Harris, E.D. (1992). Copper as a cofactor and regulator of copper,zinc superoxide dismutase. J. Nutr. *122*, 636–640.

85. Hartter, D.E., and Barnea, A. (1988). Evidence for release of copper in the brain: depolarization-induced release of newly taken-up 67copper. Synap. N. Y. N *2*, 412–415.

86. Hegde, R.S., Mastrianni, J.A., Scott, M.R., DeFea, K.A., Tremblay, P., Torchia, M., DeArmond, S.J., Prusiner, S.B., and Lingappa, V.R. (1998). A transmembrane form of the prion protein in neurodegenerative disease. Science *279*, 827–834.

87. Hegde, R.S., Tremblay, P., Groth, D., DeArmond, S.J., Prusiner, S.B., and Lingappa, V.R. (1999). Transmissible and genetic prion diseases share a common pathway of neurodegeneration. Nature *402*, 822–826.

88. Herms, J., Tings, T., Gall, S., Madlung, A., Giese, A., Siebert, H., Schürmann, P., Windl, O., Brose, N., and Kretzschmar, H. (1999). Evidence of presynaptic location and function of the prion protein. J. Neurosci. Off. J. Soc. Neurosci. *19*, 8866–8875.

89. Hiraga, C., Kobayashi, A., and Kitamoto, T. (2009). The number of octapeptide repeat affects the expression and conversion of prion protein. Biochem. Biophys. Res. Commun. *382*, 715–719.

90. Hopt, A., Korte, S., Fink, H., Panne, U., Niessner, R., Jahn, R., Kretzschmar, H., and Herms, J. (2003). Methods for studying synaptosomal copper release. J. Neurosci. Methods *128*, 159–172.

91. Hornemann, S., and Glockshuber, R. (1998). A scrapie-like unfolding intermediate of the prion protein domain PrP(121-231) induced by acidic pH. Proc. Natl. Acad. Sci. U. S. A. *95*, 6010–6014.

92. Hornshaw, M.P., McDermott, J.R., Candy, J.M., and Lakey, J.H. (1995). Copper binding to the N-terminal tandem repeat region of mammalian and avian prion protein: structural studies using synthetic peptides. Biochem. Biophys. Res. Commun. *214*, 993–999.

93. Hung, Y.H., Bush, A.I., and Cherny, R.A. (2010). Copper in the brain and Alzheimer's disease. J. Biol. Inorg. Chem. JBIC Publ. Soc. Biol. Inorg. Chem. *15*, 61–76.

94. Hutter, G., Heppner, F.L., and Aguzzi, A. (2003). No superoxide dismutase activity of cellular prion protein in vivo. Biol. Chem. *384*, 1279–1285.

95. Ilc, G., Giachin, G., Jaremko, M., Jaremko, L., Benetti, F., Plavec, J., Zhukov, I., and Legname, G. (2010). NMR Structure of the Human Prion Protein with the Pathological Q212P Mutation Reveals Unique Structural Features. PLoS ONE *5*.

96. Isaacs, J.D., Jackson, G.S., and Altmann, D.M. (2006). The role of the cellular prion protein in the immune system. Clin. Exp. Immunol. *146*, 1–8.

97. Ivanova, L., Barmada, S., Kummer, T., and Harris, D.A. (2001). Mutant prion proteins are partially retained in the endoplasmic reticulum. J. Biol. Chem. *276*, 42409–42421.

98. Jackson, G.S., and Collinge, J. (2001). The molecular pathology of CJD: old and new variants. Mol. Pathol. MP *54*, 393–399.

99. Jackson, G.S., Murray, I., Hosszu, L.L., Gibbs, N., Waltho, J.P., Clarke, A.R., and Collinge, J. (2001). Location and properties of metal-binding sites on the human prion protein. Proc. Natl. Acad. Sci. U. S. A. *98*, 8531–8535.

100. Jobling, M.F., Huang, X., Stewart, L.R., Barnham, K.J., Curtain, C., Volitakis, I., Perugini, M., White, A.R., Cherny, R.A., Masters, C.L., et al. (2001). Copper and zinc binding modulates the aggregation and neurotoxic properties of the prion peptide PrP106-126. Biochemistry (Mosc.) *40*, 8073–8084.

101. Jones, C.E., Abdelraheim, S.R., Brown, D.R., and Viles, J.H. (2004). Preferential Cu2+ coordination by His96 and His111 induces beta-sheet formation in the unstructured amyloidogenic region of the prion protein. J. Biol. Chem. *279*, 32018–32027.

102. Jones, C.E., Klewpatinond, M., Abdelraheim, S.R., Brown, D.R., and Viles, J.H. (2005). Probing copper2+ binding to the prion protein using diamagnetic nickel2+ and 1H NMR: the unstructured N terminus facilitates the coordination of six copper2+ ions at physiological concentrations. J. Mol. Biol. *346*, 1393–1407.

103. Jouvin-Marche, E., Attuil-Audenis, V., Aude-Garcia, C., Rachidi, W., Zabel, M., Podevin-Dimster, V., Siret, C., Huber, C., Martinic, M., Riondel, J., et al. (2006). Overexpression of cellular prion protein induces an antioxidant environment altering T cell development in the thymus. J. Immunol. Baltim. Md 1950 *176*, 3490–3497.

104. Kanaani, J., Prusiner, S.B., Diacovo, J., Baekkeskov, S., and Legname, G. (2005). Recombinant prion protein induces rapid polarization and development of synapses in embryonic rat hippocampal neurons in vitro. J. Neurochem. *95*, 1373–1386.

105. Kaneko, K., Zulianello, L., Scott, M., Cooper, C.M., Wallace, A.C., James, T.L., Cohen, F.E., and Prusiner, S.B. (1997a). Evidence for protein X binding to a discontinuous epitope on the cellular prion protein during scrapie prion propagation. Proc. Natl. Acad. Sci. U. S. A. *94*, 10069–10074.

106. Kaneko, K., Zulianello, L., Scott, M., Cooper, C.M., Wallace, A.C., James, T.L., Cohen, F.E., and Prusiner, S.B. (1997b). Evidence for protein X binding to a discontinuous epitope on the cellular prion protein during scrapie prion propagation. Proc. Natl. Acad. Sci. U. S. A. *94*, 10069–10074.

107. Kaplan, J. (2002). Mechanisms of cellular iron acquisition: another iron in the fire. Cell *111*, 603–606.

108. Kardos, J., Kovács, I., Hajós, F., Kálmán, M., and Simonyi, M. (1989). Nerve endings from rat brain tissue release copper upon depolarization. A possible role in regulating neuronal excitability. Neurosci. Lett. *103*, 139–144.

109. Kascsak, R.J., Rubenstein, R., Merz, P.A., Tonna-DeMasi, M., Fersko, R., Carp, R.I., Wisniewski, H.M., and Diringer, H. (1987). Mouse polyclonal and monoclonal antibody to scrapie-associated fibril proteins. J. Virol. *61*, 3688–3693.

110. Kim, B.-H., Lee, H.-G., Choi, J.-K., Kim, J.-I., Choi, E.-K., Carp, R.I., and Kim, Y.-S. (2004). The cellular prion protein (PrPC) prevents apoptotic neuronal cell death and mitochondrial dysfunction induced by serum deprivation. Brain Res. Mol. Brain Res. *124*, 40–50.

111. Kim, N.-H., Choi, J.-K., Jeong, B.-H., Kim, J.-I., Kwon, M.-S., Carp, R.I., and Kim, Y.-S. (2005). Effect of transition metals (Mn, Cu, Fe) and deoxycholic acid (DA) on the conversion of PrPC to PrPres. FASEB J. Off. Publ. Fed. Am. Soc. Exp. Biol. *19*, 783–785.

112. Kimberlin, R.H., and Millson, G.C. (1976). The effects of cuprizone toxicity on the incubation period of scrapie in mice. J. Comp. Pathol. *86*, 489–496.

113. Klamt, F., Dal-Pizzol, F., Conte da Frota, M.L., Jr, Walz, R., Andrades, M.E., da Silva, E.G., Brentani, R.R., Izquierdo, I., and Fonseca Moreira, J.C. (2001). Imbalance of antioxidant defense in mice lacking cellular prion protein. Free Radic. Biol. Med. *30*, 1137–1144.

114. Kramer, M.L., Kratzin, H.D., Schmidt, B., Römer, A., Windl, O., Liemann, S., Hornemann, S., and Kretzschmar, H. (2001). Prion protein binds copper within the physiological concentration range. J. Biol. Chem. *276*, 16711–16719.

115. Krammer, C., Schätzl, H.M., and Vorberg, I. (2009). Prion-like propagation of cytosolic protein aggregates: insights from cell culture models. Prion *3*, 206–212.

116. Kretzschmar, H.A., Prusiner, S.B., Stowring, L.E., and DeArmond, S.J. (1986). Scrapie prion proteins are synthesized in neurons. Am. J. Pathol. *122*, 1–5.

117. Lainé, J., Marc, M.E., Sy, M.S., and Axelrad, H. (2001). Cellular and subcellular morphological localization of normal prion protein in rodent cerebellum. Eur. J. Neurosci. *14*, 47–56.

118. Lauren, J., Gimbel, D.A., Nygaard, H.B., Gilbert, J.W., and Strittmatter, S.M. (2009). Cellular Prion Protein Mediates Impairment of Synaptic Plasticity by Amyloid-? Oligomers. Nature *457*, 1128–1132.

119. Lee, K.S., Magalhães, A.C., Zanata, S.M., Brentani, R.R., Martins, V.R., and Prado, M.A. (2001). Internalization of mammalian fluorescent cellular prion protein and N-terminal deletion mutants in living cells. J. Neurochem. *79*, 79–87.

120. Lee, K.S., Raymond, L.D., Schoen, B., Raymond, G.J., Kett, L., Moore, R.A., Johnson, L.M., Taubner, L., Speare, J.O., Onwubiko, H.A., et al. (2007). Hemin interactions and alterations of the subcellular localization of prion protein. J. Biol. Chem. *282*, 36525–36533.

121. Lehmann, S. (2002). Metal ions and prion diseases. Curr. Opin. Chem. Biol. *6*, 187–192.

122. Lehmann, S., and Harris, D.A. (1996). Two mutant prion proteins expressed in cultured cells acquire biochemical properties reminiscent of the scrapie isoform. Proc. Natl. Acad. Sci. U. S. A. *93*, 5610–5614.

123. Lekishvili, T., Sassoon, J., Thompsett, A.R., Green, A., Ironside, J.W., and Brown, D.R. (2004). BSE and vCJD cause disturbance to uric acid levels. Exp. Neurol. *190*, 233–244.

124. Liang, J., and Kong, Q. (2012). α-Cleavage of cellular prion protein. Prion *6*, 453–460.

125. Ma, J., and Lindquist, S. (2001). Wild-type PrP and a mutant associated with prion disease are subject to retrograde transport and proteasome degradation. Proc. Natl. Acad. Sci. U. S. A. *98*, 14955–14960.

126. Maley, F., Trimble, R.B., Tarentino, A.L., and Plummer, T.H., Jr (1989). Characterization of glycoproteins and their associated oligosaccharides through the use of endoglycosidases. Anal. Biochem. *180*, 195–204.

127. Marijanovic, Z., Caputo, A., Campana, V., and Zurzolo, C. (2009). Identification of an intracellular site of prion conversion. PLoS Pathog. *5*, e1000426.

128. Massignan, T., Biasini, E., Lauranzano, E., Veglianese, P., Pignataro, M., Fioriti, L., Harris, D.A., Salmona, M., Chiesa, R., and Bonetto, V. (2010). Mutant prion protein expression is associated with an alteration of the Rab GDP dissociation inhibitor alpha (GDI)/Rab11 pathway. Mol. Cell. Proteomics MCP *9*, 611–622.

129. Mattei, V., Garofalo, T., Misasi, R., Circella, A., Manganelli, V., Lucania, G., Pavan, A., and Sorice, M. (2004). Prion protein is a component of the multimolecular signaling complex involved in T cell activation. FEBS Lett. *560*, 14–18.

130. Mayer, R.J., Landon, M., Laszlo, L., Lennox, G., and Lowe, J. (1992). Protein processing in lysosomes: the new therapeutic target in neurodegenerative disease. Lancet *340*, 156–159.

131. McKenzie, D., Bartz, J., Mirwald, J., Olander, D., Marsh, R., and Aiken, J. (1998). Reversibility of scrapie inactivation is enhanced by copper. J. Biol. Chem. *273*, 25545–25547.

132. McKinley, M.P., Bolton, D.C., and Prusiner, S.B. (1983). A protease-resistant protein is a structural component of the scrapie prion. Cell *35*, 57–62.

133. McKinley, M.P., Taraboulos, A., Kenaga, L., Serban, D., Stieber, A., DeArmond, S.J., Prusiner, S.B., and Gonatas, N. (1991). Ultrastructural localization of scrapie prion proteins in cytoplasmic vesicles of infected cultured cells. Lab. Investig. J. Tech. Methods Pathol. *65*, 622–630.

134. McLennan, N.F., Brennan, P.M., McNeill, A., Davies, I., Fotheringham, A., Rennison, K.A., Ritchie, D., Brannan, F., Head, M.W., Ironside, J.W., et al. (2004). Prion protein accumulation and neuroprotection in hypoxic brain damage. Am. J. Pathol. *165*, 227–235.

135. Meier, P., Genoud, N., Prinz, M., Maissen, M., Rülicke, T., Zurbriggen, A., Raeber, A.J., and Aguzzi, A. (2003). Soluble dimeric prion protein binds PrP(Sc) in vivo and antagonizes prion disease. Cell *113*, 49–60.

136. Millhauser, G.L. (2004). Copper binding in the prion protein. Acc. Chem. Res. *37*, 79–85.

137. Millhauser, G.L. (2007). Copper and the prion protein: methods, structures, function, and disease. Annu. Rev. Phys. Chem. *58*, 299–320.

138. Mironov, A., Jr, Latawiec, D., Wille, H., Bouzamondo-Bernstein, E., Legname, G., Williamson, R.A., Burton, D., DeArmond, S.J., Prusiner, S.B., and Peters, P.J. (2003). Cytosolic prion protein in neurons. J. Neurosci. Off. J. Soc. Neurosci. *23*, 7183–7193.

139. Miura, T., Hori-i, A., and Takeuchi, H. (1996). Metal-dependent alpha-helix formation promoted by the glycine-rich octapeptide region of prion protein. FEBS Lett. *396*, 248–252.

140. Miura, T., Hori-i, A., Mototani, H., and Takeuchi, H. (1999). Raman spectroscopic study on the copper(II) binding mode of prion octapeptide and its pH dependence. Biochemistry (Mosc.) *38*, 11560–11569.

141. Miura, T., Sasaki, S., Toyama, A., and Takeuchi, H. (2005). Copper reduction by the octapeptide repeat region of prion protein: pH dependence and implications in cellular copper uptake. Biochemistry (Mosc.) *44*, 8712–8720.

142. Moore, R.C., Lee, I.Y., Silverman, G.L., Harrison, P.M., Strome, R., Heinrich, C., Karunaratne, A., Pasternak, S.H., Chishti, M.A., Liang, Y., et al. (1999). Ataxia in prion protein (PrP)-deficient mice is associated with upregulation of the novel PrP-like protein doppel. J. Mol. Biol. *292*, 797–817.

143. Moreno-Gonzalez, I., and Soto, C. (2011). Misfolded protein aggregates: mechanisms, structures and potential for disease transmission. Semin. Cell Dev. Biol. *22*, 482–487.

144. Mouillet-Richard, S., Ermonval, M., Chebassier, C., Laplanche, J.L., Lehmann, S., Launay, J.M., and Kellermann, O. (2000). Signal transduction through prion protein. Science *289*, 1925–1928.

145. Nazor, K.E., Seward, T., and Telling, G.C. (2007). Motor behavioral and neuropathological deficits in mice deficient for normal prion protein expression. Biochim. Biophys. Acta *1772*, 645–653.

146. Negro, A., Ballarin, C., Bertoli, A., Massimino, M.L., and Sorgato, M.C. (2001). The metabolism and imaging in live cells of the bovine prion protein in its native form or carrying single amino acid substitutions. Mol. Cell. Neurosci. *17*, 521–538.

147. Nishina, K., Jenks, S., and Supattapone, S. (2004). Ionic strength and transition metals control PrPSc protease resistance and conversion-inducing activity. J. Biol. Chem. *279*, 40788–40794.

148. Oesch, B., Westaway, D., Wälchli, M., McKinley, M.P., Kent, S.B., Aebersold, R., Barry, R.A., Tempst, P., Teplow, D.B., and Hood, L.E. (1985). A cellular gene encodes scrapie PrP 27-30 protein. Cell *40*, 735–746.

149. Ostrerova-Golts, N., Petrucelli, L., Hardy, J., Lee, J.M., Farer, M., and Wolozin, B. (2000). The A53T alpha-synuclein mutation increases iron-dependent aggregation and toxicity. J. Neurosci. Off. J. Soc. Neurosci. *20*, 6048–6054.

150. Pan, K.M., Baldwin, M., Nguyen, J., Gasset, M., Serban, A., Groth, D., Mehlhorn, I., Huang, Z., Fletterick, R.J., and Cohen, F.E. (1993). Conversion of alpha-helices into beta-sheets features in the formation of the scrapie prion proteins. Proc. Natl. Acad. Sci. U. S. A. *90*, 10962–10966.

151. Pattison, I.H., and Jebbett, J.N. (1973). Clinical and histological recovery from the scrapie-like spongiform encephalopathy produced in mice by feeding them with cuprizone. J. Pathol. *109*, 245–250.

152. Pauly, P.C., and Harris, D.A. (1998). Copper stimulates endocytosis of the prion protein. J. Biol. Chem. *273*, 33107–33110.

153. Perera, W.S., and Hooper, N.M. (2001a). Ablation of the metal ion-induced endocytosis of the prion protein by disease-associated mutation of the octarepeat region. Curr. Biol. CB *11*, 519–523.

154. Perera, W.S., and Hooper, N.M. (2001b). Ablation of the metal ion-induced endocytosis of the prion protein by disease-associated mutation of the octarepeat region. Curr. Biol. CB *11*, 519–523.

155. Peretz, D., Williamson, R.A., Matsunaga, Y., Serban, H., Pinilla, C., Bastidas, R.B., Rozenshteyn, R., James, T.L., Houghten, R.A., Cohen, F.E., et al. (1997). A conformational transition at the N terminus of the prion protein features in formation of the scrapie isoform. J. Mol. Biol. *273*, 614–622.

156. Petersen, R.B., Parchi, P., Richardson, S.L., Urig, C.B., and Gambetti, P. (1996). Effect of the D178N mutation and the codon 129 polymorphism on the metabolism of the prion protein. J. Biol. Chem. *271*, 12661–12668.

157. Pimpinelli, F., Lehmann, S., and Maridonneau-Parini, I. (2005). The scrapie prion protein is present in flotillin-1-positive vesicles in central- but not peripheral-derived neuronal cell lines. Eur. J. Neurosci. *21*, 2063–2072.

158. Polano, M., Bek, A., Benetti, F., Lazzarino, M., and Legname, G. (2009). Structural Insights into Alternate Aggregated Prion Protein Forms. J. Mol. Biol. *393*, 1033–1042.

159. Prestori, F., Rossi, P., Bearzatto, B., Lainé, J., Necchi, D., Diwakar, S., Schiffmann, S.N., Axelrad, H., and D'Angelo, E. (2008). Altered neuron excitability and synaptic plasticity in the cerebellar granular layer of juvenile prion protein knock-out mice with impaired motor control. J. Neurosci. Off. J. Soc. Neurosci. *28*, 7091–7103.

160. Priola, S.A., and Chesebro, B. (1998). Abnormal properties of prion protein with insertional mutations in different cell types. J. Biol. Chem. *273*, 11980–11985.

161. Prusiner, S.B. (1982). Novel proteinaceous infectious particles cause scrapie. Science *216*, 136–144.

162. Prusiner, S.B. (1984). Prions. Sci. Am. *251*, 50–59.

163. Prusiner, S.B., Scott, M.R., DeArmond, S.J., and Cohen, F.E. (1998). Prion protein biology. Cell *93*, 337–348.

164. Qin, K., Yang, D.S., Yang, Y., Chishti, M.A., Meng, L.J., Kretzschmar, H.A., Yip, C.M., Fraser, P.E., and Westaway, D. (2000). Copper(II)-induced conformational changes and protease resistance in recombinant and cellular PrP. Effect of protein age and deamidation. J. Biol. Chem. *275*, 19121–19131.

165. Qin, K., Yang, Y., Mastrangelo, P., and Westaway, D. (2002). Mapping Cu(II) binding sites in prion proteins by diethyl pyrocarbonate modification and matrix-assisted laser desorption ionization-time of flight (MALDI-TOF) mass spectrometric footprinting. J. Biol. Chem. *277*, 1981–1990.

166. Quaglio, E., Chiesa, R., and Harris, D.A. (2001). Copper converts the cellular prion protein into a protease-resistant species that is distinct from the scrapie isoform. J. Biol. Chem. *276*, 11432–11438.

167. Rachidi, W., Vilette, D., Guiraud, P., Arlotto, M., Riondel, J., Laude, H., Lehmann, S., and Favier, A. (2003). Expression of prion protein increases cellular copper binding and antioxidant enzyme activities but not copper delivery. J. Biol. Chem. *278*, 9064–9072.

168. Rajendran, L., Udayar, V., and Goodger, Z.V. (2012). Lipid-anchored drugs for delivery into subcellular compartments. Trends Pharmacol. Sci. *33*, 215–222.

169. Rial, D., Duarte, F.S., Xikota, J.C., Schmitz, A.E., Dafré, A.L., Figueiredo, C.P., Walz, R., and Prediger, R.D.S. (2009). Cellular prion protein modulates age-related behavioral and neurochemical alterations in mice. Neuroscience *164*, 896–907.

170. Rogers, M., Yehiely, F., Scott, M., and Prusiner, S.B. (1993). Conversion of truncated and elongated prion proteins into the scrapie isoform in cultured cells. Proc. Natl. Acad. Sci. U. S. A. *90*, 3182–3186.

171. Rogers, d.r. (1965). Screening for amyloid with the thioflavin-T fluorescent method. Am. J. Clin. Pathol. *44*, 59–61.

172. Rossi, D., Cozzio, A., Flechsig, E., Klein, M.A., Rülicke, T., Aguzzi, A., and Weissmann, C. (2001). Onset of ataxia and Purkinje cell loss in PrP null mice inversely correlated with Dpl level in brain. EMBO J. *20*, 694–702.

173. Roucou, X., Gains, M., and LeBlanc, A.C. (2004). Neuroprotective functions of prion protein. J. Neurosci. Res. *75*, 153–161.

174. Rustom, A. (2009). Hen or egg?: some thoughts on tunneling nanotubes. Ann. N. Y. Acad. Sci. *1178*, 129–136.

175. Safar, J., Roller, P.P., Gajdusek, D.C., and Gibbs, C.J., Jr (1993). Conformational transitions, dissociation, and unfolding of scrapie amyloid (prion) protein. J. Biol. Chem. *268*, 20276–20284.

176. Sakudo, A., Wu, G., Onodera, T., and Ikuta, K. (2008). Octapeptide repeat region of prion protein (PrP) is required at an early stage for production of abnormal prion protein in PrP-deficient neuronal cell line. Biochem. Biophys. Res. Commun. *365*, 164–169.

177. Scheiber, I.F., Mercer, J.F.B., and Dringen, R. Metabolism and functions of copper in brain. Prog. Neurobiol.

178. Scott, M.R., Will, R., Ironside, J., Nguyen, H.O., Tremblay, P., DeArmond, S.J., and Prusiner, S.B. (1999). Compelling transgenetic evidence for transmission of bovine spongiform encephalopathy prions to humans. Proc. Natl. Acad. Sci. U. S. A. *96*, 15137–15142.

179. Shyng, S.L., Huber, M.T., and Harris, D.A. (1993). A prion protein cycles between the cell surface and an endocytic compartment in cultured neuroblastoma cells. J. Biol. Chem. *268*, 15922–15928.

180. Sigurdsson, E.M., Brown, D.R., Alim, M.A., Scholtzova, H., Carp, R., Meeker, H.C., Prelli, F., Frangione, B., and Wisniewski, T. (2003). Copper chelation delays the onset of prion disease. J. Biol. Chem. *278*, 46199–46202.

181. Singh, A., Kong, Q., Luo, X., Petersen, R.B., Meyerson, H., and Singh, N. (2009). Prion protein (PrP) knock-out mice show altered iron metabolism: a functional role for PrP in iron uptake and transport. PloS One *4*, e6115.

182. Singh, N., Das, D., Singh, A., and Mohan, M.L. (2010). Prion protein and metal interaction: physiological and pathological implications. Curr. Issues Mol. Biol. *12*, 99–107.

183. Solforosi, L., Criado, J.R., McGavern, D.B., Wirz, S., Sánchez-Alavez, M., Sugama, S., DeGiorgio, L.A., Volpe, B.T., Wiseman, E., Abalos, G., et al. (2004). Cross-linking cellular prion protein triggers neuronal apoptosis in vivo. Science *303*, 1514–1516.

184. Stahl, N., Borchelt, D.R., Hsiao, K., and Prusiner, S.B. (1987). Scrapie prion protein contains a phosphatidylinositol glycolipid. Cell *51*, 229–240.

185. Stahl, N., Baldwin, M.A., Teplow, D.B., Hood, L., Gibson, B.W., Burlingame, A.L., and Prusiner, S.B. (1993). Structural studies of the scrapie prion protein using mass spectrometry and amino acid sequencing. Biochemistry (Mosc.) *32*, 1991–2002.

186. Steele, A.D., Lindquist, S., and Aguzzi, A. (2007). The prion protein knockout mouse: a phenotype under challenge. Prion *1*, 83–93.

187. Stevens, D.J., Walter, E.D., Rodríguez, A., Draper, D., Davies, P., Brown, D.R., and Millhauser, G.L. (2009). Early onset prion disease from octarepeat expansion correlates with copper binding properties. PLoS Pathog. *5*, e1000390.

188. Stöckel, J., Safar, J., Wallace, A.C., Cohen, F.E., and Prusiner, S.B. (1998a). Prion protein selectively binds copper(II) ions. Biochemistry (Mosc.) *37*, 7185–7193.

189. Stöckel, J., Safar, J., Wallace, A.C., Cohen, F.E., and Prusiner, S.B. (1998b). Prion protein selectively binds copper(II) ions. Biochemistry (Mosc.) *37*, 7185–7193.

190. Sunyach, C., Jen, A., Deng, J., Fitzgerald, K.T., Frobert, Y., Grassi, J., McCaffrey, M.W., and Morris, R. (2003). The mechanism of internalization of glycosylphosphatidylinositol-anchored prion protein. EMBO J. *22*, 3591–3601.

191. Supattapone, S. (2004). Prion protein conversion in vitro. J. Mol. Med. Berl. Ger. *82*, 348–356.

192. Surewicz, W.K., and Apostol, M.I. (2011). Prion protein and its conformational conversion: a structural perspective. Top. Curr. Chem. *305*, 135–167.

193. Taraboulos, A., Serban, D., and Prusiner, S.B. (1990). Scrapie prion proteins accumulate in the cytoplasm of persistently infected cultured cells. J. Cell Biol. *110*, 2117–2132.

194. Taraboulos, A., Scott, M., Semenov, A., Avrahami, D., Laszlo, L., Prusiner, S.B., and Avraham, D. (1995). Cholesterol depletion and modification of COOH-terminal targeting sequence of the prion protein inhibit formation of the scrapie isoform. J. Cell Biol. *129*, 121–132.

195. Telling, G.C., Scott, M., Hsiao, K.K., Foster, D., Yang, S.L., Torchia, M., Sidle, K.C., Collinge, J., DeArmond, S.J., and Prusiner, S.B. (1994). Transmission of Creutzfeldt-Jakob disease from humans to transgenic mice expressing chimeric human-mouse prion protein. Proc. Natl. Acad. Sci. U. S. A. *91*, 9936–9940.

196. Telling, G.C., Scott, M., Mastrianni, J., Gabizon, R., Torchia, M., Cohen, F.E., DeArmond, S.J., and Prusiner, S.B. (1995). Prion propagation in mice expressing human and chimeric PrP transgenes implicates the interaction of cellular PrP with another protein. Cell *83*, 79–90.

197. Thackray, A.M., Knight, R., Haswell, S.J., Bujdoso, R., and Brown, D.R. (2002). Metal imbalance and compromised antioxidant function are early changes in prion disease. Biochem. J. *362*, 253–258.

198. Thompson, K.J., Shoham, S., and Connor, J.R. (2001). Iron and neurodegenerative disorders. Brain Res. Bull. *55*, 155–164.

199. Tobler, I., Gaus, S.E., Deboer, T., Achermann, P., Fischer, M., Rülicke, T., Moser, M., Oesch, B., McBride, P.A., and Manson, J.C. (1996). Altered circadian activity rhythms and sleep in mice devoid of prion protein. Nature *380*, 639–642.

200. Ai Tran, H.N., Sousa, F., Moda, F., Mandal, S., Chanana, M., Vimercati, C., Morbin, M., Krol, S., Tagliavini, F., and Legname, G. (2010). A novel class of potential prion drugs: preliminary in vitro and in vivo data for multilayer coated gold nanoparticles. Nanoscale *2*, 2724–2732.

201. Treiber, C., Thompsett, A.R., Pipkorn, R., Brown, D.R., and Multhaup, G. (2007). Real-time kinetics of discontinuous and highly conformational metal-ion binding sites of prion protein. J. Biol. Inorg. Chem. JBIC Publ. Soc. Biol. Inorg. Chem. *12*, 711–720.

202. Tsenkova, R.N., Iordanova, I.K., Toyoda, K., and Brown, D.R. (2004). Prion protein fate governed by metal binding. Biochem. Biophys. Res. Commun. *325*, 1005–1012.

203. Turk, E., Teplow, D.B., Hood, L.E., and Prusiner, S.B. (1988). Purification and properties of the cellular and scrapie hamster prion proteins. Eur. J. Biochem. FEBS *176*, 21–30.

204. Uchiyama, K., Muramatsu, N., Yano, M., Usui, T., Miyata, H., and Sakaguchi, S. (2013). Prions disturb post-Golgi trafficking of membrane proteins. Nat. Commun. *4*, 1846.

205. Urso, E., Rizzello, A., Acierno, R., Lionetto, M.G., Salvato, B., Storelli, C., and Maffia, M. (2010). Fluorimetric analysis of copper transport mechanisms in the b104 neuroblastoma cell model: a contribution from cellular prion protein to copper supplying. J. Membr. Biol. *233*, 13–21.

206. Urso, E., Manno, D., Serra, A., Buccolieri, A., Rizzello, A., Danieli, A., Acierno, R., Salvato, B., and Maffia, M. (2012). Role of the cellular prion protein in the neuron adaptation strategy to copper deficiency. Cell. Mol. Neurobiol. *32*, 989–1001.

207. Valensin, D., Luczkowski, M., Mancini, F.M., Legowska, A., Gaggelli, E., Valensin, G., Rolka, K., and Kozlowski, H. (2004). The dimeric and tetrameric octarepeat fragments of prion protein behave differently to its monomeric unit. Dalton Trans. Camb. Engl. 2003 1284–1293.

208. Vassallo, N., and Herms, J. (2003). Cellular prion protein function in copper homeostasis and redox signalling at the synapse. J. Neurochem. *86*, 538–544.

209. Veith, N.M., Plattner, H., Stuermer, C.A.O., Schulz-Schaeffer, W.J., and Bürkle, A. (2009a). Immunolocalisation of PrPSc in scrapie-infected N2a mouse neuroblastoma cells by light and electron microscopy. Eur. J. Cell Biol. *88*, 45–63.

210. Veith, N.M., Plattner, H., Stuermer, C.A.O., Schulz-Schaeffer, W.J., and Bürkle, A. (2009b). Immunolocalisation of PrPSc in scrapie-infected N2a mouse neuroblastoma cells by light and electron microscopy. Eur. J. Cell Biol. *88*, 45–63.

211. Viles, J.H., Cohen, F.E., Prusiner, S.B., Goodin, D.B., Wright, P.E., and Dyson, H.J. (1999). Copper binding to the prion protein: structural implications of four identical cooperative binding sites. Proc. Natl. Acad. Sci. U. S. A. *96*, 2042–2047.

212. Volpicelli-Daley, L.A., Luk, K.C., Patel, T.P., Tanik, S.A., Riddle, D.M., Stieber, A., Meaney, D.F., Trojanowski, J.Q., and Lee, V.M.-Y. (2011). Exogenous α-synuclein fibrils induce Lewy body pathology leading to synaptic dysfunction and neuron death. Neuron *72*, 57–71.

213. Wadsworth, J.D., Hill, A.F., Joiner, S., Jackson, G.S., Clarke, A.R., and Collinge, J. (1999). Strain-specific prion-protein conformation determined by metal ions. Nat. Cell Biol. *1*, 55–59.

214. Waggoner, D.J., Drisaldi, B., Bartnikas, T.B., Casareno, R.L., Prohaska, J.R., Gitlin, J.D., and Harris, D.A. (2000). Brain copper content and cuproenzyme activity do not vary with prion protein expression level. J. Biol. Chem. *275*, 7455–7458.

215. Waheed, A., Grubb, J.H., Zhou, X.Y., Tomatsu, S., Fleming, R.E., Costaldi, M.E., Britton, R.S., Bacon, B.R., and Sly, W.S. (2002). Regulation of transferrin-mediated iron uptake by HFE, the protein defective in hereditary hemochromatosis. Proc. Natl. Acad. Sci. U. S. A. *99*, 3117–3122.

216. Walter, E.D., Stevens, D.J., Visconte, M.P., and Millhauser, G.L. (2007). The prion protein is a combined zinc and copper binding protein: Zn2+ alters the distribution of Cu2+ coordination modes. J. Am. Chem. Soc. *129*, 15440–15441.

217. Walter, E.D., Stevens, D.J., Spevacek, A.R., Visconte, M.P., Dei Rossi, A., and Millhauser, G.L. (2009). Copper binding extrinsic to the octarepeat region in the prion protein. Curr. Protein Pept. Sci. *10*, 529–535.

218. Watt, N.T., and Hooper, N.M. (2003). The prion protein and neuronal zinc homeostasis. Trends Biochem. Sci. *28*, 406–410.

219. Weiss, J.H., Sensi, S.L., and Koh, J.Y. (2000). Zn(2+): a novel ionic mediator of neural injury in brain disease. Trends Pharmacol. Sci. *21*, 395–401.

220. Wells, M.A., Jackson, G.S., Jones, S., Hosszu, L.L.P., Craven, C.J., Clarke, A.R., Collinge, J., and Waltho, J.P. (2006). A reassessment of copper(II) binding in the full-length prion protein. Biochem. J. *399*, 435–444.

221. Westergard, L., Turnbaugh, J.A., and Harris, D.A. (2011). A nine amino acid domain is essential for mutant prion protein toxicity. J. Neurosci. Off. J. Soc. Neurosci. *31*, 14005–14017.

222. Whittal, R.M., Ball, H.L., Cohen, F.E., Burlingame, A.L., Prusiner, S.B., and Baldwin, M.A. (2000). Copper binding to octarepeat peptides of the prion protein monitored by mass spectrometry. Protein Sci. Publ. Protein Soc. *9*, 332–343.

223. Wong, B.S., Pan, T., Liu, T., Li, R., Petersen, R.B., Jones, I.M., Gambetti, P., Brown, D.R., and Sy, M.S. (2000). Prion disease: A loss of antioxidant function? Biochem. Biophys. Res. Commun. *275*, 249–252.

224. Wong, B.S., Brown, D.R., and Sy, M.S. (2001). A Yin-Yang role for metals in prion disease. Panminerva Med. *43*, 283–287.

225. Wopfner, F., Weidenhöfer, G., Schneider, R., von Brunn, A., Gilch, S., Schwarz, T.F., Werner, T., and Schätzl, H.M. (1999). Analysis of 27 mammalian and 9 avian PrPs reveals high conservation of flexible regions of the prion protein. J. Mol. Biol. *289*, 1163–1178.

226. Yamasaki, T., Suzuki, A., Shimizu, T., Watarai, M., Hasebe, R., and Horiuchi, M. (2012). Characterization of intracellular localization of PrP(Sc) in prion-infected cells using a mAb that recognizes the region consisting of aa 119-127 of mouse PrP. J. Gen. Virol. *93*, 668–680.

227. Yedidia, Y., Horonchik, L., Tzaban, S., Yanai, A., and Taraboulos, A. (2001). Proteasomes and ubiquitin are involved in the turnover of the wild-type prion protein. EMBO J. *20*, 5383–5391.

228. Zanusso, G., and Monaco, S. (2005). Molecular mechanisms of human prion diseases. Drug Discov. Today Dis. Mech. *2*, 511–518.

229. Zanusso, G., Petersen, R.B., Jin, T., Jing, Y., Kanoush, R., Ferrari, S., Gambetti, P., and Singh, N. (1999). Proteasomal Degradation and N-terminal Protease Resistance of the Codon 145 Mutant Prion Protein. J. Biol. Chem. *274*, 23396–23404.

230. Zatta, P., Drago, D., Bolognin, S., and Sensi, S.L. (2009). Alzheimer's disease, metal ions and metal homeostatic therapy. Trends Pharmacol. Sci. *30*, 346–355.

231. Zhang, C.C., Steele, A.D., Lindquist, S., and Lodish, H.F. (2006). Prion protein is expressed on long-term repopulating hematopoietic stem cells and is important for their self-renewal. Proc. Natl. Acad. Sci. U. S. A. *103*, 2184–2189.

232. Zhou, Z., and Xiao, G. (2013). Conformational conversion of prion protein in prion diseases. Acta Biochim. Biophys. Sin. *45*, 465–476.